STATISTICAL SYSTEM IDENTIFICATION OF STRUCTURES WITH FLEXIBLE JOINTS

by

Sathya N. Gangadharan

Dissertation submitted to the Faculty of the

Virginia Polytechnic Institute and State University

in partial fulfillment of the requirements for the degree of

Doctor of Philosophy

in

Aerospace and Ocean Engineering

APPROVED:

E. Nikolaidis, Chairman

Z. Gurdal

R. T. Haftka

R. Heller

O. Hughes

E. Johnson

R. K. Kapania

P. Kaplan

M. P. Singh

April, 1990

Blacksburg, Virginia

STATISTICAL SYSTEM IDENTIFICATION OF STRUCTURES WITH FLEXIBLE JOINTS

by

Sathya N. Gangadharan

E. Nikolaidis, Chairman

Aerospace and Ocean Engineering

(ABSTRACT)

The flexibility of welded joints is an important issue in design of car bodies. Two generic, 3-D, design-oriented models (simple and complex) are developed to represent the compliant behavior of multibranch flexible joints. The simple model consists of torsional springs restraining the relative rotation of the joint branches in the three planes, while all branches are assumed to be rigidly connected in translation. Coupling between motions in different planes is neglected. The complex model accounts for such coupling. A statistical system identification method is proposed for inferring the model parameters from the static response of the structure. The method is demonstrated by applying it to a simple cube frame structure and a car body. Finally, the two models are compared in terms of their ability to predict static response.

Acknowledgements

I am greatly indebted to my advisor Dr. Nikolaidis for his guidance and support. The advice and guidance received from Dr. Haftka is unequalled. The sincerity and constant encouragement I have enjoyed under them is deeply appreciated. I shall be eternally obliged to them for their help in this dissertation. My special thanks are to Dr. Haftka for his timely financial support to make this dissertation a success.

I wish to thank Dr. Heller, Dr. Johnson, Dr. Kapania, Dr. Kaplan, and Dr. Singh for serving on my committee. I thank Dr. Gurdal and Dr. Hughes for serving on my committee during my final defense. I would love to take this opportunity to thank all my fellow friends and colleagues for all their arguments, discussions and insight.

This research was supported in part by a grant from FORD Motor Company, Dearborn, Michigan and from NASA Langley Research Center, Virginia.

Thanks are also to Dr. C. T. Chon for his valuable suggestions and to technical monitor Dr. T. G. Adams of FORD Motor Company.

Finally, I wish to thank my parents Dr. Gopal Gangadharan, professor of electrical engineering, and Dr. Kousalya Gangadharan, professor of plant pathology, for their continued strong moral support towards this dissertation.

Dedication

To my loving sister and to my wonderful parents

1.0 Table of Contents

2.0 List of Figures

3.0 List of Tables

Page

4.0 List of Symbols

$\mathbf{B}$ ..... Equilibrium matrix

CPU ..... Central processing time of the computer

$E_{complex}$ .....Strain energy of complex model

$\mathbf{E}_m$ ..... Error vector

E_{simple} .....Strain energy of simple model

$\mathbf{f}^p$ ..... Pseudo load vector

$\mathbf{F}$ ..... Force vector

$\mathbf{F}_R$ ..... Reduced force vector

$\mathbf{K}$ ..... Stiffness matrix

k_{ij} ..... Stiffness quantities of flexible joint

$\mathbf{k}_J$ ..... Joint stiffness parameter vector

$\mathbf{K}_C$ ..... Stiffness matrix of constrained joint

$\mathbf{K}_J$ ..... Joint stiffness matrix

K_{ij} ..... Element of joint stiffness matrix

$\mathbf{K}_{overall}$ ..... Stiffness matrix of entire structure

$\mathbf{K}_R$ ..... Reduced stiffness matrix of super-element

$\mathbf{K}_U$ ..... Stiffness matrix of unconstrained joint

L_f ..... Length of force vector

$\mathbf{u}$ ..... Rotation vector

$\mathbf{U}$ ..... Displacement vector

$\mathbf{U}_A$ ..... Actual displacement vector

U_E ..... Strain energy stored by the springs

$\mathbf{U}_m$ ..... Measured displacement vector

$\mathbf{V}_e$ ..... Quality matrix (Covariance matrix)

$\mathbf{V}_m$ ..... Covariance matrix of measurement errors

x ..... Parameter of interest

$\mathbf{X}_m$ ..... Matrix formed from the measured displacements

$'$ ..... Derivative with respect to parameter

θ_{ij} ..... Rotational degrees of freedom at joint

SUBSCRIPTS

B ..... Boundary degrees of freedom

I ..... Internal degrees of freedom

BI ..... Cross terms between boundary-internal degrees of freedom

IB ..... Cross terms between internal-boundary degrees of freedom

J ..... Joint related characteristic

R ..... Reduced (condensed) form

Chapter 1: Introduction

1.1 Overview

Flexible characteristics of joints are important in analysis and design of structures because, in some cases, they dominate the static and dynamic response. An example of a typical structure with flexible joints is an automotive structure. Complex finite element models developed to analyze welded joints are too complicated to be used in design. Therefore, simple, but reasonably accurate models, which are computationally inexpensive to analyze and enable to perform many design iterations, are preferred.

The present research is primarily directed towards this goal by developing such simple design-oriented models for joints. A finite element analysis of the automotive structure that incorporates these models must be able to predict the response of the overall vehicle to a set of loading conditions which represent real

life loads. It should also predict the natural frequencies and the first few modes with reasonable accuracy.

Two generic joint models are proposed. These are called simple and complex models. The first model neglects the coupling between the parameters in various planes while the second accounts for it. The parameters of these models are estimated by calibrating them in a way that theoretically predicted displacements agree with measurements. Alternatively, displacements from very detailed finite element models of the automotive structure can be used as measurements in identifying the joint models.

The following are some of the important questions confronted by the designer of an automotive structure as regards to flexibility of welded joints:

(i) How complicated should the joint model be for reasonable accuracy ?

(ii) Should the coupling be considered in the model ?

(iii) Can complications induced by considering coupling be justified ?

The present research attempts to answer these questions by comparing the two models in terms of their accuracy in predicting displacements. Previous work is reviewed and referenced in section 1.3.

1.2 Objective

The objective of this dissertation is to develop simple design-oriented models representing the compliant behavior of flexible joints, and a method to identify the model and test its accuracy.

1.3 Literature Survey

Structural analysis of car bodies is generally done by detailed finite element discretization of the entire structure into large number of elements [1]. Simpler models consisting of beams are also used at the preliminary design stages. Figure 1.1 shows the 'stick' model with typical sections of an automotive structure as modeled by Chon [2]. These simple models are preferable since many iterations need to be performed for small changes in design parameters to optimize the design.

Chang demonstrated in [3] that, in some cases, flexible characteristics of welded joints dominate the static and dynamic response. The response obtained from experiments is widely different from that when the joints are assumed to be rigid. Figure 1.2, extracted from [3], depicts the displacement of a car body under longitudinal bending calculated under the assumption of rigid joints (dashed curve) and results from measurements. Figure 1.3 shows the finite element model of an automotive vehicle with some critical joints. Flexible characteristics of the joints pose a major difficulty in design because their behavior has not been

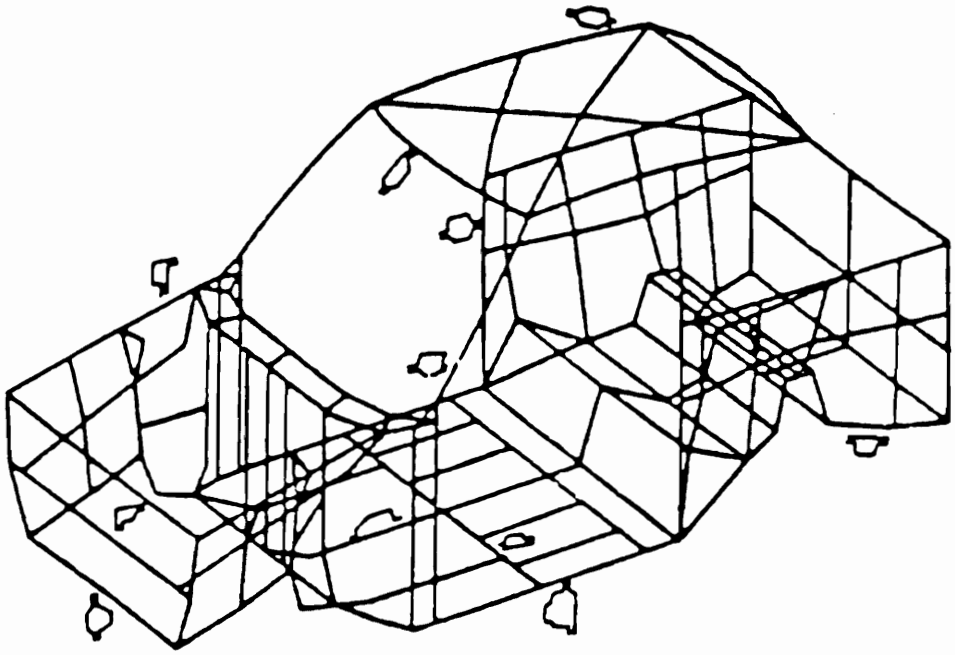

Figure 1.1 Stick model of a car with typical sections

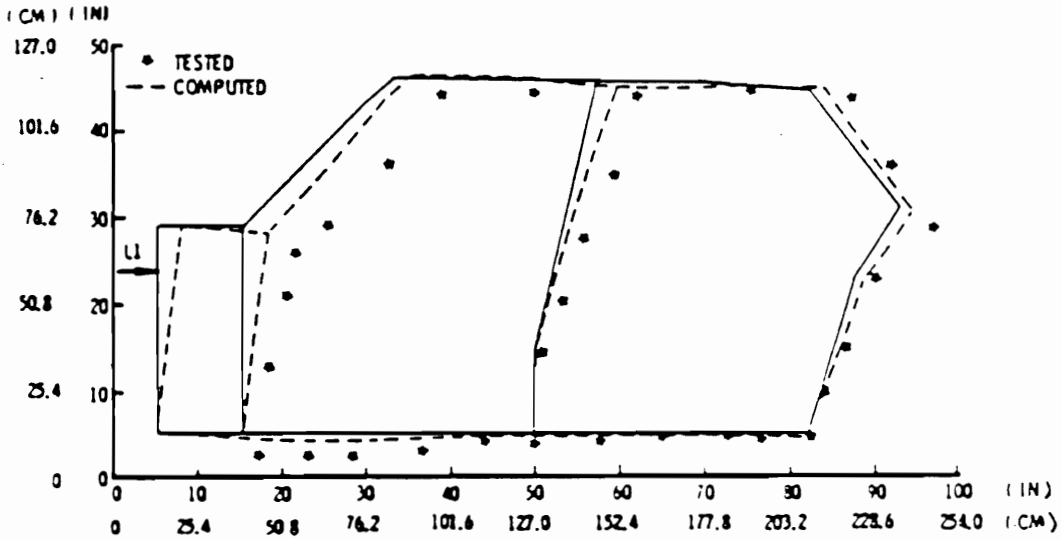

Figure 1.2 Vehicle deflections in bending test (asterisks) and deflections computed assuming all rigid connections (dashed line)

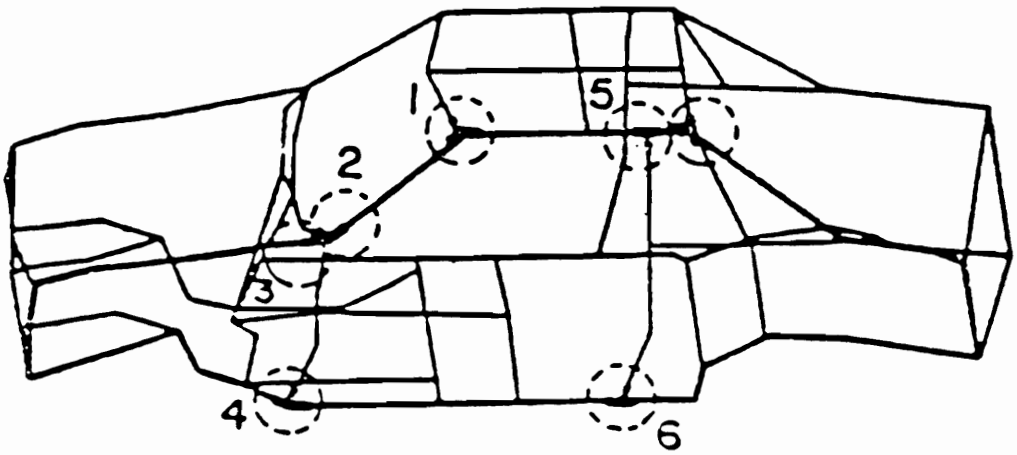

1) A-PILLAR TO ROOF RAIL
2) A-PILLAR TO FRT HINGE PILLAR
3) SHOTGUN TO FRT HINGE PILLAR
4) FRT HINGE PILLAR TO ROCKER
5) B-PILLAR TO ROOF RAIL
6) B-PILLAR TO ROCKER

Figure 1.3 Finite element model of an automotive vehicle with some crucial joints

completely understood. Detailed finite element models of the welded joints have been developed [1], but they cannot be used in design because they are very complex and they involve a high number of degrees of freedom. Simple, design-oriented models of flexible joints do not exist to the best of author's knowledge.

Significant improvement in the accuracy for structural analysis and effectiveness of design optimization is expected when the flexibility of the joints is accounted for [3,4]. Optimal design of automotive structures requires an analysis method of the vehicle stiffness that is computationally efficient and reasonably accurate. The problem of developing such a method becomes quite complex if the flexibility of the body connections, which are formed by overlapping metal sheets fastened by spot welds, is taken into consideration.

Several obstacles are encountered in developing a method that incorporates the flexibility of the joints in the analysis of the stiffness of a vehicle. These problems include the determination of joint stiffness parameters from the test measurements, the non-linear behavior of the joints, and the variation of the stiffness parameters of the joints from one vehicle to another due to manufacturing defects of the weldments which are random in nature. Chang [3] modeled flexible joints as sets of torsional springs connected to the rest of the members of a finite element model of an automotive structure. Garstecki studied optimal design of joints in linear elastic beams and frames [5]. Ioannidis and Kounadis studied the effect of joint flexibility on the non-linear buckling load of

metal portal frames using springs [6]. The analysis assumes that the performance of a joint can be simulated by using linear rotational springs.

"System Identification" is sometimes defined as the "inverse problem" of systems analysis, i.e., given the system input and output, determine the equations that describe the system behavior [7]. System identification falls into two categories. The first category is called "parametric identification", while the second, "non-parametric identification". Parametric identification procedures assume that the form of the model equations is known and only model parameter values need to be identified. Non-parametric identification techniques seek to determine (at least in part) the form of the mathematical model equations. A principal goal of the structural analyst is to develop an analytical approach whose results are in good agreement with the experimental measurements. If the theoretical results are not in good agreement with the experimental measurements, parametric system identification, is used to adjust the theoretical model until the analysis and test results agree. In the present research, parametric identification is performed.

System identification can be deterministic or statistical. In the former the measurement error is assumed to be zero. The system parameters are determined in a way that the measurements exactly agree with theoretical predictions. In statistical identification, the error in measurements is accounted for. Since the identification problem results to an algebraic system of equations in which the number of equations is larger than the number of unknown parameters, the latter are determined in a way that the discrepancy between predictions and

measurements is minimized. An advantage of statistical system identification is that it takes more information into account and provides some measures of confidence to the final estimates of the system parameters and the accuracy of the model.

Berman [8], employed a system identification procedure to estimate the parameters of a structural system from dynamic test results. The parameters were determined by identifying a set of minimum changes in the originally assumed values so that the eigensolution agree with test measurements. Berman's procedure was not iterative and does not account for the rigid body response. Since the procedure was deterministic no consideration was given to measurement errors, and no information on the level of confidence in the predicted values of the parameters was provided.

Boroski, et al. [9], introduced fictitious linear springs to represent the flexibility of joints. The analysis assumes various spring constants and then those constants are tuned to make theoretical predictions match dynamic test results. This approach is deterministic and does not yield the quality of the estimates.

A method for identification of linear dynamic systems was presented by Baruch [10]. First the stiffness matrix of the system was estimated based on the results of static test measurements. Since in most practical cases, the vector of displacement measurements obtained from static tests is incomplete, a method for filling the gaps in this matrix corresponding to the missing displacements was

used. The stiffness matrix was estimated based on the results of static tests corrected from the previous step. In both steps, a set of minimum changes to the displacement of stiffness matrix was determined so that theoretically predicted displacements are in good agreement with measurements. The reason for using static test results is that they are more easily measured and the measurement results are more reliable than that of the mode shapes. Baruch demonstrated that it is extremely important to keep the rigid body characteristics of the structure uncorrupted. An important characterstic of his approach is that it does not corrupt the rigid body modes of the dynamical system to be identified. A method proposed in [11] using law of mass conservation can be used.

An approach for system identification on non-linear systems using a recursive filtering algorithm was proposed by Yun [12]. Here the test measurements consist of forced response time histories, and the noise involved in these measurements is taken into account. The estimation procedure starts from some initial estimates of the system parameters that are continuously updated as more measurements are taken. With increasing time, the estimates of the parameters converge to certain values, and the confidence intervals for these estimates become narrower.

Collins [13] developed a statistical identification method that uses measurements of mode shapes and natural frequencies to estimate the parameters of a linear dynamic system. This method essentially consists of repeated application of a sequential linearization technique (see for example Draper [14]). One of its features is that the random error in the measurements as well as the quality of the

initial estimates of the parameters are considered. Assuming that both these quantities are normally distributed, the errors can be quantified by defining the covariance matrices of the vectors of the measurements and the initial estimates of the parameters. Information on the level of confidence in the final estimates of the system parameters was provided by the covariance matrix of the random vector consisting of the final estimates of these parameters. Two disadvantages of the estimation method employed by Collins [13] are associated with the convergence of the iterative algorithm being used and the determination of the covariance matrix of the initial estimates of the random parameters. Collins also performed a statistical analysis of modal properties of large structural systems [15]. He underestimated the variances of the estimates by treating measurements at every iteration to be independent and updating the covariance matrix of the parameters accordingly.

A serious problem when measurements of mode shapes are used arises from the inaccuracies in these measurements, especially those associated with the higher natural frequencies. In addressing this problem, system identification methods have been recently introduced for estimating the mode shapes from dynamic response measurements [16]. Butkunas [17] was successful in identifying regions in the models for large automotive structures that should be changed to bring finite element predictions in exact agreement with experimental results. The approach is deterministic and the model is calibrated so that theoretically predicted natural frequencies and mode shapes exactly match measurements.

Allen [18] used Newton's method and followed weighted least squares approach in identification of structural model parameters. The iterative methods [19-22] includes both deterministic and statistical framework for both the model and the experimental data. The former framework is assumed in non-linear least squares based techniques while the latter framework in Bayesian based techniques. These approaches require design sensitivity information and include both batch and recursive solution procedures. They also permit simple constraints to be imposed on the estimated parameters. The drawback with these methods is that the analyst has to select the uncertain parameters beforehand, which is sometimes very difficult.

Chen [19] proposed a matrix perturbation method to calculate the Jacobian matrix (matrix of sensitivity derivatives) and to compute the new eigendata for the parameter estimation procedure. The model updating procedure requires the sensitivity derivative matrix to identify the model parameters that are affected by the eigenvectors and eigenvalues. The advantage of the method is the applicability to large complex structures without knowing the analytical expressions for the mass and stiffness matrices. Chrostowski [22] discussed the practical considerations of system identification process. He introduced a computer code that links finite element analysis and statistical estimation procedures.

Isenberg [23] reviews and unifies concisely the class of least-squares estimators. The advantages and limitations of each method are discussed. The approach is

based on formulating and then minimizing an objective function for each method. It emphasizes the importance of determining the uncertainties associated with the data.

The behavior of flexible joints in automotive structures has not been understood. The present research attempts to fill some of the gaps in understanding and modeling flexible joint behavior. This is done by developing two flexible joint models and a method for identifying their parameters in a way that the best possible agreement is achieved between the model predictions and the behavior of the car body under static loads.

1.4 Assumptions of the Proposed Method

The development of the joint model and the identification method is based on the following assumptions:

(i) The branches of the flexible joint are rigidly connected in translation.

(ii) The branches rotate around the same point.

(iii) The response of the structure is linear.

(iv) Systematic error due to finite element approximations and idealizations is neglected when estimating the model parameters.

The assumption that the branches are rigidly connected in translation is justified because the branches of the joint are much shorter than the rest of the structural members comprising the automotive structure. Therefore, the translational

degrees of freedom can be assumed to be rigid compared to the rotational degrees of freedom. Modeling error might be significant compared to the error due to the assumption that the joints are rigid. Bias to the parameter estimates is introduced by attributing the discrepancy between predictions and measurements at the joint. This study has shown that the bias is relatively low and that the parameter estimates are still reasonably accurately. This research is a first step towards understanding flexible joint behavior. Hence, although assumptions (ii), (iii) and (iv) may not be realistic for some cases, they are adopted to simplify the analysis and make it easier to identify various trends.

1.5 Outline

The material in the following chapters is arranged as follows:

In Chapter 2, two generic flexible joint models, which will be called simple and complex models, are presented. The simple model of the flexible joint is simulated by linear torsional springs. Each spring constrains the relative rotation in a plane for different elements forming the joint. Coupling between the motions in the various planes is neglected. The complex model of the flexible joint is more realistic because it takes into account the coupling between the motions in the various planes. On the other hand, the number of parameters necessary to represent the complex model is more than that for the simple model. The stiffness matrices for both models are derived.

Chapter 3 suggests an alternate version of static condensation for sensitivity calculations which is easy to implement without access to the source code of the finite element program. The proposed approach is demonstrated by applying it in system identification of joint parameters of 3-D frame structures (cube model and car model) using a direct method for evaluating the sensitivity derivatives of the response of a structure with flexible joints with respect to the joint parameters. The efficiency of the proposed method when applied to estimate sensitivity derivatives is compared to that of various methods.

In Chapter 4, the estimation method is presented. More specifically, we formulate the identification problem, and present some approaches for solving it and for interpreting the parameter estimates. The estimation problem reduces to the minimization of the residual of the displacements of the reduced stiffness matrix which is a non-linear function of the stiffness parameters. In the first stages of the estimation procedure, the fixed point iteration method is used to obtain a first approximation to the joint parameters. Newton's method is employed to refine the approximation. Newton's method requires repeated evaluation of the derivatives of displacements with respect to the joint stiffness parameters. These derivatives are efficiently evaluated using substructuring to condense all the degrees of freedom that are neither included in the estimation process nor belong to an element being estimated. This strategy reduces the cost of sensitivity calculations to a small fraction of the cost of a detailed finite element analysis.

In Chapter 5, examples are used to illustrate the identification method. The cube frame and a car body are used as examples and modeled with 3-D frame elements with 6 degrees of freedom per node. The method for simulating experimental measurements is also discussed.

Chapter 6 deals with the comparison of the simple and complex models. For the purpose of the examples, an actual joint which behaves according to the assumptions stated in section 1.4 is considered. Therefore, the complex model can exactly predict the behavior of the actual joint. Simulated measurements are used to estimate the parameters of simple and complex models. The behavior of two identified joint models is compared. Since the only difference between the two models is in accounting for coupling, the results from their comparison can be used to assess the importance of coupling.

Finally, in Chapter 7, conclusions, inferences and suggestions for future work are summarized.

Chapter 2: Flexible Joint Models

2.1 Overview

Two generic, 3-D, design-oriented flexible joint models that represent the compliant behavior of joints are described in this chapter. These are called simple and complex models. The models are generic because they can be utilized for modeling the joints of any framed structure such as for example an offshore platform. These are design-oriented because they are simple and are far less complicated than detailed finite element models [1].

The simple model includes torsional springs restraining the relative rotation of the joint branches in the three planes, while all branches are assumed to have the same linear displacements. Coupling between the different planes is neglected. The complex model of the flexible joint takes into account the coupling between the parameters in the various planes. These joint models are incorporated in the

finite element model of the overall vehicle to form a finite element model that accounts for the flexibility of the welded joints.

2.2 Simple Model

There are many ways to represent a flexible joint. In this study, a joint connecting n space frame elements is simulated by $3\binom{n}{2}$ linear torsional springs. Each spring constrains the relative rotation of two elements in a plane. The torsional spring constants are represented by three subscripts. Each torsional spring connects a pair of elements represented by the second and third subscripts and constrains their relative rotation in the plane represented by the first subscript. Care is taken not to connect the two members more than once. Figure 2.1 depicts a model of a joint with three branches in X-plane. Here, for example, spring $k_{x_{12}}$ connects pair of elements 1 and 2 in the X-plane and constrains the relative rotation between these two elements in the X-plane. θ_{x1} refers to the rotation of member 1 in the X-plane.

Consider the case of a joint with 3 elements shown in Figure 2.1. Similar simulations in the Y-plane and in the Z-plane incorporate 9 torsional springs for the 3 element joint. The strain energy stored by the springs is given by

$$U_E = \frac{1}{2}\begin{bmatrix} k_{x_{12}}(\theta_{x1}-\theta_{x2})^2 + k_{x_{23}}(\theta_{x2}-\theta_{x3})^2 + k_{x_{31}}(\theta_{x3}-\theta_{x1})^2 \\ + k_{y_{12}}(\theta_{y1}-\theta_{y2})^2 + k_{y_{23}}(\theta_{y2}-\theta_{y3})^2 + k_{y_{31}}(\theta_{y3}-\theta_{y1})^2 \\ + k_{z_{12}}(\theta_{z1}-\theta_{z2})^2 + k_{z_{23}}(\theta_{z2}-\theta_{z3})^2 + k_{z_{31}}(\theta_{z3}-\theta_{z1})^2 \end{bmatrix} \quad (1)$$

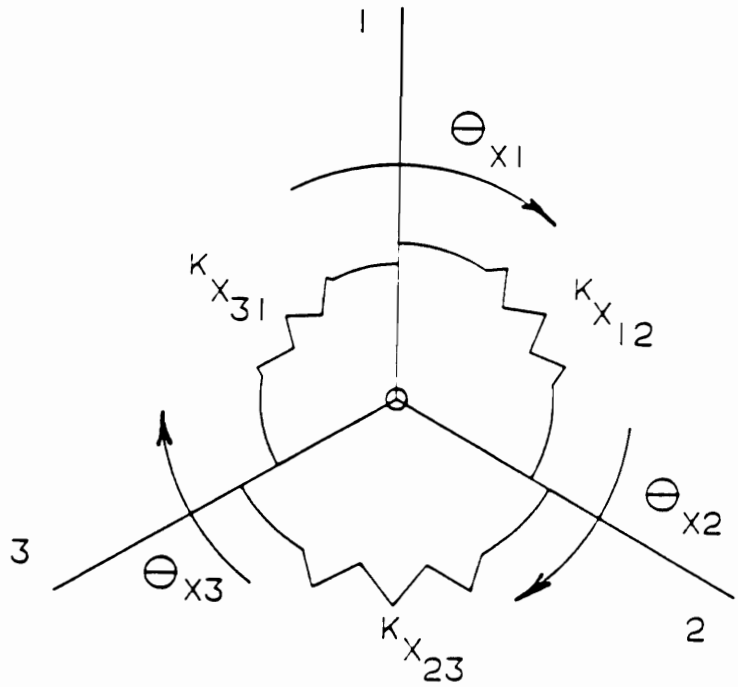

Figure 2.1 Joint simulation in X-plane (simple model)

The joint stiffness matrix (Table 2.1) is obtained by differentiating the total strain energy stored by springs with respect to rotational degrees of freedom at the joint i.e.,

$$K_{ij} = \frac{\partial^2 U_E}{\partial\theta_j \partial\theta_i} \Big|_{i=1,2,.....9\ ;j=1,2,.....9} \tag{2}$$

where

$$\theta_i \Big|_{i=1,2,.....9} = [\theta_{x1}, \theta_{y1}, \theta_{z1}, \theta_{x2}, \theta_{y2}, \theta_{z2}, \theta_{x3}, \theta_{y3}, \theta_{z3}] \tag{3}$$

There are cases for which the connection between certain degrees of freedom forming the joint is practically rigid. In such cases, the joint stiffness matrix is obtained by ignoring the springs connecting those degrees of freedom and deleting the rows and columns corresponding to the rotations not included in the model. This is equivalent to setting the corresponding degrees of freedom to be the same. For example, if the connections between branches 1 and 2 are rigid, then set $\theta_{x1} = \theta_{x2}$, $\theta_{y1} = \theta_{y2}$ and $\theta_{z1} = \theta_{z2}$. This implies that 3 springs are sufficient to characterize the joint.

2.3 Complex Model

A more complete representation would be to model a joint with n branches by an element with $6n$ degrees of freedom. The stiffness matrix of such an element is a $6n \times 6n$ matrix. The displacement due to stretching or warping of the

$(K_{X_{12}} + K_{X_{31}})$	0	0	$-K_{X_{12}}$	0	0	$-K_{X_{31}}$	0	0	Θ_{X1}
	$(K_{Y_{12}} + K_{Y_{31}})$	0	0	$-K_{Y_{12}}$	0	0	$-K_{Y_{31}}$	0	Θ_{Y1}
		$(K_{Z_{12}} + K_{Z_{31}})$	0	0	$-K_{Z_{12}}$	0	0	$-K_{Z_{31}}$	Θ_{Z1}
			$(K_{X_{12}} + K_{X_{23}})$	0	0	$-K_{X_{23}}$	0	0	Θ_{X2}
				$(K_{Y_{12}} + K_{Y_{23}})$	0	0	$-K_{Y_{23}}$	0	Θ_{Y2}
	S	Y	M		$(K_{Z_{12}} + K_{Z_{23}})$	0	0	$-K_{Z_{23}}$	Θ_{Z2}
						$(K_{X_{23}} + K_{X_{31}})$	0	0	Θ_{X3}
							$(K_{Y_{23}} + K_{Y_{31}})$	0	Θ_{Y3}
								$(K_{Z_{23}} + K_{Z_{31}})$	Θ_{Z3}

Table 2.1 Joint stiffness matrix (simple model)

members comprising the joint is negligible compared to that due to bending or torsion. The joint is assumed to be rigid in translation which reduces the translational degrees of freedom to 3. The degrees of freedom corresponding to rotations of the ends of the joint members which play an important role in the behavior of the overall joint is $3\,n$.

The elements of the reduced stiffness matrix of the joint constrained against rigid body motion are sufficient to determine the complete stiffness matrix of the unconstrained joint. The number of d.o.f. of a constrained joint, considering rotations only, is $(3n-3)$. As a result the number of parameters necessary to determine the full stiffness matrix of the element representing an $n-$ branch joint is $3(n-1)(3n-2)/2$ because the stiffness matrix is symmetric. If the branches are constrained to move in a plane, the number of unknown parameters reduces to n.

The stiffness matrix of the unconstrained joint is given by

$$\mathbf{K}_U = \mathbf{B}\,\mathbf{K}_C\,\mathbf{B}^T \tag{4}$$

where,

$\mathbf{K}_U$ is the stiffness matrix of the unconstrained joint of order $3n \times 3n$,

$\mathbf{K}_C$ is the stiffness matrix of the constrained joint (reduced stiffness matrix) of order $(3n-3) \times (3n-3)$, and

B is the equilibrium matrix of size $3n \times (3n - 3)$, whose columns include a unit load in one of the d.o.f. (corresponding to rotations) of the constrained joint and the reactions of the statically determinate joint caused by the unit load.

For example, consider a 3-branch joint as shown in Figure 2.2. This is represented by an element with 18 degrees of freedom. Since the joint is assumed to be rigid in translation, only 12 degrees of freedom are important. The 9 degrees of freedom corresponding to rotations of its ends play an important role in the behavior of the overall joint. The reduced stiffness matrix of such a joint is of order 6 x 6. If node 3 is clamped, the simulation of the constrained joint in 3-D requires 21 parameters (Table 2.2). The equilibrium matrix **B** of order 9 x 6 is obtained by constraining node 3 and applying a unit load at one of the free ends corresponding to rotational degree of freedom as shown in Figure 2.3. The reactions at all the other degrees of freedom constitute a column corresponding to the respective rotational degree of freedom in the equilibrium matrix. The process is repeated for all 6 rotational degrees of freedom to obtain all the 6 columns columns of the equilibrium matrix **B** as shown in Table 2.3. The stiffness matrix of the unconstrained joint in terms of the 21 parameters of the constrained joint obtained by using equation (4) is shown in Table 2.4.

The stiffness matrix of the joint model is assembled with the stiffness matrix of the rest of the structure to form the stiffness matrix of the model of the car body which accounts for the flexibility of the welded joints. The response of the overall

system at the internal degrees of freedom can be obtained by the recovery process used in static condensation.

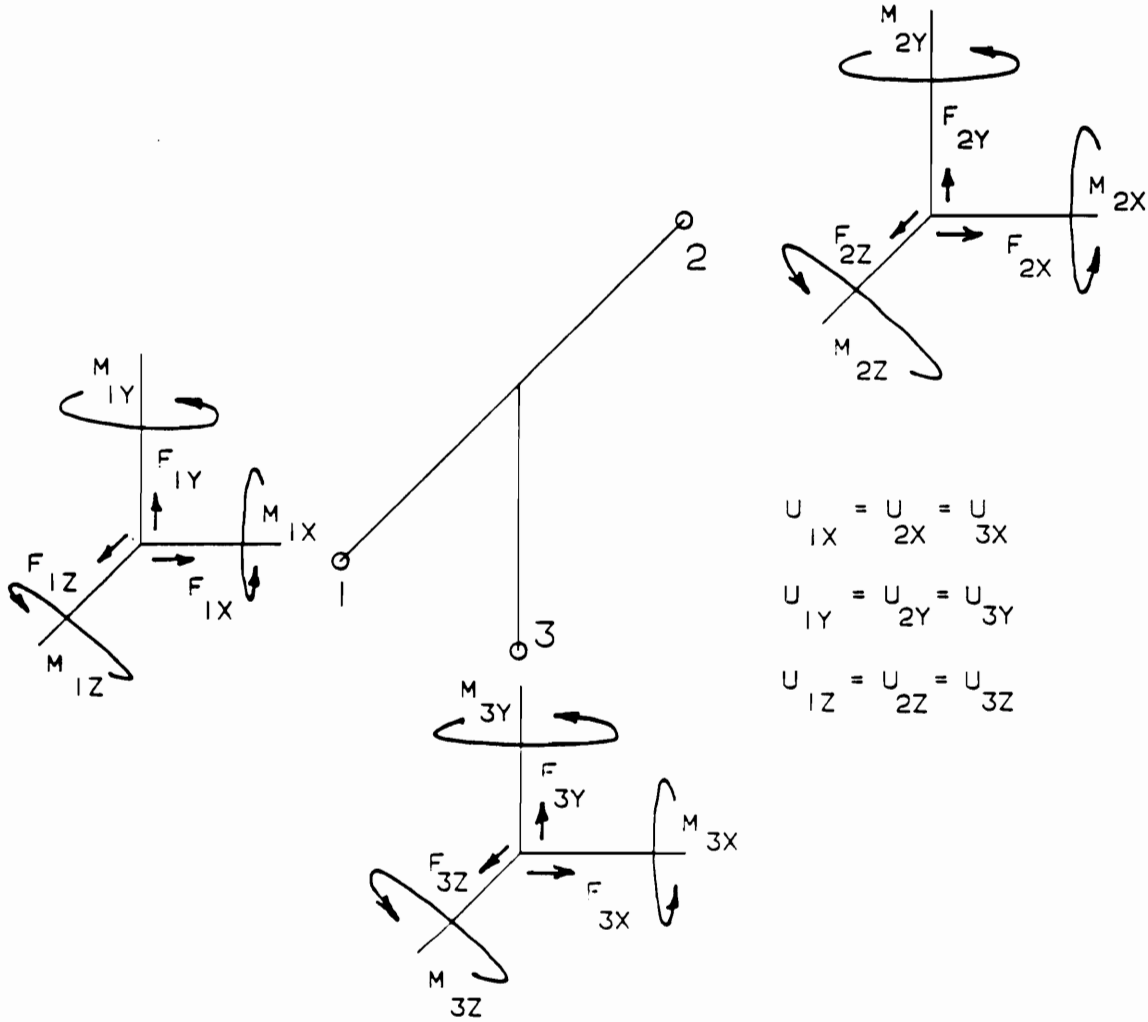

Figure 2.2 3-branch joint with 18 d.o.f

K_{11}	K_{12}	K_{13}	K_{14}	K_{15}	K_{16}	Θ_{X1}
	K_{22}	K_{23}	K_{24}	K_{25}	K_{26}	Θ_{Y1}
		K_{33}	K_{34}	K_{35}	K_{36}	Θ_{Z1}
			K_{44}	K_{45}	K_{46}	Θ_{X2}
	S	Y	M	K_{55}	K_{56}	Θ_{Y2}
					K_{66}	Θ_{Z2}

Table 2.2 Reduced stiffness matrix

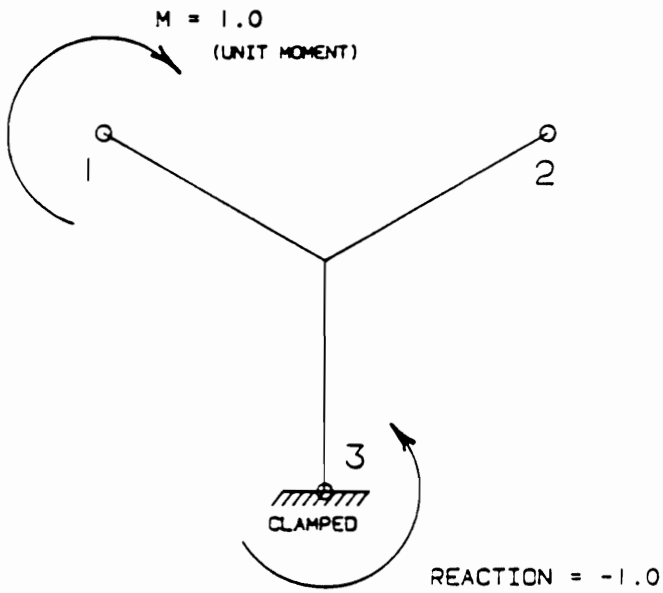

Figure 2.3 Simulation of Complex Joint Model

1	0	0	0	0	0
0	1	0	0	0	0
0	0	1	0	0	0
0	0	0	1	0	0
0	0	0	0	1	0
0	0	0	0	0	1
-1	0	0	-1	0	0
0	-1	0	0	-1	0
0	0	-1	0	0	-1

Table 2.3 The equilibrium matrix [B]

K_{11}	K_{12}	K_{13}	K_{14}	K_{15}	K_{16}	$-K_{11}-K_{14}$	$-K_{12}-K_{15}$	$-K_{13}-K_{16}$
	K_{22}	K_{23}	K_{24}	K_{25}	K_{26}	$-K_{12}-K_{24}$	$-K_{22}-K_{25}$	$-K_{23}-K_{26}$
		K_{33}	K_{34}	K_{35}	K_{36}	$-K_{13}-K_{34}$	$-K_{23}-K_{35}$	$-K_{33}-K_{36}$
			K_{44}	K_{45}	K_{46}	$-K_{14}-K_{44}$	$-K_{24}-K_{45}$	$-K_{34}-K_{46}$
				K_{55}	K_{56}	$-K_{15}-K_{45}$	$-K_{25}-K_{55}$	$-K_{35}-K_{56}$
					K_{66}	$-K_{16}-K_{46}$	$-K_{26}-K_{56}$	$-K_{36}-K_{66}$
		S	Y	M		$K_{11}+K_{14}$ $+K_{14}+K_{44}$	$K_{12}+K_{15}$ $+K_{24}+K_{45}$	$K_{13}+K_{16}$ $+K_{34}+K_{46}$
							$K_{22}+K_{25}$ $+K_{25}+K_{55}$	$K_{23}+K_{26}$ $+K_{35}+K_{56}$
								$K_{33}+K_{36}$ $+K_{36}+K_{66}$

Table 2.4 Stiffness matrix of unconstrained joint (complex model)

Chapter 3: Simple and Easy to Implement Static Condensation Method

3.1 Overview

Modern structural analyses typically require operations with very large stiffness matrices obtained by the finite element method. Procedures for structural optimization and structural identification require costly repeated analysis and sensitivity calculations. Most of the computational cost is often associated with the calculation of sensitivity derivatives of the response with respect to parameters employed for optimization or identification. For this reason, there has been considerable effort invested in the development of efficient algorithms for sensitivity calculations [24].

In many cases, the processes of optimization and identification involve repeated changes in only a small part of the structural model. In this case it is possible to

take advantage of sub-structuring techniques [25-28] or to employ the static condensation technique and eliminate degrees of freedom associated with the fixed part of the structure [29].

The static condensation technique (a.k.a Guyan reduction) [30] is available in some general purpose finite element packages (e.g. NASTRAN) [31] but not in others. The technique is difficult to implement without access to and familiarity with the source code of the finite element package, which is usually not available to the user. This chapter suggests an alternative version of the static condensation technique which is easy to implement with a general purpose program. The proposed approach shall be called 'black-box' method because it allows one to use the finite element package as a black-box. The method is slightly more expensive than the standard static condensation, but for large number of analyses and sensitivity calculations, it is considerably more efficient than no condensation at all. This chapter focuses on the use of the static condensation for the calculation of sensitivity derivatives.

One application where only a small part of the structure has to be repeatedly remodeled is the identification of joint stiffness in frame models. Such joint stiffnesses are typically not known, but they can have large effects on structural response [32]. The joint stiffnesses can be estimated from static deflections of the structure. The estimation procedure requires calculation of the sensitivity derivatives of the joint displacements with respect to the joint stiffnesses. A cube

example as well as a car frame example are used for demonstrating the efficiency of using static condensation for sensitivity calculation.

3.2 Background on Methods for Sensitivity Analysis

In this section, the methods of sensitivity analysis used later are briefly reviewed. These methods include: two finite-difference methods, the direct method, and the semi-analytical implementation of the direct method [33]. The review is limited to sensitivity with respect to parameters which do not affect the loads on the structure.

The finite element method is used in the sensitivity analysis. The matrix form of the equation describing the response of the structure under static loads is

$$\mathbf{K}(x)\,\mathbf{U} = \mathbf{F} \tag{5}$$

where, $\mathbf{K}(x)$ is the global stiffness matrix; $\mathbf{U}$ is the structural displacement vector; $\mathbf{F}$ is the load vector; and x is the parameter of interest.

3.2.1 Forward-Difference Scheme

The displacement $\mathbf{U}$ is found for a perturbed value $(x + \Delta x)$ of the design parameter. The derivative of $\mathbf{U}$ with respect to x is denoted by $\mathbf{U}'$ and is given by

$$\mathbf{U}' = \frac{\mathbf{U}(x + \Delta x) - \mathbf{U}(x)}{\Delta x} + O(\Delta x) \tag{6}$$

3.2.2 Central-Difference Scheme

Both a positive and a negative perturbation is used, and the sensitivity derivative is given by

$$\mathbf{U}' = \frac{\mathbf{U}(x + \Delta x) - \mathbf{U}(x - \Delta x)}{2\,\Delta x} + O\left(\Delta x^2\right) \tag{7}$$

The step size chosen is very critical to the accuracy of the sensitivity derivatives calculated using finite-difference schemes. The central-difference method is more accurate. However, if the derivative of the structural response with respect to n design variables is required, the forward-difference approximation requires n additional analyses and the central-difference approximation $2n$ additional analyses. Higher order approximations of the sensitivity derivative are even more expensive.

Because of the cost associated with finite-difference derivatives and possible accuracy problems, analytical methods are gaining popularity.

3.2.3 Direct Method

In this method, equation (5) can be differentiated with respect to the design variable x to yield:

$$\mathbf{K}(x)\ \mathbf{U}' = \mathbf{f}^p \tag{8}$$

where the pseudo load vector $\mathbf{f}^p$ is given by

$$\mathbf{f}^p = -\mathbf{K}(x)'\mathbf{U} \tag{9}$$

The sensitivity of the displacement can be calculated by evaluating the response of the structure to a static load equal to the right hand side of equation (8). Since equation (8) has the same global stiffness matrix as equation (5), there is no need to assemble and factor a new stiffness matrix for the calculation of sensitivities.

3.2.4 Semi-Analytical Implementation Scheme

The derivatives of the stiffness matrix with respect to the design variables are often difficult to calculate analytically, especially for shape design variables which change element geometry. For this reason a semi-analytical approach, where the derivatives of the stiffness matrix are approximated by finite differences can be employed. The derivative thus obtained is used in equation (8) to find the sensitivity derivative $\mathbf{U}'$.

3.3 Static Condensation Technique

The static condensation technique is useful when an interest is only in a subset of the displacement components, and when this subset needs to be calculated for several load conditions. It is also very useful when needed to recalculate the

response after repeated changes to a limited part of the structure. Both these conditions occur when it is needed to calculate sensitivities with respect to parameters which affect only a small part of the structure. The technique is summarized below:

Consider a structure where interest is only in a subset $\mathbf{U}_B$ of the displacement vector. This subset includes degrees of freedom associated with parts of the structure that change as well as other degrees of freedom that are of interest. The rest of the displacement vector is denoted by $\mathbf{U}_I$.

Equation (5) can be partitioned as follows:

$$\begin{bmatrix} \mathbf{K}_{BB} & \mathbf{K}_{BI} \\ \mathbf{K}_{IB} & \mathbf{K}_{II} \end{bmatrix} \begin{Bmatrix} \mathbf{U}_B \\ \mathbf{U}_I \end{Bmatrix} = \begin{Bmatrix} \mathbf{F}_B \\ \mathbf{F}_I \end{Bmatrix} \tag{10}$$

where $\mathbf{K}_{II}$ is associated with the part of the structure that does not change. Solving for $\mathbf{U}_I$ from the second row of equation (10) yields

$$\mathbf{U}_I = \mathbf{K}_{II}^{-1} \left[\mathbf{F}_I - \mathbf{K}_{IB}\, \mathbf{U}_B\right] \tag{11}$$

Substituting equation (11) in the first row of equation (10), yields the statically condensed equations :

$$\mathbf{K}_R\, \mathbf{U}_B = \mathbf{F}_R \tag{12}$$

where,

$$\mathbf{K}_R = \mathbf{K}_{BB} - \mathbf{K}_{BI}\mathbf{K}_{II}^{-1}\mathbf{K}_{IB} \tag{13}$$

and $$\mathbf{F}_R = \mathbf{F}_B - \mathbf{K}_{BI}\mathbf{K}_{II}^{-1}\mathbf{F}_I \tag{14}$$

Static condensation is computationally efficient because when the structure is changed, only $\mathbf{K}_{BB}$ changes. Hence, $\mathbf{K}_R$ can be updated without repeating the condensation process.

3.4 Black-box Approach for Static Condensation

Performing the operations indicated in equations (13) and (14) typically requires access to the source code of the finite element program. This section presents a procedure for obtaining $\mathbf{K}_R$ and $\mathbf{F}_R$ without using equations (13) and (14).

Consider a structure subjected to external loads as shown in Figure 3.1. Joint A is the node of interest. The rest of the structure apart from the boundary degrees of freedom is termed as the super-element.

Equation (12) can then be written as

$$\mathbf{U}_B = \mathbf{K}_R^{-1}\,\mathbf{F}_B \tag{15}$$

Equation (15) implies that each column of the flexibility matrix $\mathbf{K}_R^{-1}$ is the displacement $\mathbf{U}_B$ due to a unit load applied at the corresponding degrees of

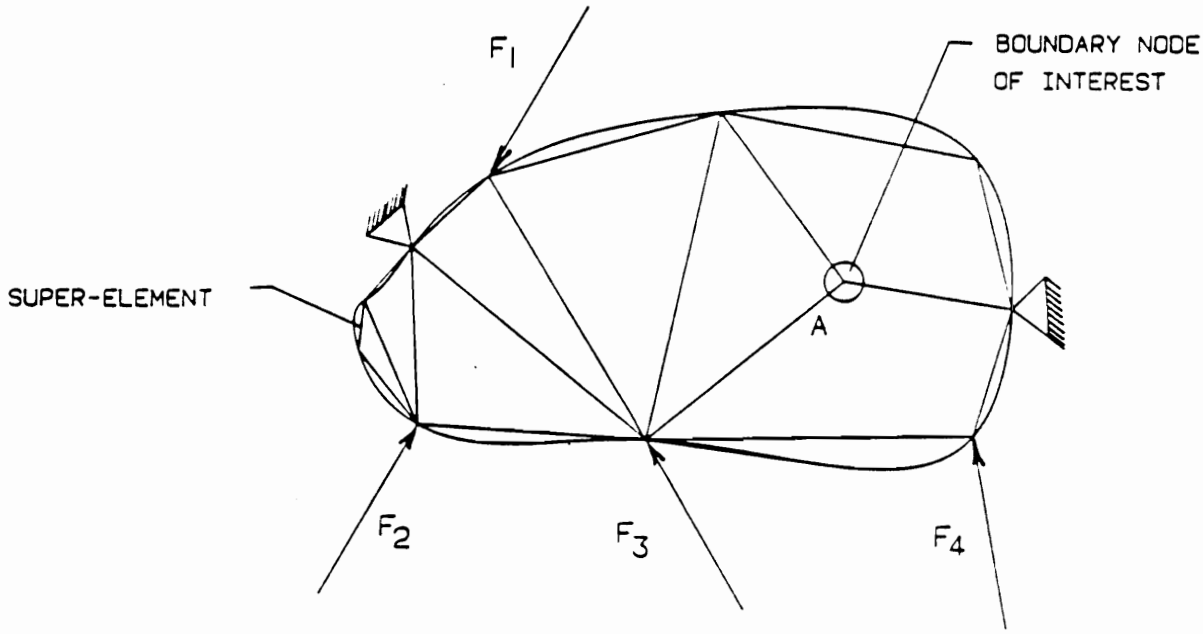

Figure 3.1 Boundary node and super-element

freedom. Hence, one column of $\mathbf{K}_R{}^{-1}$ can be obtained by applying such a unit load to the structure only at the boundary degrees of freedom and extracting from displacement vector the $\mathbf{U}_B$ components as in Figure 3.2. The process is repeated for all the $\mathbf{U}_B$ degrees of freedom to obtain all the columns of $\mathbf{K}_R{}^{-1}$. Finally, $\mathbf{K}_R$ is obtained by inverting $\mathbf{K}_R{}^{-1}$.

To calculate $\mathbf{F}_R$, the response of the structure to the actual loads as in Figure 3.3 is calculated and then the resulting $\mathbf{U}_B$ is multiplied by $\mathbf{K}_R$ (equation (12)).

3.5 Application to Local Variation and Sensitivity Analysis

The method outlined in the previous section for obtaining $\mathbf{K}_R$ and $\mathbf{F}_R$ is of no value for small number of analyses. The response of the structure is calculated from the unreduced system for $(n_B + 1)$ load cases where n_B is the number of components of $\mathbf{U}_B$. However, the method is economical for an application (such as optimization or system identification) where $\mathbf{K}_{BB}$ is repeatedly changed and derivatives of the response with respect to parameters that affect only $\mathbf{K}_{BB}$ is sought. In fact, equation (13) indicates that the change $\Delta\mathbf{K}_R$ in $\mathbf{K}_R$ due to a change $\Delta\mathbf{K}_{BB}$ in $\mathbf{K}_{BB}$ is

$$\Delta\mathbf{K}_R = \Delta\mathbf{K}_{BB} \tag{16}$$

Similarly, for changes that affect only $\mathbf{K}_{BB}$ the partitioned form of equation (10) is

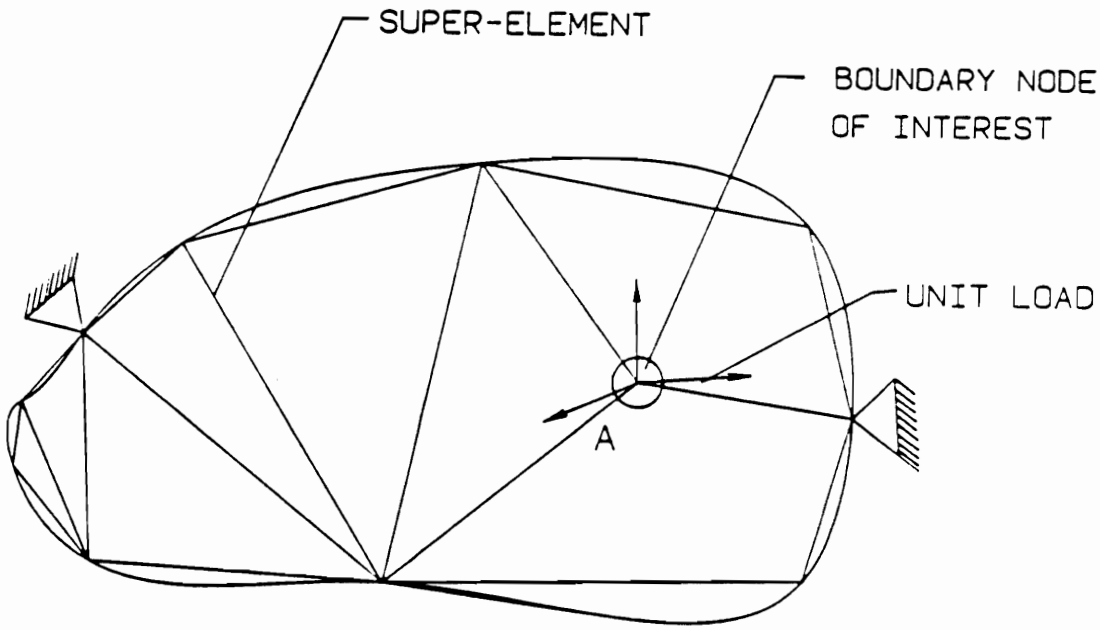

Figure 3.2 Evaluation of flexibility matrix

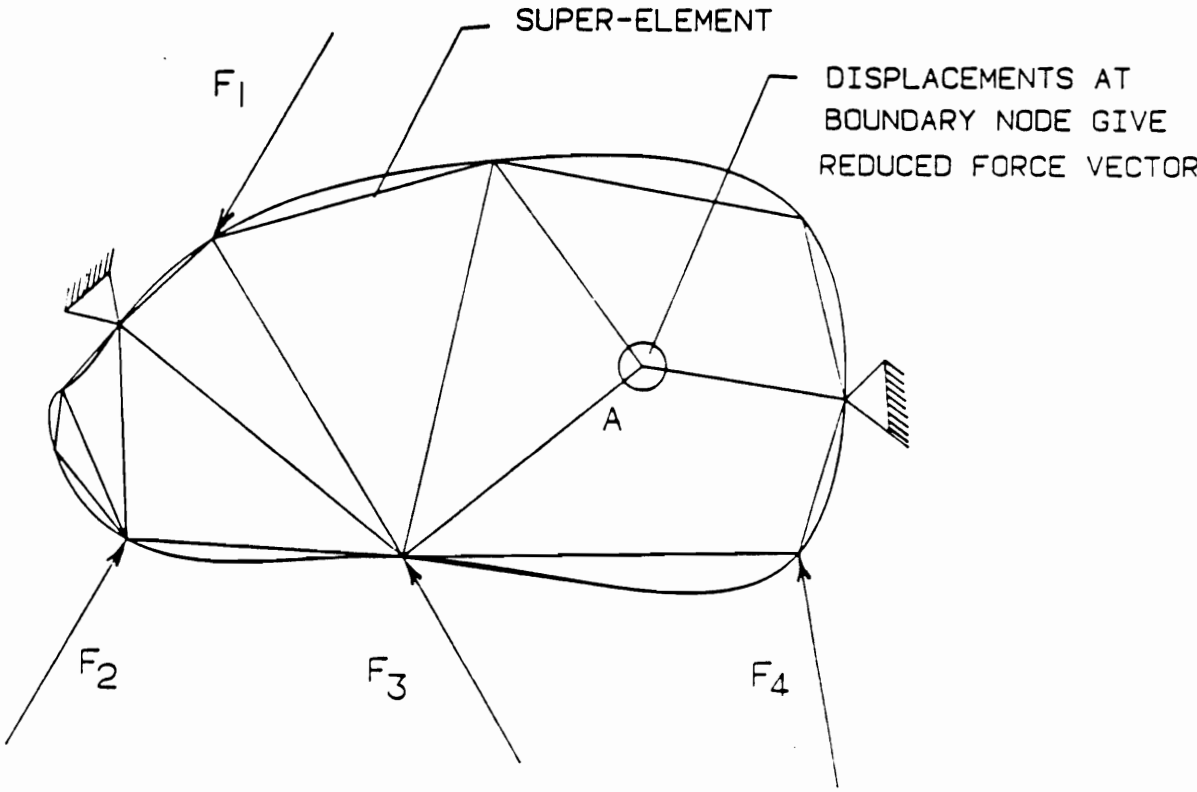

Figure 3.3 Evaluation of reduced force vector

$$\begin{bmatrix} \mathbf{K}_{BB} & \mathbf{K}_{BI} \\ \mathbf{K}_{IB} & \mathbf{K}_{II} \end{bmatrix} \begin{Bmatrix} \mathbf{U}_B' \\ \mathbf{U}_I' \end{Bmatrix} = \begin{Bmatrix} -\mathbf{K}_{BB}'\mathbf{U}_B \\ \mathbf{0} \end{Bmatrix} \tag{17}$$

which reduces to

$$\mathbf{K}_R \mathbf{U}_B' = -\mathbf{K}_{BB}' \mathbf{U}_B \tag{18}$$

Hence, the sensitivity $\mathbf{U}_B'$ can be calculated from the condensed system of equations at relatively low cost.

3.6 Application to Joint Stiffness Variation

Engineering structures are produced commercially utilizing formed sections connected by simple joint configurations either temporary (bolted joints) or permanent (welded joints). Welded joints are the most common permanent type of joint configuration in body structures such as automotive structures. The flexibility of the joints often dominates the static and dynamic response of these structures, so that large errors in the analysis and design of such structures are incurred when the flexibility of the joints is neglected. Because simple analytical models of joint stiffnesses are not available at present, it is expected that system identification methods will be utilized to create such simple models.

The applicability of the black-box method and its computational efficiency relative to the methods using no static condensation was demonstrated by applying it to identify the joint stiffness parameters.

There are many ways to represent a flexible joint. To demonstrate the method developed, a simple joint model is simulated by n space frame elements with $3\binom{n}{2}$ torsional springs as discussed in Chapter 2.

The proposed model of a flexible joint (Chapter 2) is not complete unless the parameters describing the joint are identified. There are two approaches to identify the joint stiffness parameters:

(i) Finite element analysis of a detailed model of the joint.

(ii) Estimation of the parameters from measured deflections of the structure.

The second process requires repeated analysis and sensitivity calculations and was simulated for two examples here. The Newton-Raphson iteration scheme was used for the numerical implementation of the identification.

An initial guess of the joint stiffness parameters is used to perform a finite element analysis of flexible joint model. The response of the structure when all the joint stiffness parameters have the same chosen value, is taken as the measured response to simulate the experimental results. The finite element analysis yields the displacements and the sensitivity derivatives with respect to joint parameters of interest. The sensitivity derivatives and the difference between the measured response and the response based on the current joint stiffness parameters are used to update the stiffness parameters by Newton-Raphson procedure. The updated value of the parameters are then used

in the next iteration and the process is repeated for convergence as shown in Figure 3.4.

3.7 Illustrative Examples

In this section, the 'black-box' method is illustrated with a cube frame and a car model examples.

3.7.1 Cube Frame Example

A cube frame with a flexible joint at node 7 shown in Figure 3.5 is used as the first example. Concentrated moments of magnitude 0.5 N-m are applied at nodes 5, 6 and 8 about the z axis. Node 1 is fixed and node 7 is the joint under consideration. Geometry and material property data are given in Table 3.1. The frame is analyzed using space frame elements having 6 d.o.f. per node. In the example, the spring stiffnesses k_{ij} are all taken to be equal to a single number k chosen as $1.0 \times 10^4 \ N-m/radian$. This value corresponds to potential energy (work done by external loads) which lies way half between the value for a rigid joint and the value for $k = 0$.

The sensitivity of the structural response with respect to the joint stiffness k is evaluated using the direct method with static condensation (equation (18)); the forward difference scheme and the central difference scheme. The results are almost identical and the sensitivity derivatives at the joint boundary are given in Table 3.2.

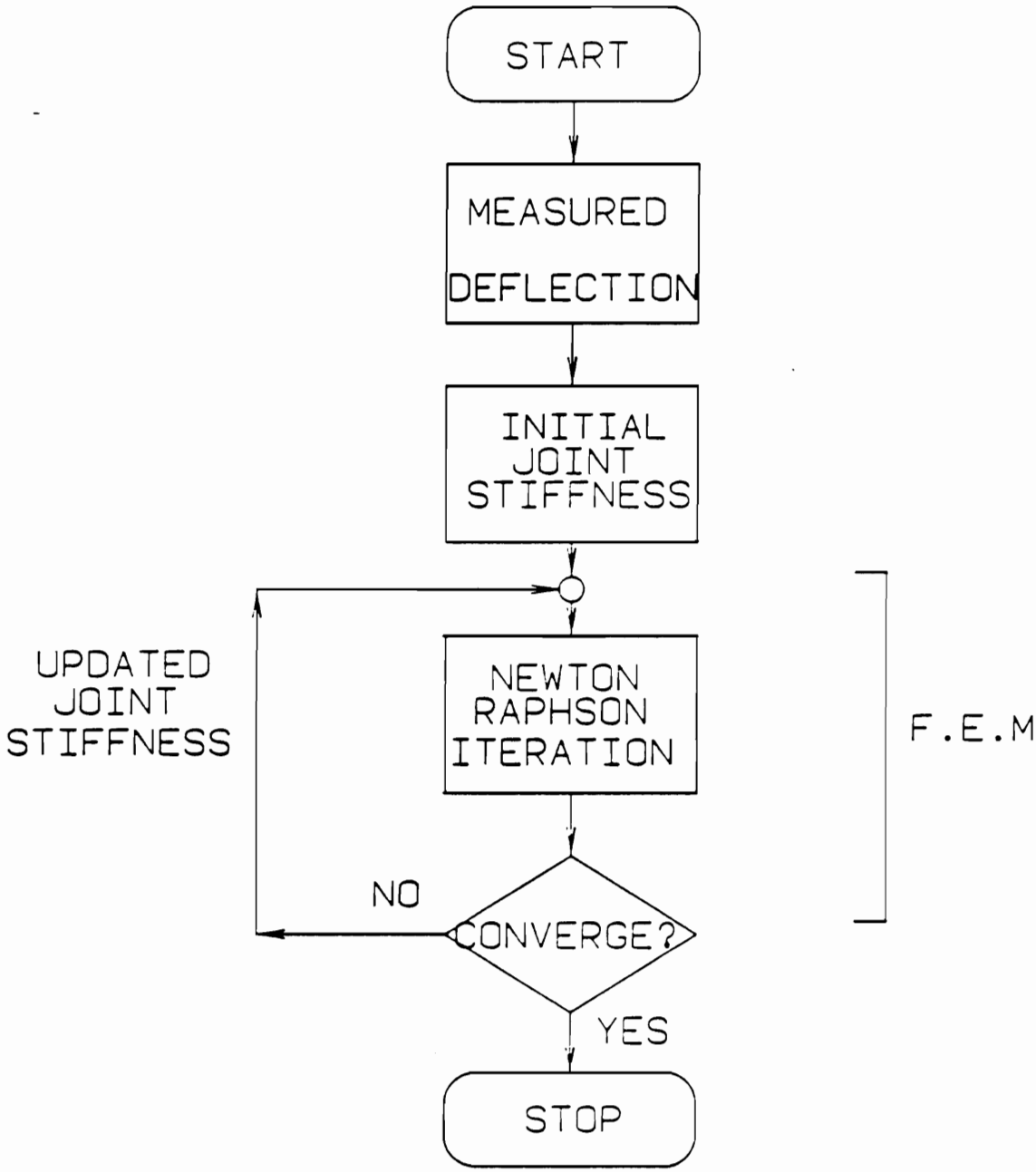

Figure 3.4 System identification process

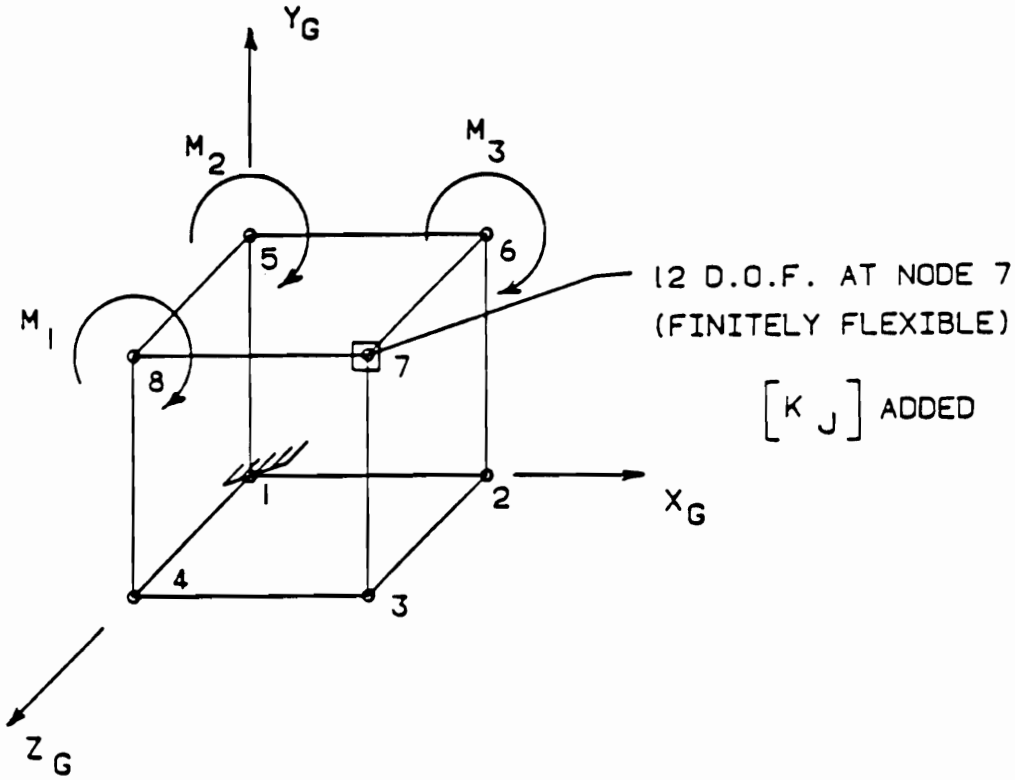

Figure 3.5 Cube frame example with flexible joint at node 7

Property	Value
Young's Modulus, E	200 GPa
Shear Modulus, G	80 GPa
Torsional Constant, J	0.4E-08 m^4
Cross-sectional Area, A	4.0E-04 m^2
Moment of Inertia, I_{yy}	1.333E-08 m^4
Moment of Inertia, I_{zz}	1.333E-08 m^4
Length of Element, L	0.2 m

Table 3.1 Frame element properties for cube model

Joint Degrees of Freedom	Sensitivity *		
	Direct Method	Central Differences	Forward Differences
u_x	-7.7415	-7.7414	-7.7372
u_y	2.2233	2.2235	2.2226
u_z	2.6074	2.6073	2.6066
θ_{x1}	-0.5140	-0.5141	-0.5138
θ_{y1}	-0.7863	-0.7863	-0.7859
θ_{z1}	0.2206	0.2206	0.2205
θ_{x2}	0.5293	0.5294	0.5291
θ_{y2}	-0.1090	-0.1090	-0.1091
θ_{z2}	0.8165	0.8166	0.8161
θ_{x3}	0.1012	0.1012	0.1011
θ_{y3}	0.2725	0.2724	0.2723
θ_{z3}	0.3263	0.3263	0.3261

* The sensitivity with respect to torsional spring constants for translational displacements is in 10^{-10} $radian/N$

* The sensitivity with respet to torsional spring constants for rotational displacements is in 10^{-14} $radian^2/N-m$

Table 3.2 Sensitivity derivatives at joint boundary (cube model)

To demonstrate the practicality and efficiency of the black-box static condensation, the computer times for identification of the joint parameters using static condensation (direct method), black-box implementation of static condensation, forward difference scheme and central difference schemes are compared. In the last two methods, sub-structuring technique was not employed; so the entire analysis was repeated each time that a joint parameter was changed.

The system identification process involves repeated calculations of sensitivity derivatives which dominate the CPU time. Results of the comparison between the various methods for the cube model is shown in Table 3.3. Figure 3.6 shows the estimated values of two joint parameters $k_{x_{12}}$ and $k_{x_{23}}$ as a function of the number of iterations for the cube model. The initial value of the parameters used in the identification process is $1.0 \times 10^3 \ N - m/radian$. It is observed that the values converge after 6 iterations.

The black-box static condensation is only slightly more costly than the standard static condensation with analytical derivatives. Compared to the finite difference schemes without condensation, the static condensation with analytical derivatives proves to be very efficient. The reason is that the former requires the whole solution process be repeated for small changes in the design parameters used for sensitivity calculations. The analysis is repeated once for each parameter when a forward difference scheme is employed, and twice if a central difference scheme is employed.

Model	CPU Time (seconds)				Number of Iterations
	Black-box Static Condensation & analytical derivative	Standard Static Condensation & analytical derivative	Forward Differences derivatives (no condensation)	Central Differences derivatives (no condensation)	
Cube	0.14	0.12	0.58	0.93	6
Car	8.89	8.85	58.49	86.71	4

Table 3.3 Comparison of CPU time between various methods (IBM3090-600E mainframe)

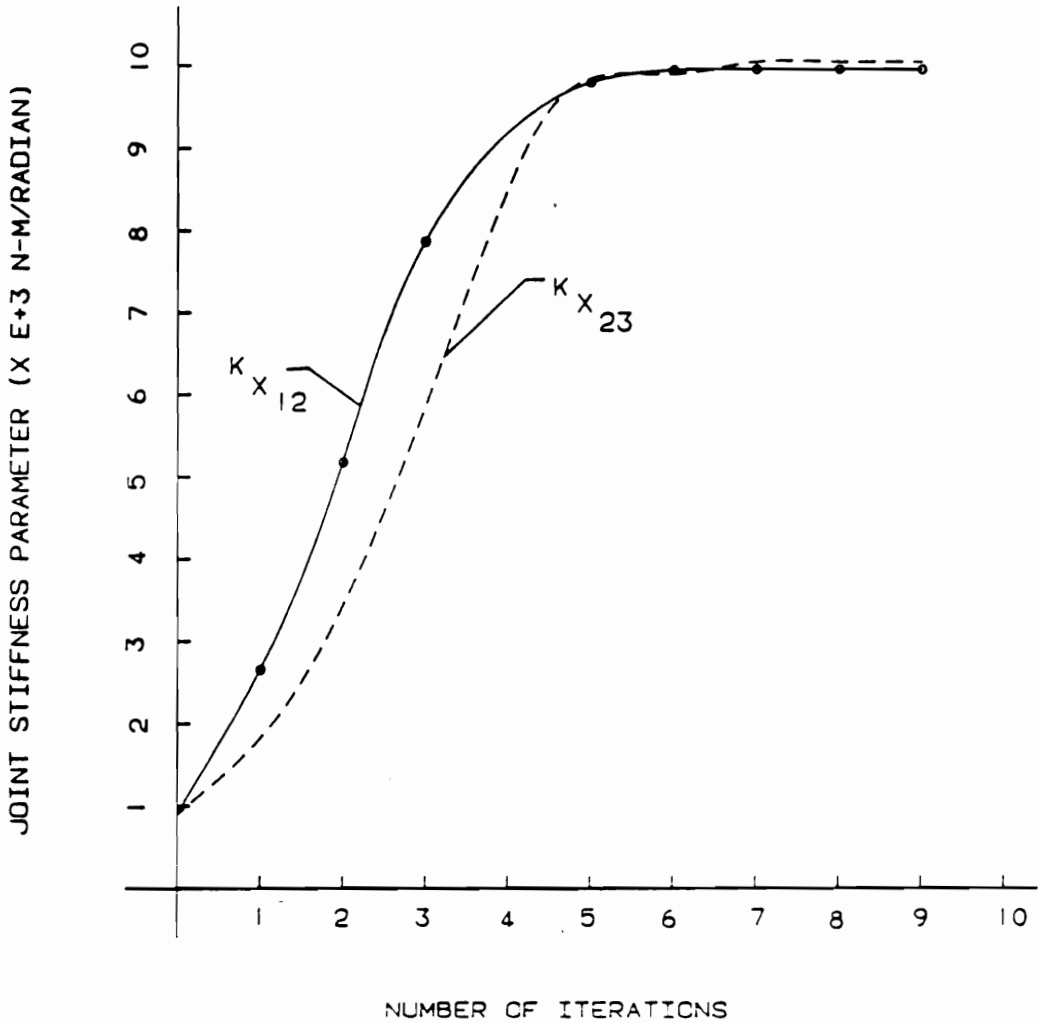

Figure 3.6 Identification of parameters $k_{x_{12}}$ and $k_{x_{23}}$ (cube model)

3.7.2 Illustrative Car Model

A 'stick' frame model of a car is analyzed with a flexible joint. The applied vertical loads of magnitude 1000 N and the boundary conditions are shown in Figure 3.7. Table 3.4 gives the property constants used for the car model. This model has 63 nodes and 115 elements with 384 degrees of freedom totally, including 12 degrees of freedom for the flexible joint. For the car model, the value of k which lies half way between the rigid and totally flexible joint is $1.0 \times 10^5 \ N-m/radian$. The sensitivity derivatives evaluated by various methods are given in Table 3.5. The CPU times required for estimating the joint parameters with various sensitivity methods are presented in Table 3.3. Figure 3.8 shows the estimated values of one joint parameter $k_{x_{12}}$ as a function of the number of iterations. The initial value of the unknown parameter $k_{x_{12}}$ used in the identification process is $1.0 \times 10^4 \ N-m/radian$. The value of other parameters, $1.0 \times 10^5 \ N-m/radian$ is assumed to be known. It is observed that $k_{x_{12}}$ converges after 4 iterations.

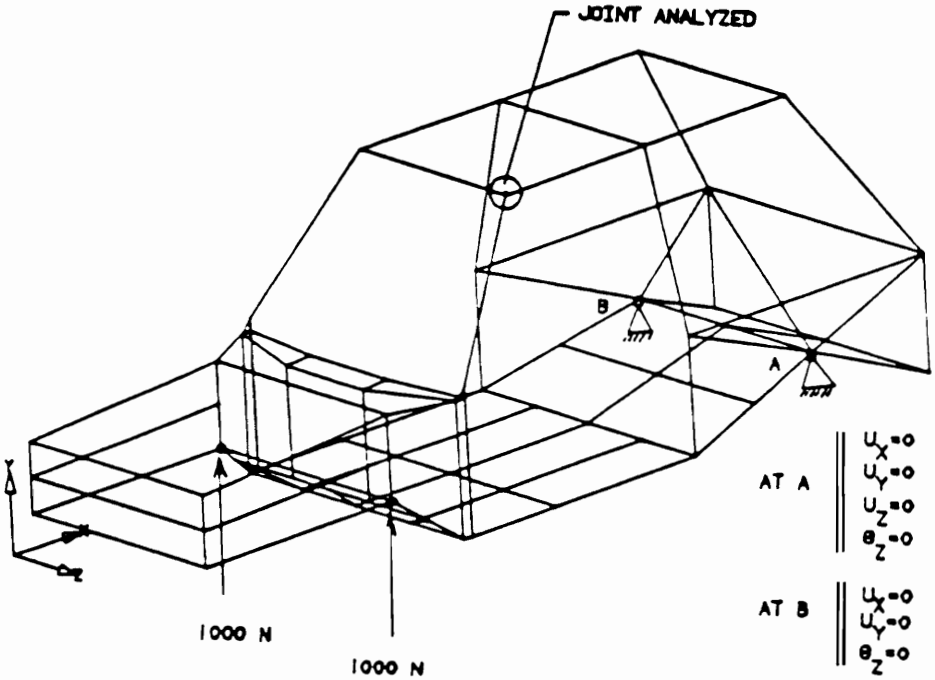

Figure 3.7 Space frame stick model of car

Property	Value
Young's Modulus, E	206.85 GPa
Shear Modulus, G	82.7 GPa
Torsional Constant, J	35.40E-08 m^4
Cross-sectional Area, A	2.99E-04 m^2
Moment of Inertia, I_{yy}	16.65E-08 m^4
Moment of Inertia, I_{zz}	77.42E-08 m^4

Table 3.4 Frame element properties for car model

Joint Degrees of Freedom	Sensitivity *		
	Direct Method	Central Differences	Forward Differences
u_x	-0.8084	-0.8083	-0.8082
u_y	3.2251	3.2251	3.2249
u_z	-1.5142	-1.5143	-1.5145
θ_{x1}	-0.3874	-0.3874	-0.3877
θ_{y1}	-1.0313	-1.0313	-1.0315
θ_{z1}	0.5575	0.5575	0.5575
θ_{x2}	-0.1976	-0.1975	-0.1978
θ_{y2}	1.1743	1.1743	1.1745
θ_{z2}	0.7509	0.7509	0.7508
θ_{x3}	-0.2715	-0.2715	-0.2714
θ_{y3}	-0.3723	-0.3722	-0.3725
θ_{z3}	-0.7733	-0.7732	-0.7729

* The sensitivity with respect to torsional spring constants for translational displacements is in 10^{-8} $radian/N$

* The sensitivity with respet to torsional spring constants for rotational displacements is in 10^{-11} $radian^2/N-m$

Table 3.5 Sensitivity derivatives at joint boundary (car model)

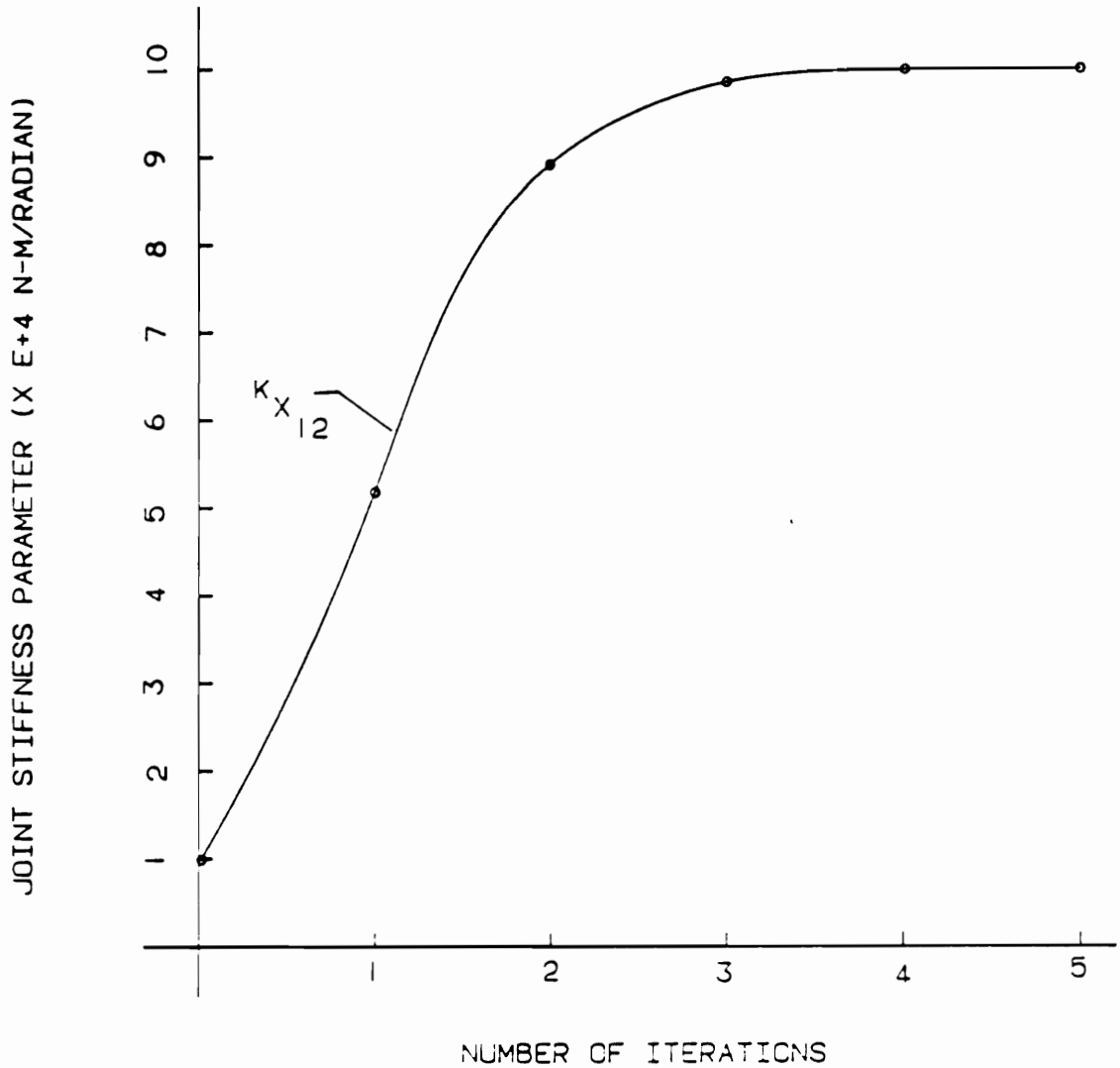

Figure 3.8 Identification of parameters $k_{x_{12}}$ (car model)

Chapter 4: Identification of Joint Models

4.1 Overview

The proposed models of flexible joints described in Chapter 2 are not complete unless the parameters describing the joint are identified. The parameters of the joint models can be quantified by tuning them so that theoretically predicted displacements agree as much as possible with measurements. The approach employs a weighted regression analysis (Allen [18]) applied to experimental measurements or results from very detailed finite element analysis to estimate joint parameters. The solution to the estimation problem consists of two iterative procedures for rapid convergence. In the first stages of the estimation procedure, the fixed point iteration method is used to obtain a first approximation to the joint parameters. Newton's method is employed to refine the approximation. The quality of the estimates are assessed by the length of the confidence intervals of each estimate.

4.2 Formulation of the Estimation Problem

In this section, the problem of determining the values of the stiffness parameters of the joint by bringing it into the form of a non-linear estimation model is formulated.

Consider a finite element model of the overall vehicle structure or a part of it. The matrix form of the equation describing the response of the structure under static loads is:

$$\mathbf{K}(\mathbf{k}_j)\ \mathbf{U} = \mathbf{F} \tag{19}$$

where, $\mathbf{K}$ is the stiffness matrix that is a function of the joint stiffness parameters, $\mathbf{U}$ is the displacement vector, and $\mathbf{F}$ is the force vector.

Consider a small subset of stiffness parameters, $\mathbf{k}_j$, and a set of measured displacements, $\mathbf{U}_m$, that is expected to be sensitive only to the above parameters. Furthermore, let $\mathbf{E}_m$ denote the error between analytical predictions and measured displacements. The following equation relates the measurements with the stiffness parameters.

$$\mathbf{U}_m = \mathbf{K}(\mathbf{k}_j)^{-1}\ \mathbf{F} + \mathbf{E}_m \tag{20}$$

Observing that the inverse stiffness matrix is a known function of the stiffness parameters, equation (20) can be recast into the form

$$\mathbf{U}_m = \mathbf{U}_A(\mathbf{k}_J) + \mathbf{E}_m \tag{21}$$

where, $\mathbf{U}_A(\mathbf{k}_J) = \mathbf{K}(\mathbf{k}_J)^{-1}\,\mathbf{F}$ is a vector of known functions of the parameters in $\mathbf{k}_J$ that are in general non-linear.

Equation (21) represents a non-linear estimation model [14,34,35]. The objective when solving a problem of the form of equation (21) is to estimate the vector of parameters $\mathbf{k}_J$ from the observation vector $\mathbf{U}_m$ and the statistics of the vector of measurement errors $\mathbf{E}_m$. The latter is assumed to be a Gaussian random vector with zero mean, so that its covariance matrix, $\mathbf{V}_e$, called quality matrix, is sufficient to describe its statistics.

The discrepancy between experimental and analytically predicted displacements comes from,

(a) random errors in measuring deflections, and

(b) systematic errors resulting from approximations and idealizations on which the finite element model is based.

The effect of random measurement error can be averaged out by taking a large number of displacement measurements. Unfortunately, the same cannot be done with the systematic modeling error. Therefore, this systematic error is neglected when estimating the model parameters. This simplification induces bias in the estimates. The effect of this simplification is investigated in Chapter 5.

Measured displacements are sub-divided into two classes:

(i) Measurements at the joint boundary degrees of freedom.

(ii) Measurements at degrees of freedom away from the joint boundary.

The method proposed takes into account both types of measurements. However, the method requires measurement of all displacements at the joint boundaries for all loading cases in order to estimate the parameters of interest.

For the case that only measurements at the degrees of freedom at the joint boundary are used in estimation, the global stiffness matrix is condensed to the reduced stiffness matrix with those degrees of freedom at the boundary. For the case that the measurements away from the joint boundary are also considered, the corresponding degrees of freedom are not condensed and the super-structure consists of the remaining structure apart from the joint as well as the degrees of freedom at which displacements are measured. The 'black-box' method [36] is used effectively in both cases to derive the condensed stiffness matrix. If n is the number of joint degrees of freedom and m is the number of additional measurements away from the joint, then the condensed flexibility matrix will be of the order $(m + n) \times (m + n)$. This is used in equation (21).

The model represented by equation (21) is solved by the procedure described in the following section in order to estimate the model parameters.

4.3 Solution to the Estimation Problem

The most popular solution methods of the estimation model is to find the values of the parameters by minimizing a norm of the vector of residuals. The norm used in this dissertation is the inner product of the vector of residuals weighted by the inverse of the quality matrix. This leads to the weighted least square estimation [14]. The estimation problem reduces to the minimization of a non-linear function of the stiffness parameters.

This problem is solved by two iterative procedures for fast convergence. The system identification process is shown in Figure 4.1. The solution is started with a fixed point iteration and concluded with Newton's method. In the following sections, the two iterative procedures are described.

4.3.1 Fixed Point Iterative Scheme

The flexible joint model is formed by adding the joint stiffness matrix, $\mathbf{K}_J$, to the reduced (statically condensed) stiffness matrix, $\mathbf{K}_R$ (equation 11), of the super-element.

$$[\mathbf{K}_R + \mathbf{K}_J]\,\mathbf{U}_A = \mathbf{F}_R \tag{22}$$

Introducing the error in measured displacements,

$$\mathbf{U}_A = \mathbf{U}_m - \mathbf{E}_m \tag{23}$$

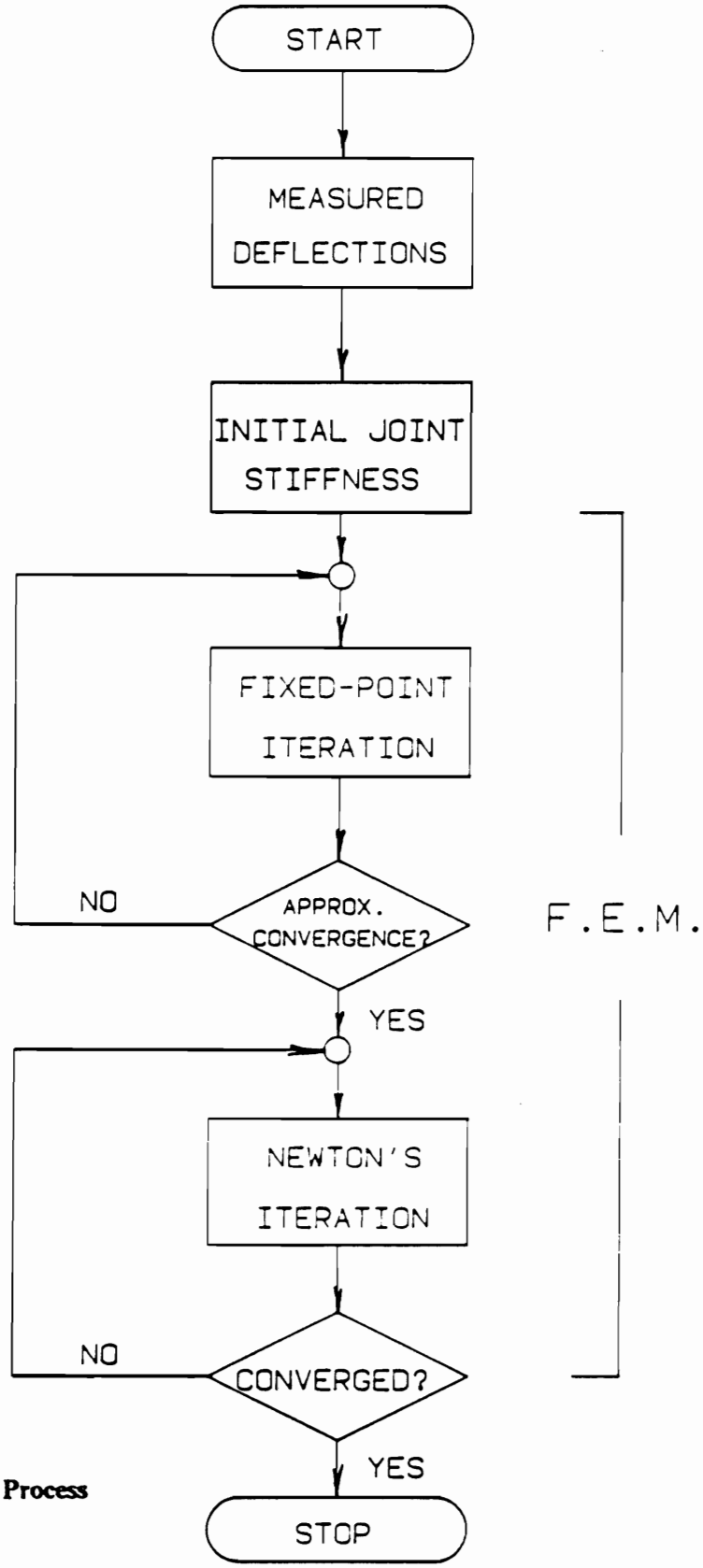

Figure 4.1 System Identification Process

Substituting back into equation (22) yields

$$\mathbf{K}_J \mathbf{U}_m = \mathbf{F}_R - \mathbf{K}_R \mathbf{U}_m + [\mathbf{K}_R + \mathbf{K}_J] \mathbf{E}_m \tag{24}$$

Equation (24) can be written as

$$\mathbf{X}_m \mathbf{k}_J = \mathbf{F}_R - \mathbf{F}_m + \mathbf{K}_{overall} \mathbf{E}_m \tag{25}$$

where,

$$\mathbf{F}_m = \mathbf{K}_R \mathbf{U}_m \quad and \quad \mathbf{K}_{overall} = \mathbf{K}_R + \mathbf{K}_J \tag{25a}$$

Due to the form of matrix $\mathbf{X}_m$, all rotations at the joint boundaries for all loading cases must be measured in order to estimate the joint parameters.

Fixed-point iteration is a solution procedure that is based on successive substitutions. If an initial approximation x_1 to a root α of the system $x = F(x)$ is provided, a sequence $x_2, x_3, \ldots$ may be defined by the recursive relation $x_{j+1} = F(x_j)$ with the hope that the sequence will converge to α.

Equation (25) is of the form

$$\mathbf{Y} = \mathbf{X}\mathbf{b} + \mathbf{E} \tag{26}$$

where,

$$\mathbf{Y} = \mathbf{F}_R - \mathbf{F}_m \tag{27a}$$

$$\mathbf{X} = \mathbf{X}_m \tag{27b}$$

$$\mathbf{b} = \mathbf{k}_J \tag{27c}$$

$$\text{and} \quad \mathbf{E} = \mathbf{K}_{overall}\, \mathbf{E}_m \tag{27d}$$

Start with an initial guess of the joint parameters and use it to calculate the matrix $\mathbf{K}_J$ on the right hand side of equation (24). Then, update the vector of joint parameters, $\mathbf{k}_J$, by obtaining a weighted residual regression solution for equation (26) given below.

$$\mathbf{b} = \left[\mathbf{X}^T\, \mathbf{V}_e^{-1}\, \mathbf{X}\right]^{-1} \mathbf{X}^T\, \mathbf{V}_e^{-1}\, \mathbf{Y} \tag{28}$$

The quality matrix $\mathbf{V}_e$ is given as

$$\mathbf{V}_e = \mathbf{K}_{overall}\, \mathbf{V}_m\, \mathbf{K}_{overall}^T \tag{29}$$

where $\mathbf{V}_m$ is a covariance matrix of measurement errors. It was observed that the solution from fixed point iteration approaches the neighborhood of the solution but it does not converge to it. Therefore, apply Newton's iteration after the solution from fixed point iteration starts to oscillate.

4.3.2 Newton's Iterative Scheme

The sequential linearization method, also known as Newton's method, uses the results of linear estimation in a succession of stages [37].

Equation (22) can be rewritten as

$$\mathbf{U}_A = [\mathbf{K}_R + \mathbf{K}_J]^{-1} \mathbf{F}_R \tag{30}$$

The equation relating measurements with the joint stiffness parameters is

$$\mathbf{U}_m = [\mathbf{K}_R + \mathbf{K}_J]^{-1} \mathbf{F}_R + \mathbf{E}_m \tag{31}$$

This equation is linearized about the nominal values of the stiffness parameters. The resulting linearized equation is,

$$\mathbf{U}_m = [\mathbf{K}_R + \mathbf{K}_J]^{-1} \mathbf{F}_R + \left[\frac{\partial \mathbf{U}}{\partial \mathbf{k}_J} \right]_{nominal} \Delta\mathbf{k} + \mathbf{E}_m \tag{32}$$

Newton's iteration uses equation (32) which is in the form of equation (26). Equation (28) is used to estimate the solution and confidence intervals.

4.4 Interpretation of Estimates (confidence intervals)

It is important to assess the quality of the estimates of the joint stiffness parameters. This usually is done by constructing confidence intervals for the estimated values of these parameters.

A confidence interval is an interval of length equal to twice the standard deviation of the parameter which is centered around estimated value of the parameter of interest. A number of such intervals corresponding to various probability levels could be estimated. The smaller the length of the confidence interval, the higher the quality of the stiffness estimates. The confidence interval indicates the effect of measurement error on the estimates. Therefore, it cane be used to decide whether enough loading cases have been considered so that the effect of this error can be averaged out.

Chapter 5: Examples

5.1 Overview

The proposed models for flexible joints are not complete unless the parameters describing the joint are identified. The proposed method is demonstrated by applying it to a cube frame structure and a car body. Both the simple and complex flexible joint models are estimated using computer simulated experimental measurements.

5.2 Simulation of Measurements

An actual joint is not simply a set of beams whose ends coincide. It is a geometrically complex assembly of overlapping metal sheets joined together. For each branch measure the rotations of a number of nodes in the vicinity of the branch end. Then, consider their average as measured rotations of the node at the branch end in the joint model.

For example, consider one branch of a joint as shown in Figure 5.1. Then, the rotation vector u of the corresponding branch in the model is,

$$u = \sum_{i=1}^{n} u_i/n \tag{33}$$

which is the average of all the rotation vectors. The statistics of the error at a point can be estimated by considering the experimental results in the neighborhood of the point of interest. These rotations can be analyzed to infer the statistics of the error in these rotations.

The rotations of a joint branch are superpositions of rotations due to movement of the joint as a rigid body and due to relative motions between the joint members. Only the relative motions are useful in estimating the joint parameters. Unfortunately, the former are considerably larger than the latter. Therefore, it is difficult to extract the relative rotations of the joint branches from their measured rotations. This results in a very high sensitivity of the estimated joint parameters to the error in measurements.

This undesirable effect of measurement errors can be significantly reduced as follows: The displacement of a reference point in the vicinity of a joint is to be measured first. Then, measure the relative displacements of all other points on the joint branches with respect to this reference point. Finally, the displacement of each point is derived by adding the relative displacements to the

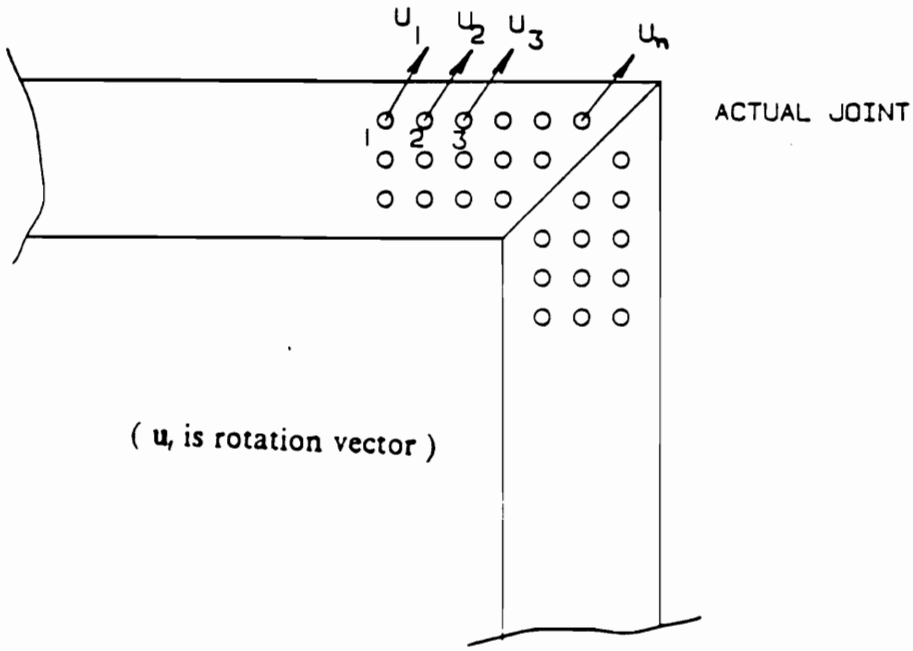

Figure 5.1 Method of simulation for 1-branch joint

displacement of the reference point. In that case, the relative branch rotations which are entries of matrix $\mathbf{X}_m$ are not contaminated with rigid body displacements. Therefore, the parameters estimated are significantly more accurate.

The error in the displacements consists of three parts.

(a) Error due to model simplification

(b) Error due to measurement error and

(c) Error due to the representation of all displacements by one equal to their average.

Only the error in (b) can be averaged out by taking many loading cases. The standard deviation of the measurement error used in V_m matrix is only for parts (b) and (c). The procedure of measuring displacements is simulated by using random noise to represent the measurement error. These values are then used in the statistical system identification procedure. Because errors (a) and (c) are not simulated, the results below may be expected to be better than those obtained in actual experiments.

Figure 5.2 depicts the procedure for simulating measurements. The finite element analysis yields the exact values of displacements. These are contaminated by random noise to give us the simulated measured displacements. With initially guessed values for joint stiffnesses, obtain the corresponding displacements which are compared with simulated measured displacements and the estimation

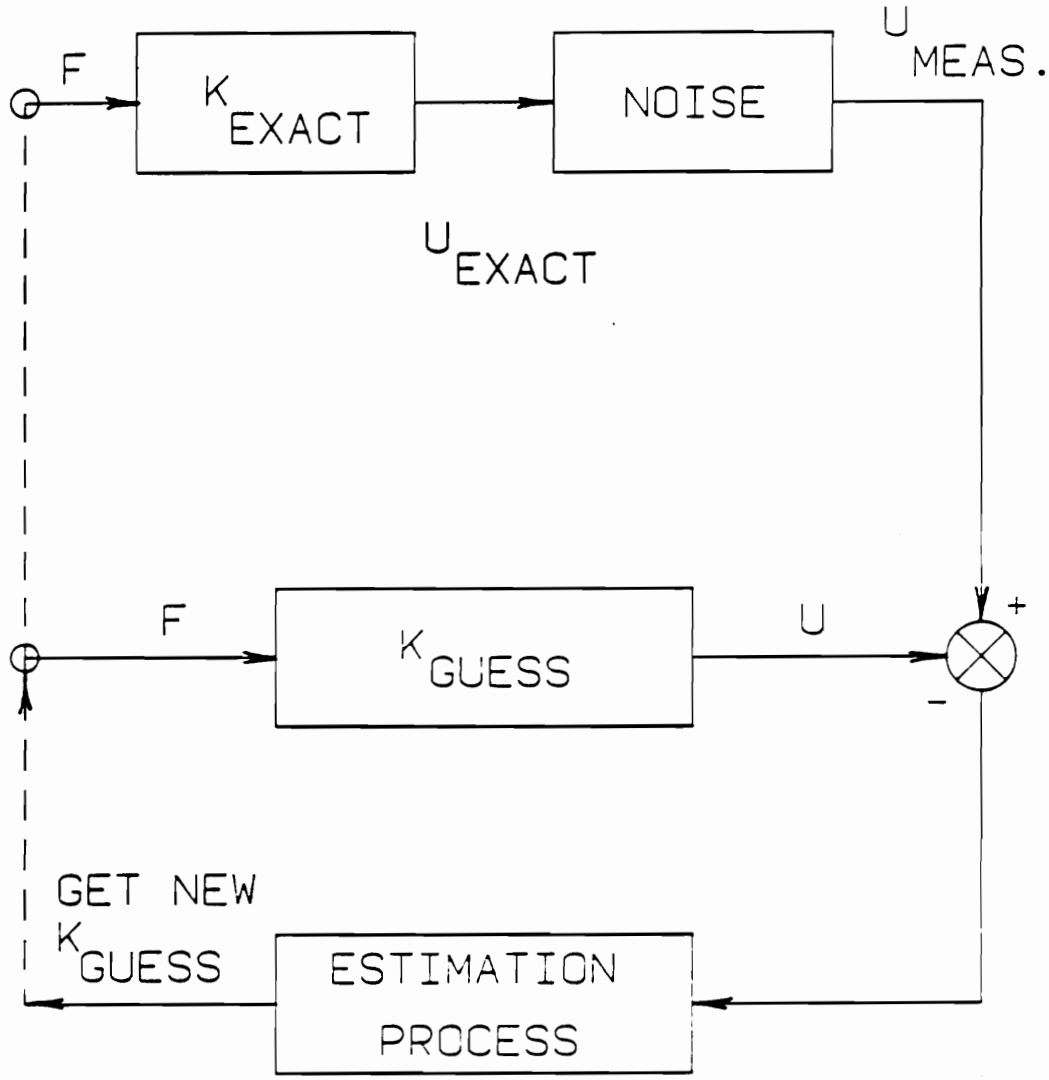

Figure 5.2 Estimation process

process is carried out. The new values of joint parameters obtained are substituted for the previously used values and the process is repeated for convergence.

5.3 Identification of Simple Model

In this section the approach is illustrated for the simple joint model with a cube frame and a car body examples. The form of $\mathbf{X}_m$ (equation (26)) is shown in Table 5.1.

5.3.1 Illustrative Cube Frame Example

A cube frame with a flexible joint at node 7 is used as the first example. This structure is shown in Figure 2.5 Node 1 is fixed and node 7 is the joint under consideration. Geometry and material property data are given in Table 2.1. The frame is analyzed using space frame elements having 6 degrees of freedom per node. In the example, the spring stiffnesses $\mathbf{k}_{ij}$ are all taken to be equal to a single number k .

The value of spring stiffness parameters $\mathbf{k}_j$ which is 1.0×10^4 $N - m/radian$, is chosen in a way that the corresponding potential energy (work done by external loads) lies way half between the value for a rigid joint and an infinitely flexible joint. A loading case is defined by a set of loads applied to the structure at the same time while measurements stand for the displacements that are used in the estimation process to identify the stiffness parameters.

$\theta_{X1}-\theta_{X2}$	0	0	0	0	0	$\theta_{X1}-\theta_{X3}$	0	0	$K_{X_{12}}$
0	$\theta_{Y1}-\theta_{Y2}$	0	0	0	0	0	$\theta_{Y1}-\theta_{Y3}$	0	$K_{Y_{12}}$
0	0	$\theta_{Z1}-\theta_{Z2}$	0	0	0	0	0	$\theta_{Z1}-\theta_{Z3}$	$K_{Z_{12}}$
$\theta_{X2}-\theta_{X1}$	0	0	$\theta_{X2}-\theta_{X3}$	0	0	0	0	0	$K_{X_{23}}$
0	$\theta_{Y2}-\theta_{Y1}$	0	0	$\theta_{Y2}-\theta_{Y3}$	0	0	0	0	$K_{Y_{23}}$
0	0	$\theta_{Z2}-\theta_{Z1}$	0	0	$\theta_{Z2}-\theta_{Z3}$	0	0	0	$K_{Z_{23}}$
0	0	0	$\theta_{X3}-\theta_{X2}$	0	0	$\theta_{X3}-\theta_{X1}$	0	0	$K_{X_{31}}$
0	0	0	0	$\theta_{Y3}-\theta_{Y2}$	0	0	$\theta_{Y3}-\theta_{Y1}$	0	$K_{Y_{31}}$
0	0	0	0	0	$\theta_{Z3}-\theta_{Z2}$	0	0	$\theta_{Z3}-\theta_{Z1}$	$K_{Z_{31}}$

Table 5.1 Form of X_m matrix (simple model)

Figure 5.3 demonstrates that the use of fixed point iteration is beneficial as compared to using only Newton's method in the identification process. The standard deviation of the error is 5% of the actual rotation. When fixed point iteration was used along with Newton's method, convergence was achieved in only 4 iterations. However, if only Newton's method is used, 9 iterations are required for convergence.

Figure 5.4 shows the weighted sum of residuals (r.m.s. error) as a function of the number of iterations for the cube model for two cases. For the first case, only displacements at the joint boundary were used in estimation. For the second case, additional displacements of nodes away from the joint boundary were considered. It is seen that when more measurements are taken, the estimates get better and the r.m.s. residual error reduces. It is better therefore to include measurements away from the joint in the estimation. Table 5.2 shows the estimated values, length of confidence intervals (also expressed as a percentage of the estimated value) for both cases for 5 loading cases. Figure 5.5 shows the estimated value with confidence intervals of parameter $k_{x_{12}}$ as a function of the number of iterations for 15 loading cases with measurements also away from the joint. It is observed that the estimates converge after 4 iterations and that the confidence interval narrows with the number of iterations to yield better estimates. Convergence rate does not change when using additional displacement measurements for nodes away from the joint in estimation.

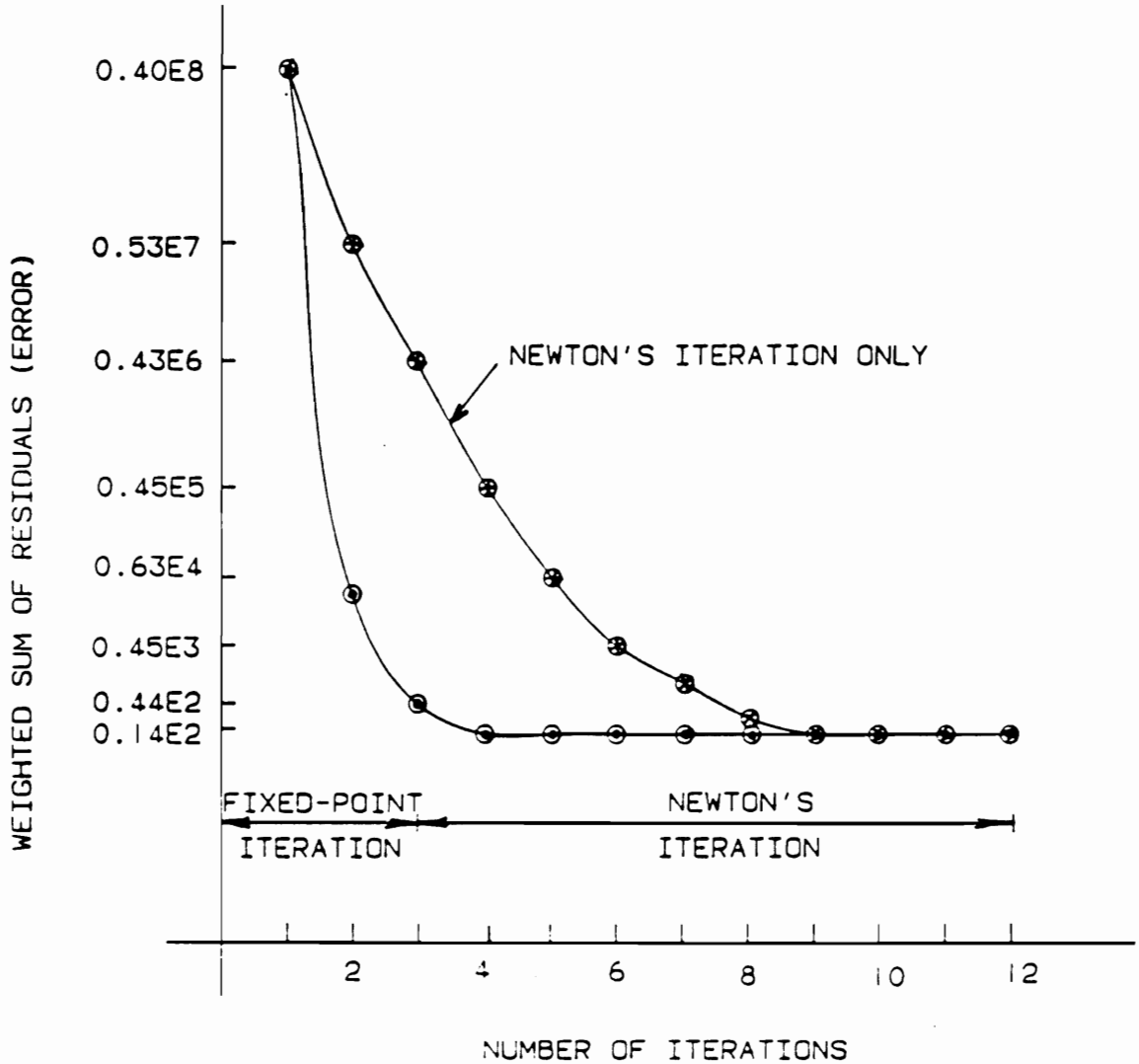

Figure 5.3 Faster convergence of proposed method (cube example; simple joint model)

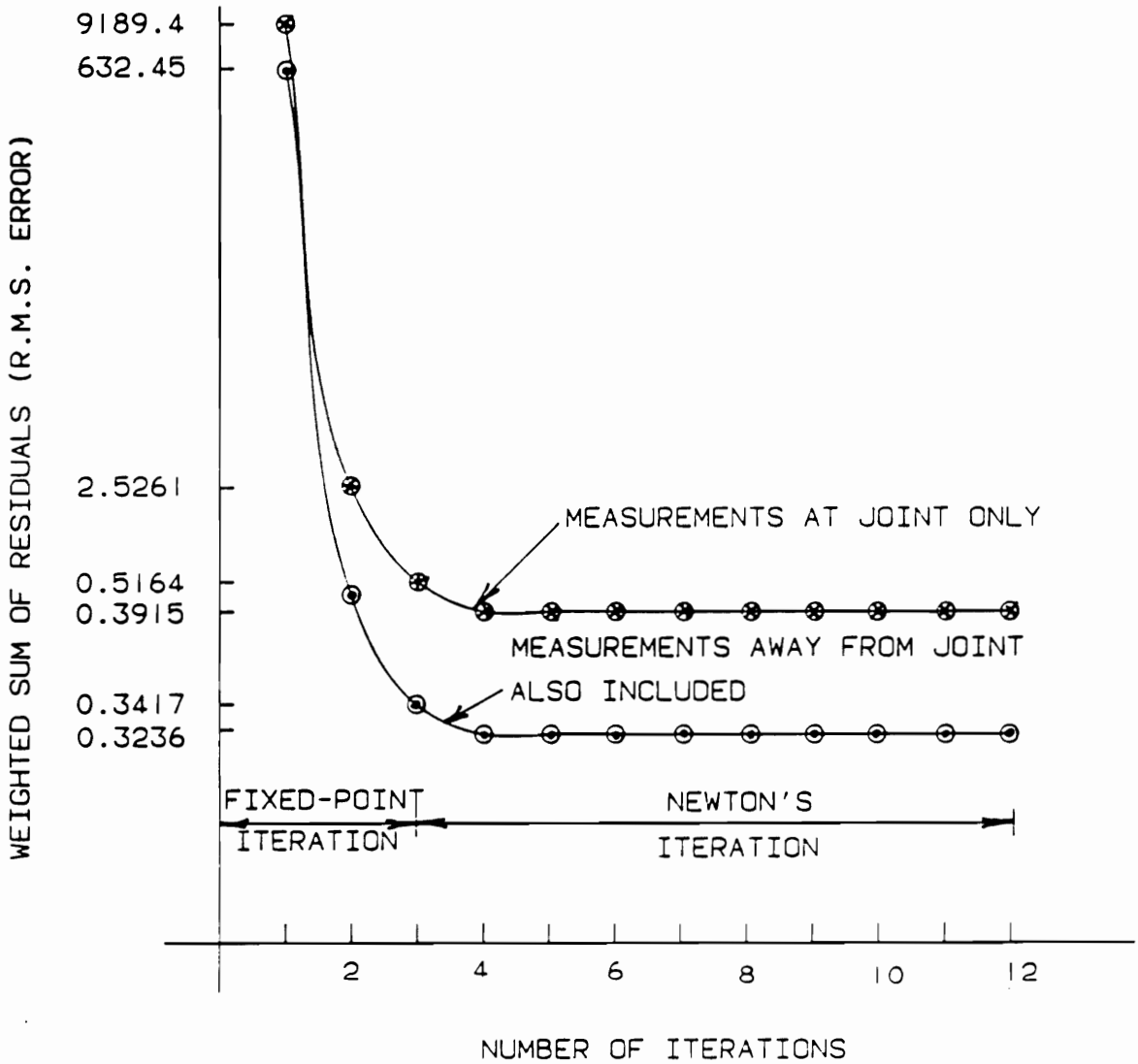

Figure 5.4 Estimation results (cube example; simple joint model)

Joint Stiffness	Measurements at Joint only			Measurements also away from Joint		
Parameter	Value	Interval	Percentage	Value	Interval	Percentage
$k_{x_{12}}$	1.1254	0.0776	6.89	1.0738	0.0691	6.44
$k_{y_{12}}$	0.9826	0.0784	7.98	1.0849	0.0745	6.86
$k_{z_{12}}$	0.9875	0.0597	6.05	1.0574	0.0442	4.18
$k_{x_{23}}$	0.9954	0.0322	3.23	1.1253	0.0406	3.61
$k_{y_{23}}$	1.0257	0.0495	4.82	1.0665	0.0329	3.08
$k_{z_{23}}$	1.2656	0.0954	8.09	0.9515	0.0625	6.57
$k_{x_{31}}$	1.1795	0.0455	3.58	0.9622	0.0299	3.11
$k_{y_{31}}$	0.9863	0.0417	4.23	1.0527	0.0392	3.72
$k_{z_{31}}$	1.1529	0.0826	7.16	0.9531	0.0681	7.15

The value and interval of parameter are represented in 10^4 $N-m/radian$

Table 5.2 Estimation results (cube example; simple joint model)

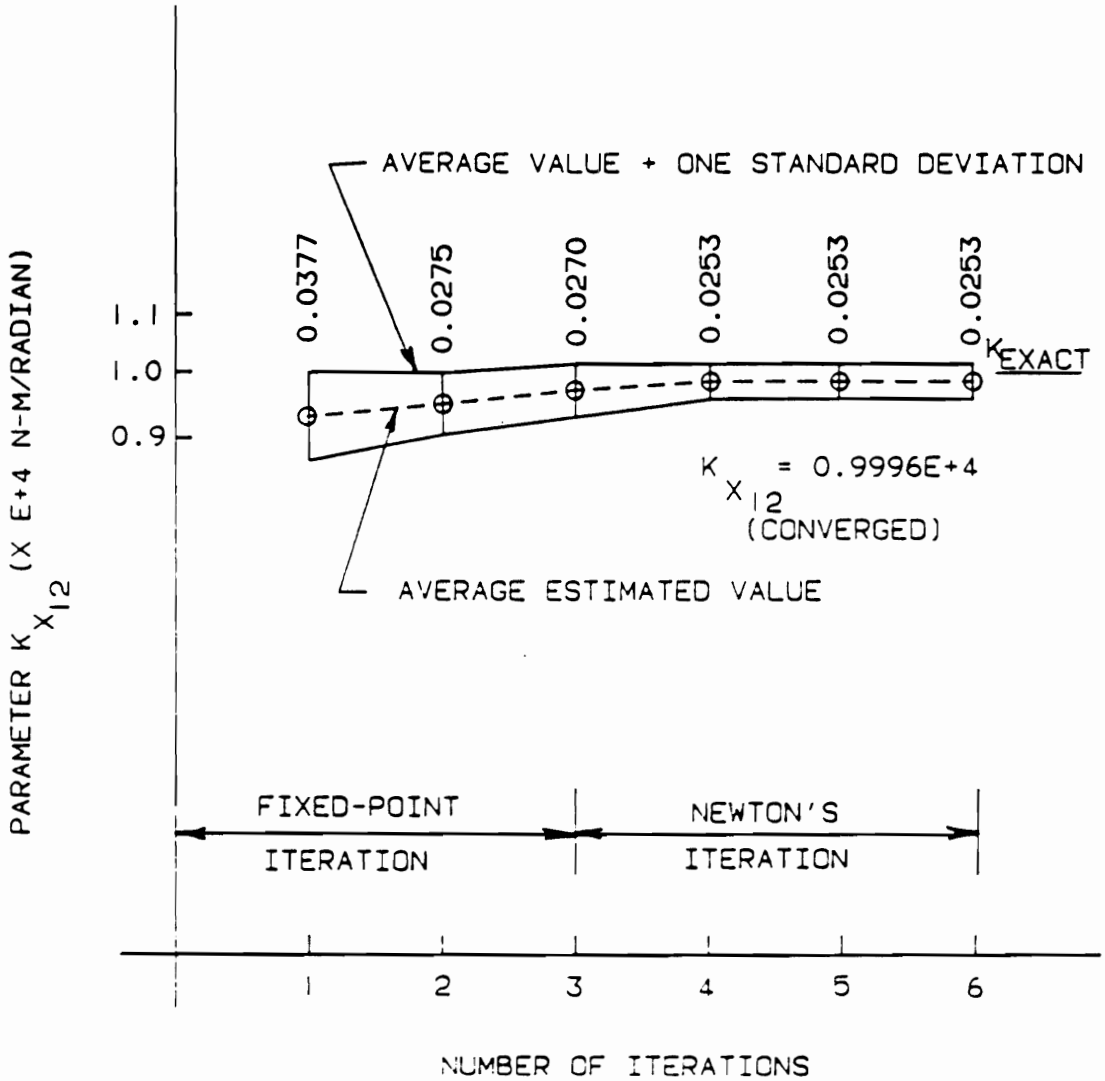

Figure 5.5 Confidence interval for $k_{x_{12}}$ (cube example; simple joint model)

Various standard deviations of the measurement error were considered in measuring deflections. It was observed that for lower error, the estimates were better than those for larger error. Table 5.3 shows the comparison of sum of squares of residuals in estimation for various levels of measurement errors for the cube frame example. The sum of square errors (SOS) increases almost proportionally with the square of the measurement error.

The stiffness parameters of the joint model can also be estimated by using a number of measurements equal to the number of parameters and by solving the system of equations relating the displacements to the parameters. Table 5.4 compares this approach to probabilistic system identification. In this table, confidence intervals are provided for the estimates obtained probabilistically for 20 loading cases. Probabilistic identification gives a better estimate of the parameters since more loading cases are considered in the estimation and an overall good fit is obtained.

The number of loading cases was gradually increased to observe the effect of such an increase in the estimation. 5, 8, 10, 15, and 20 loading cases were tried for the cube example and it was observed that as the number of loading cases increased, the confidence interval decreased to prove that the quality of estimates gets better with the number of loading cases. Tables 5.5 and Table 5.6 give the estimated parameters and confidence intervals for various loading cases. It is observed that 10 loading cases are sufficient to give reasonable estimates with a confidence interval of 5% of the estimated value.

Error Value (percent)	Sum of Squares of Residuals (mm^2)
2	0.8312E-3
5	0.5210E-2
10	0.2086E-1

$$\text{Sum of squares of residuals} = |\mathbf{U}_m - \mathbf{U}_{predicted}|^2$$

Table 5.3 Effect of error variation (cube example; simple joint model)

Joint Parameter	Deterministic Approach Value	Probabilistic Approach Value	Probabilistic Approach Error (percent)
$k_{x_{12}}$	1.2562	1.0097	1.33
$k_{y_{12}}$	0.9663	1.0112	1.18
$k_{z_{12}}$	0.9775	1.0147	0.94
$k_{x_{23}}$	0.9726	0.9982	2.45
$k_{y_{23}}$	1.3021	1.0076	1.96
$k_{z_{23}}$	1.1297	0.9978	1.23
$k_{x_{31}}$	0.9514	0.9937	2.05
$k_{y_{31}}$	0.9370	0.9945	0.83
$k_{z_{31}}$	0.9662	1.0184	1.56

The value of parameter is represented in 10^4 $N - m/radian$

Table 5.4 Probabilistic Vs. deterministic approach (cube example; simple joint model)

Joint Stiffness Parameter	Stiffness Parameter × 10^4 $N-m/radian$ (various loading cases)				
	5 Cases	8 Cases	10 Cases	15 Cases	20 Cases
$k_{x_{12}}$	1.0738	1.0556	1.0391	0.9996	1.0097
$k_{y_{12}}$	1.0849	1.0626	1.0356	1.0257	1.0112
$k_{z_{12}}$	1.0574	1.0414	1.0227	1.0199	1.0147
$k_{x_{23}}$	1.1253	1.1021	1.0933	1.0124	0.9982
$k_{y_{23}}$	1.0665	1.0227	0.9986	0.9995	1.0076
$k_{z_{23}}$	0.9515	0.9685	0.9765	0.9826	0.9978
$k_{x_{31}}$	0.9622	0.9756	0.9819	0.9912	0.9937
$k_{y_{31}}$	1.0527	1.0423	1.0267	1.0091	0.9945
$k_{z_{31}}$	0.9531	1.0382	1.0294	1.0216	1.0184

Table 5.5 Effect of loading cases on parameters (cube example; simple joint model)

Joint Stiffness Parameter	Confidence Interval × 10^4 $N-m/radian$ (various loading cases)				
	5 Cases	8 Cases	10 Cases	15 Cases	20 Cases
$k_{x_{12}}$	0.0691	0.0479	0.0326	0.0253	0.0134
$k_{y_{12}}$	0.0745	0.0513	0.0395	0.0235	0.0119
$k_{z_{12}}$	0.0442	0.0325	0.0251	0.0178	0.0095
$k_{x_{23}}$	0.0856	0.0592	0.0429	0.0347	0.0245
$k_{y_{23}}$	0.0329	0.0214	0.0205	0.0201	0.0197
$k_{z_{23}}$	0.0625	0.0528	0.0402	0.0256	0.0122
$k_{x_{31}}$	0.0299	0.0343	0.0297	0.0243	0.0204
$k_{y_{31}}$	0.0392	0.0256	0.0207	0.0139	0.0083
$k_{z_{31}}$	0.0681	0.0477	0.0363	0.0273	0.0159

Table 5.6 Effect of loading cases on confidence intervals (cube example; simple joint model)

Errors resulting from approximations and idealizations on which the finite element model is based, constitute for the systematic bias in the stiffness of the structure and the joint. In this study, this systematic bias is introduced in the estimation process by increasing or decreasing the applied forces.

Figure 5.6 shows the biased estimation process with bias in the measurements. Figure 5.7 shows the parameter $k_{z_{31}}$ as a function of the number of loading cases with confidence intervals for both the biased and unbiased cases. It is observed that 10 loading cases are enough to get reasonable estimates with confidence interval of about 5 percent of the estimates. Bias in resulting estimates does not converge to zero as the number of loading cases tends to infinity.

5.3.2 Illustrative Car Model Example

A car body with one flexible joint is analyzed. The car is represented by a finite element model consisting of frame elements with 6 degrees of freedom per node. The model and the boundary conditions is shown in Figure 2.7. Table 2.4 gives the property constants used for the car model. This model has 63 nodes and 115 elements with 384 degrees of freedom including 12 degrees of freedom for the flexible joint. For the car model, the value of $\mathbf{k}_j$ which lies approximately half way between the rigid and totally flexible joint is $1.15 \times 10^5 \ N - m/radian$.

Figure 5.8 demonstrates that the use of fixed point iteration is beneficial as compared to using only Newton's method in the identification process. The

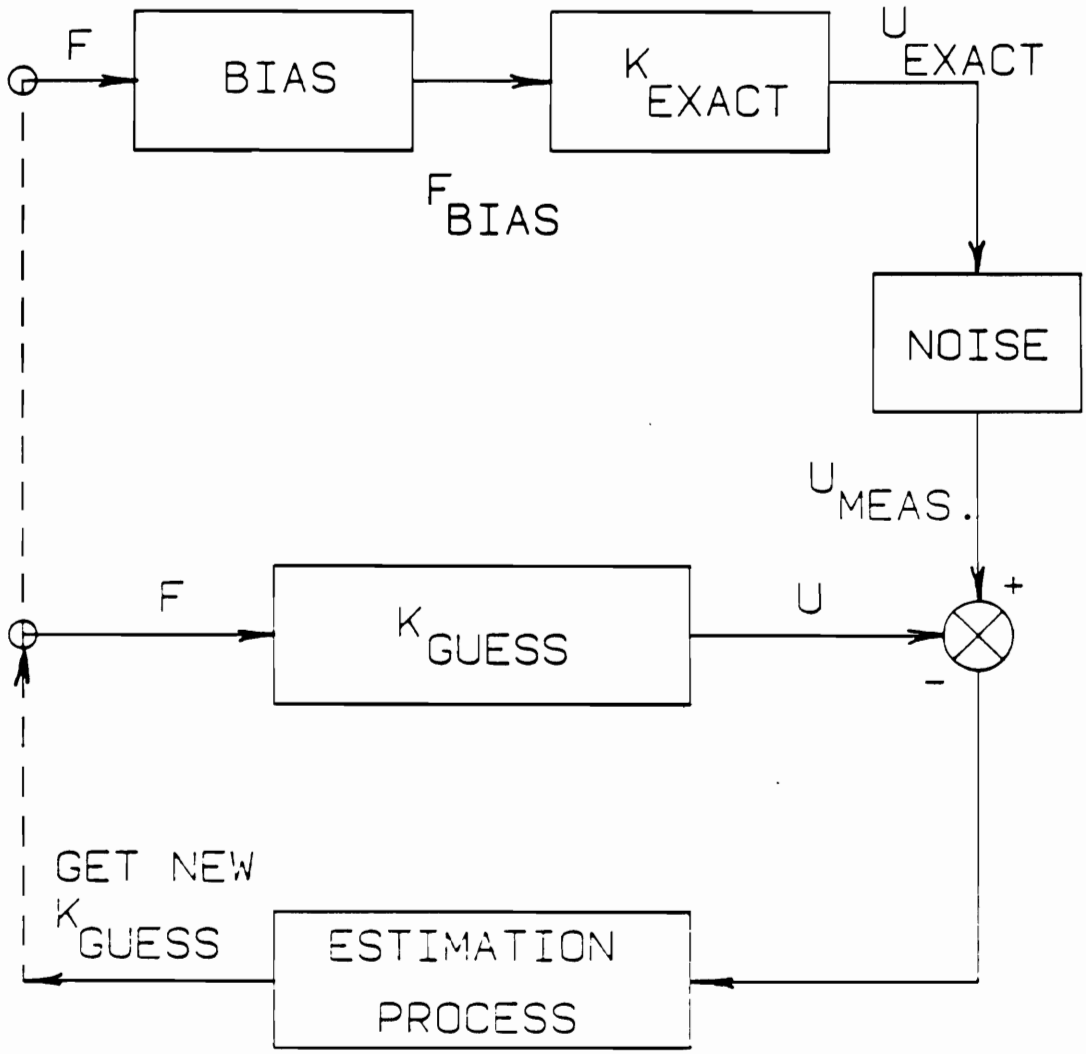

Figure 5.6 Biased estimation process

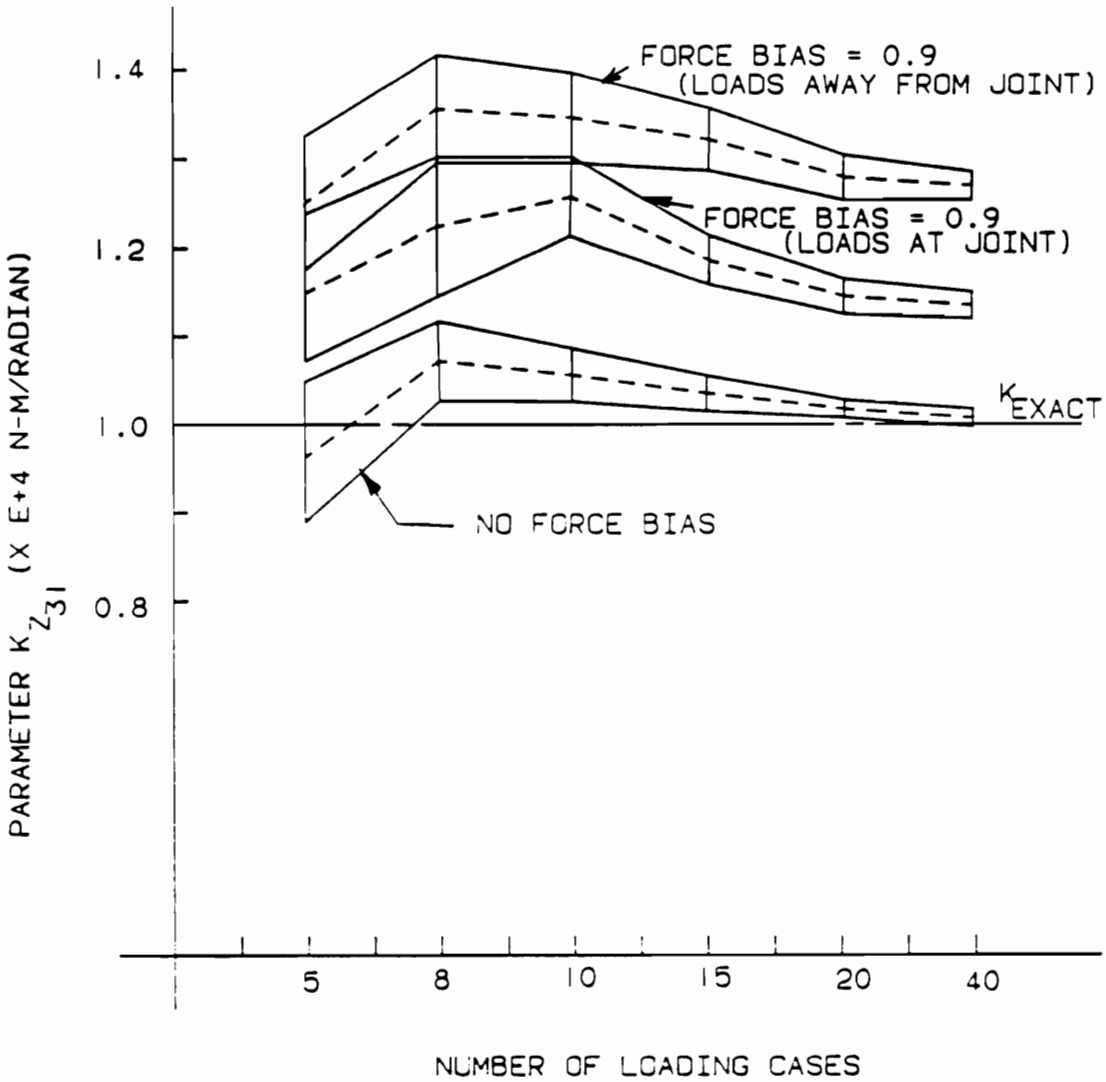

Figure 5.7 Biased and unbiased estimation results (cube example; simple joint model)

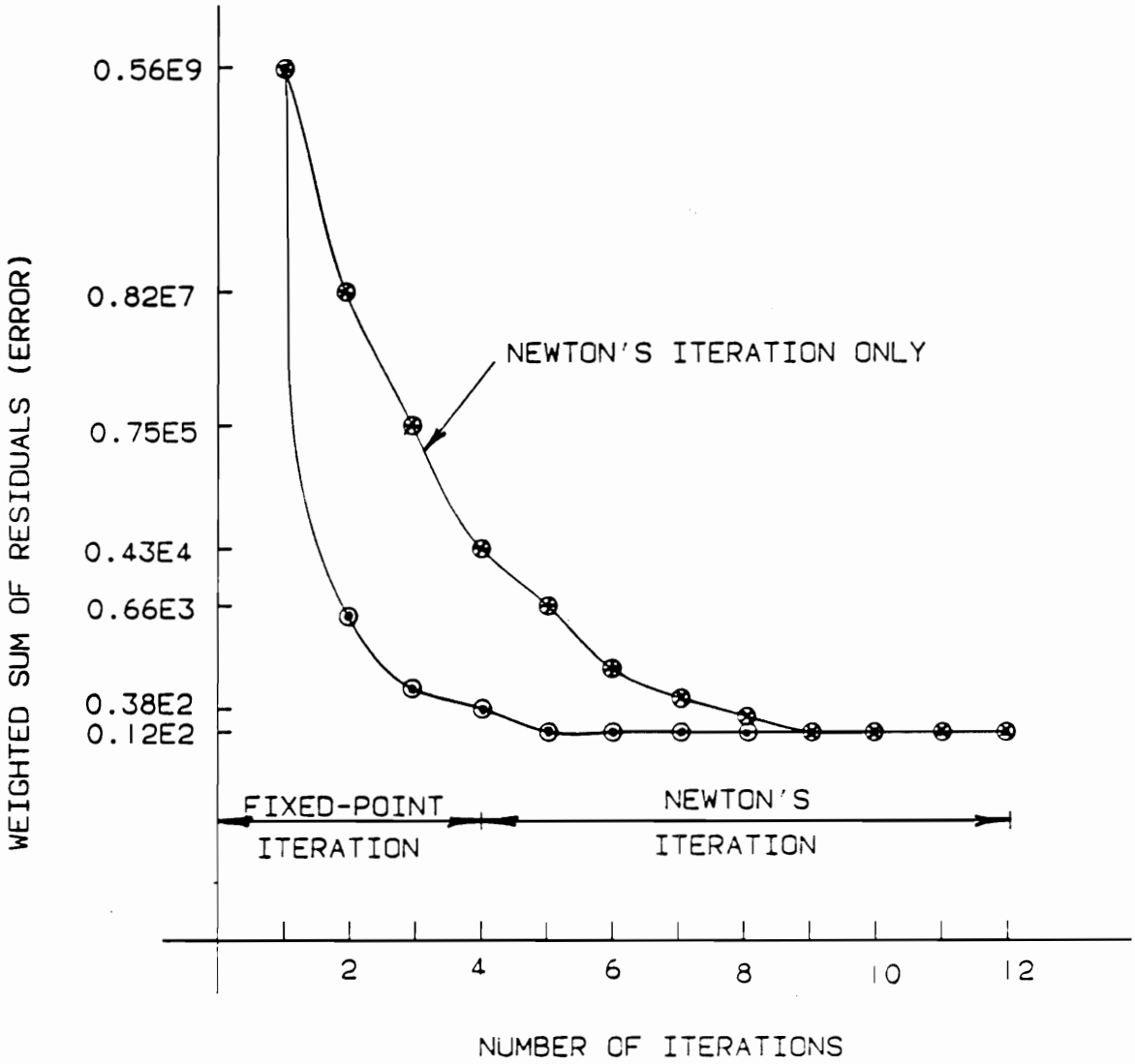

Figure 5.8 Faster convergence of proposed method (car example; simple joint model)

standard deviation of the error is 5% of the actual rotation. When fixed point iteration was used along with Newton's method, only 5 iterations were necessary for convergence. However, if only Newton's method is used, 9 iterations are required for convergence.

Figure 5.9 shows the weighted sum of residuals (r.m.s. error) as a function of the number of iterations for the cube model when only the joint degrees of freedom are considered as the boundary degrees of freedom and when degrees of freedom other than the joint degrees of freedom are considered as the boundary degrees of freedom. It is seen that when more measurements are taken, the estimates get better and the r.m.s. residual error reduces. It is better therefore to include measurements away from the joint in the estimation. Table 5.7 shows the estimated values, length of confidence intervals (also expressed as a percentage of the estimated value) for both cases for 5 loading cases. Figure 5.10 shows the estimated value with confidence intervals of parameter $k_{x_{23}}$ as a function of the number of iterations for 15 loading cases when using displacement measurements for nodes away from joint. It is observed that the estimates converge after 5 iterations and that the confidence interval narrows with the number of iterations to yield better estimates. Convergence rate does not change when using additional displacement measurements for nodes away from the joint in estimation.

Table 5.8 shows the comparison of sum of squares of residuals in estimation for various levels of measurement errors for the car frame example. The sum of

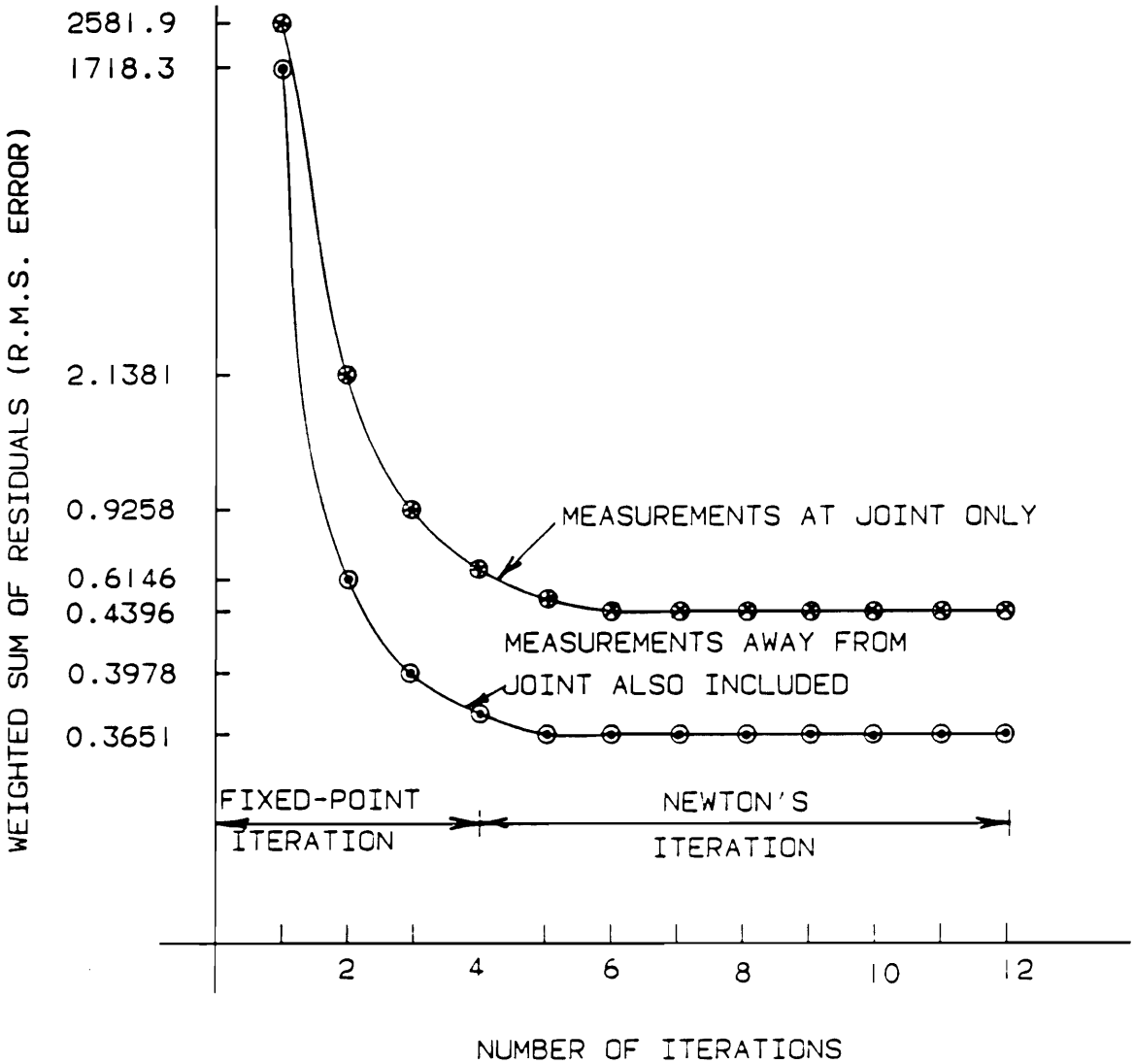

Figure 5.9 Estimation results (car example; simple joint model)

Table 5.7 Estimation results (car example; simple joint model)

Joint Stiffness Parameter	Measurements at Joint only			Measurements also away from Joint		
	Value	Interval	Percentage	Value	Interval	Percentage
k_{x12}	1.0644	0.0499	4.52	1.1892	0.0418	3.52
k_{y12}	1.1628	0.0553	4.76	1.1712	0.0484	4.13
k_{z12}	1.1423	0.0737	6.45	1.1782	0.0764	6.48
k_{x23}	1.2184	0.0797	6.54	1.1596	0.0665	5.83
k_{y23}	1.1663	0.0631	5.41	1.1783	0.0561	4.76
k_{z23}	1.1553	0.0453	3.92	1.1365	0.0413	3.59
k_{x31}	1.2624	0.1283	10.17	1.1198	0.1059	9.46
k_{y31}	1.1426	0.0294	2.58	1.1407	0.0259	2.28
k_{z31}	1.1423	0.0856	7.49	1.1876	0.0787	6.62

The value and interval of parameter are represented in 10^5 $N-m/radian$

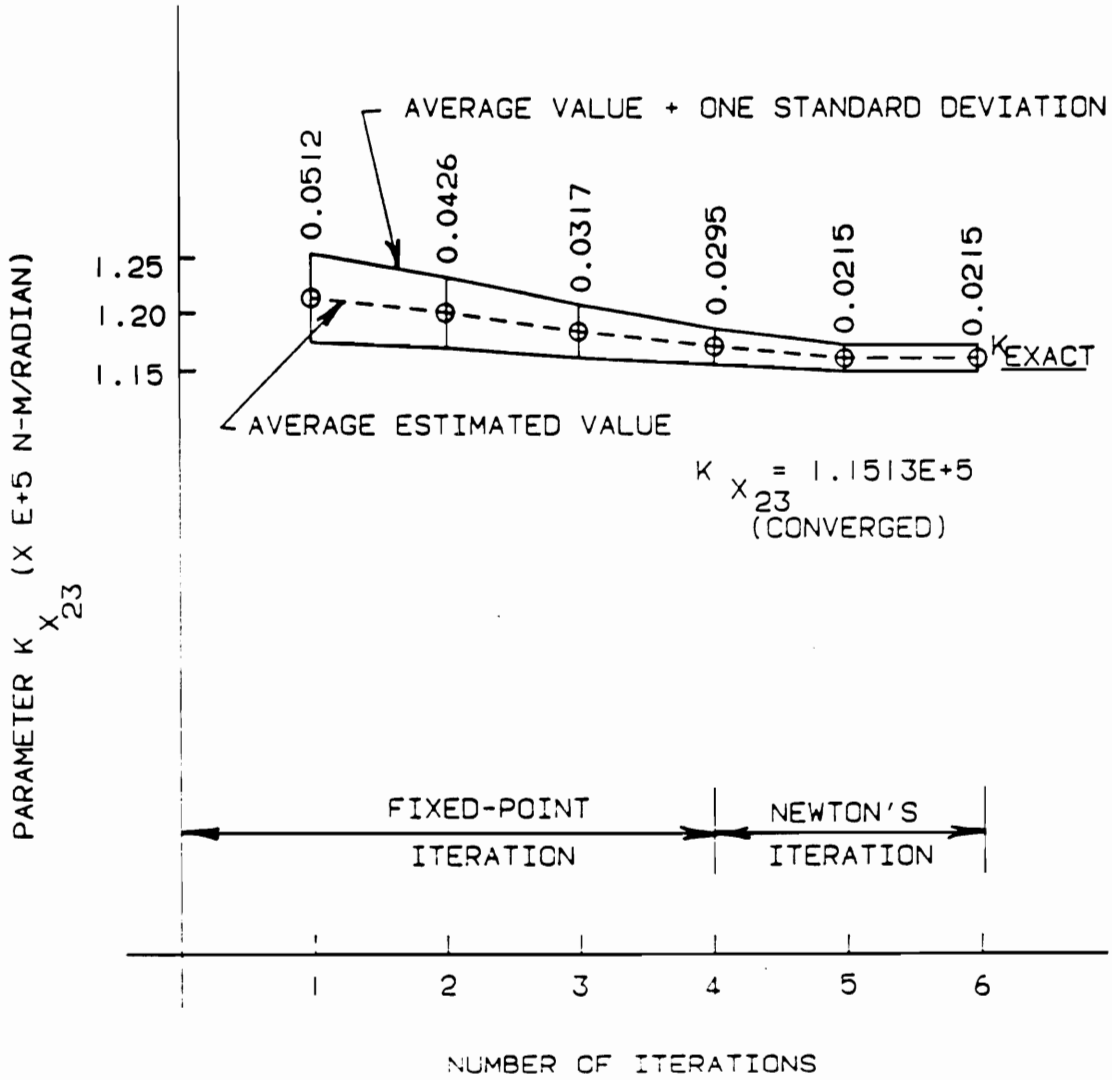

Figure 5.10 Confidence interval for $k_{x_{23}}$ (car example; simple joint model)

Error Value (percent)	Sum of Squares of Residuals (mm^2)
2	0.5473E-3
5	0.4018E-2
10	0.1992E-1

$$\text{Sum of squares of residuals} = |U_m - U_{predicted}|^2$$

Table 5.8 Effect of error variation (car example; simple joint model)

square errors (SOS) increases almost proportionally with the square of the measurement error.

The stiffness parameters of the joint model can also be estimated by using a number of measurements equal to the number of parameters and by solving the system of equations relating the displacements to the parameters. Table 5.9 compares this approach to probabilistic system identification. In this table, confidence intervals are provided for the estimates obtained probabilistically for 20 loading cases. Probabilistic identification gives a better estimate of the parameters since more loading cases are considered in the estimation and an overall good fit is obtained. Tables 5.10 and Table 5.11 give the estimated parameters and confidence intervals for various loading cases. It is observed that 10 loading cases are sufficient to give reasonable estimates with a confidence interval of 5% of the estimated value.

Figure 5.11 shows the parameter $k_{y_{23}}$ as a function of the number of loading cases with confidence intervals for both the biased and unbiased cases. It is observed that 10 loading cases are enough to obtain reasonable estimates with confidence interval of about 5 percent of the estimates. The bias in resulting estimates does not converge to zero as the number of loading cases tends to infinity.

Joint Parameter	Deterministic Approach Value	Probabilistic Approach Value	Probabilistic Approach Error (percent)
$k_{x_{12}}$	1.5341	1.1512	0.81
$k_{y_{12}}$	1.4782	1.1498	0.97
$k_{z_{12}}$	0.9824	1.1492	1.17
$k_{x_{23}}$	0.9507	1.1507	1.11
$k_{y_{23}}$	1.2936	1.1520	0.95
$k_{z_{23}}$	0.9972	1.1539	0.71
$k_{x_{31}}$	1.3563	1.1592	2.11
$k_{y_{31}}$	1.3295	1.1496	0.64
$k_{z_{31}}$	1.0274	1.1506	1.85

The value of parameter is represented in 10^5 $N - m/radian$

Table 5.9 Probabilistic Vs. deterministic approach (car example; simple joint model)

Joint Stiffness Parameter	Stiffness Parameter × 10^5 $N-m/radian$ (various loading cases)				
	5 Cases	8 Cases	10 Cases	15 Cases	20 Cases
$k_{x_{12}}$	1.1892	1.1797	1.1706	1.1697	1.1512
$k_{y_{12}}$	1.1712	1.1674	1.1625	1.1535	1.1498
$k_{z_{12}}$	1.1782	1.1625	1.1541	1.1505	1.1492
$k_{x_{23}}$	1.1596	1.1507	1.1489	1.1513	1.1507
$k_{y_{23}}$	1.1783	1.1736	1.1697	1.1526	1.1520
$k_{z_{23}}$	1.1365	1.1421	1.1432	1.1522	1.1539
$k_{x_{31}}$	1.1198	1.1395	1.1434	1.1487	1.1592
$k_{y_{31}}$	1.1407	1.1442	1.1469	1.1478	1.1496
$k_{z_{31}}$	1.1876	1.1803	1.1718	1.1654	1.1506

Table 5.10 Effect of loading cases on parameters (car example; simple joint model)

Joint Stiffness Parameter	Confidence Interval × 10^5 $N-m/radian$ (various loading cases)				
	5 Cases	8 Cases	10 Cases	15 Cases	20 Cases
$k_{x_{12}}$	0.0418	0.0322	0.0256	0.0122	0.0093
$k_{y_{12}}$	0.0484	0.0387	0.0315	0.0176	0.0112
$k_{z_{12}}$	0.0764	0.0594	0.0433	0.0226	0.0135
$k_{x_{23}}$	0.0665	0.0466	0.0369	0.0215	0.0127
$k_{y_{23}}$	0.0561	0.0395	0.0286	0.0184	0.0109
$k_{z_{23}}$	0.0413	0.0313	0.0245	0.0108	0.0082
$k_{x_{31}}$	0.1059	0.0758	0.0466	0.0399	0.0245
$k_{y_{31}}$	0.0259	0.0176	0.0125	0.0102	0.0074
$k_{z_{31}}$	0.0787	0.0623	0.0357	0.0289	0.0213

Table 5.11 Effect of loading cases on confidence intervals (car example; simple joint model)

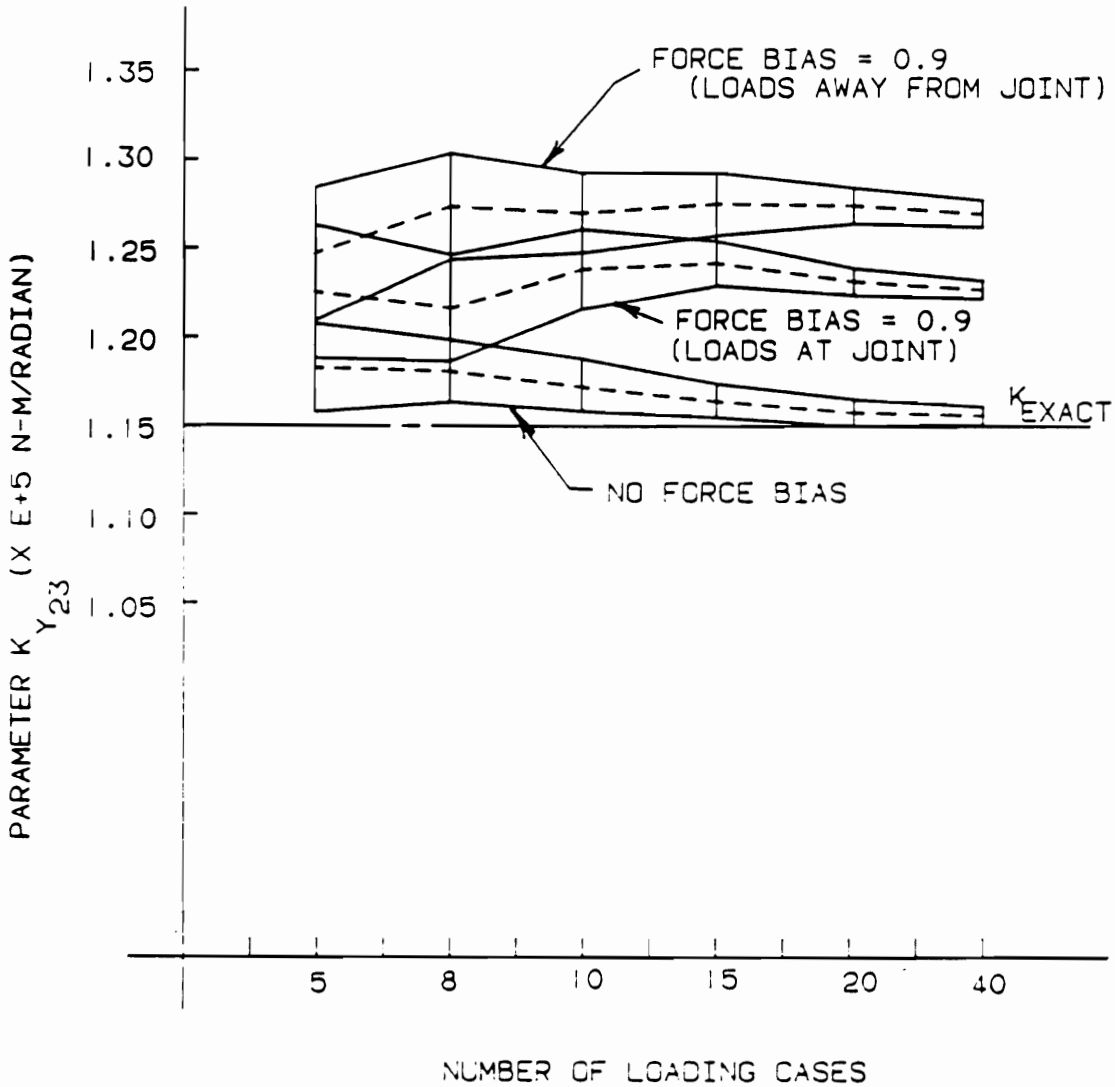

Figure 5.11 Biased and unbiased estimation results (car example; simple joint model)

5.4: Identification of Complex Model

In this section the proposed approach is illustrated for the complex model with a cube frame and a car body examples.

5.4.1 Illustrative Cube Frame Example

The identification process was applied to estimate the complex joint model. The obtain the actual values of joint stiffness parameters, a three member joint of equal length is taken and clamped at one of the ends and hinged at the remaining two ends. The 6 d.o.f. at the hinged ends form the boundary d.o.f. The stiffness matrix is reduced in terms of the boundary d.o.f. to obtain the reduced stiffness matrix of order 6×6. The unconstrained joint stiffness matrix is obtained by using equation (4). Various lengths were taken and the joint stiffness matrix was chosen in a way that the corresponding potential energy (work done by external loads) lies approximately way half between the value for a rigid joint and the value when the parameters are all zero. The length was found to be $1.0 \times 10^{-2} m$ The actual values of the joint stiffness parameters are given in Table 5.12.

Figure 5.12 demonstrates that the use of fixed point iteration is beneficial as compared to using only Newton's method in the identification process. The standard deviation of the error is 5% of the actual rotation. When fixed point iteration was used along with Newton's method, only 4 iterations were needed for

Joint Stiffness Parameter	Value $N - m/radian$
k_{11}	0.6098E + 07
k_{12}	-0.7255E + 06
k_{13}	0.7508E + 05
k_{14}	0.2627E + 05
k_{15}	-0.1502E + 06
k_{16}	0.2830E + 07
k_{22}	0.6098E + 07
k_{23}	0.7805E + 05
k_{24}	-0.2550E + 05
k_{25}	0.1374E + 06
k_{26}	-0.1502E + 06
k_{33}	0.3122E + 06
k_{34}	-0.1530E + 04
k_{35}	-0.2551E + 05
k_{36}	0.2627E + 05
k_{44}	0.3122E + 06
k_{45}	0.7805E + 05
k_{46}	0.7805E + 05
k_{55}	0.6098E + 07
k_{56}	-0.7255E + 06
k_{66}	0.6098E + 07

Table 5.12 Actual values of joint stiffness parameters (cube example; complex model)

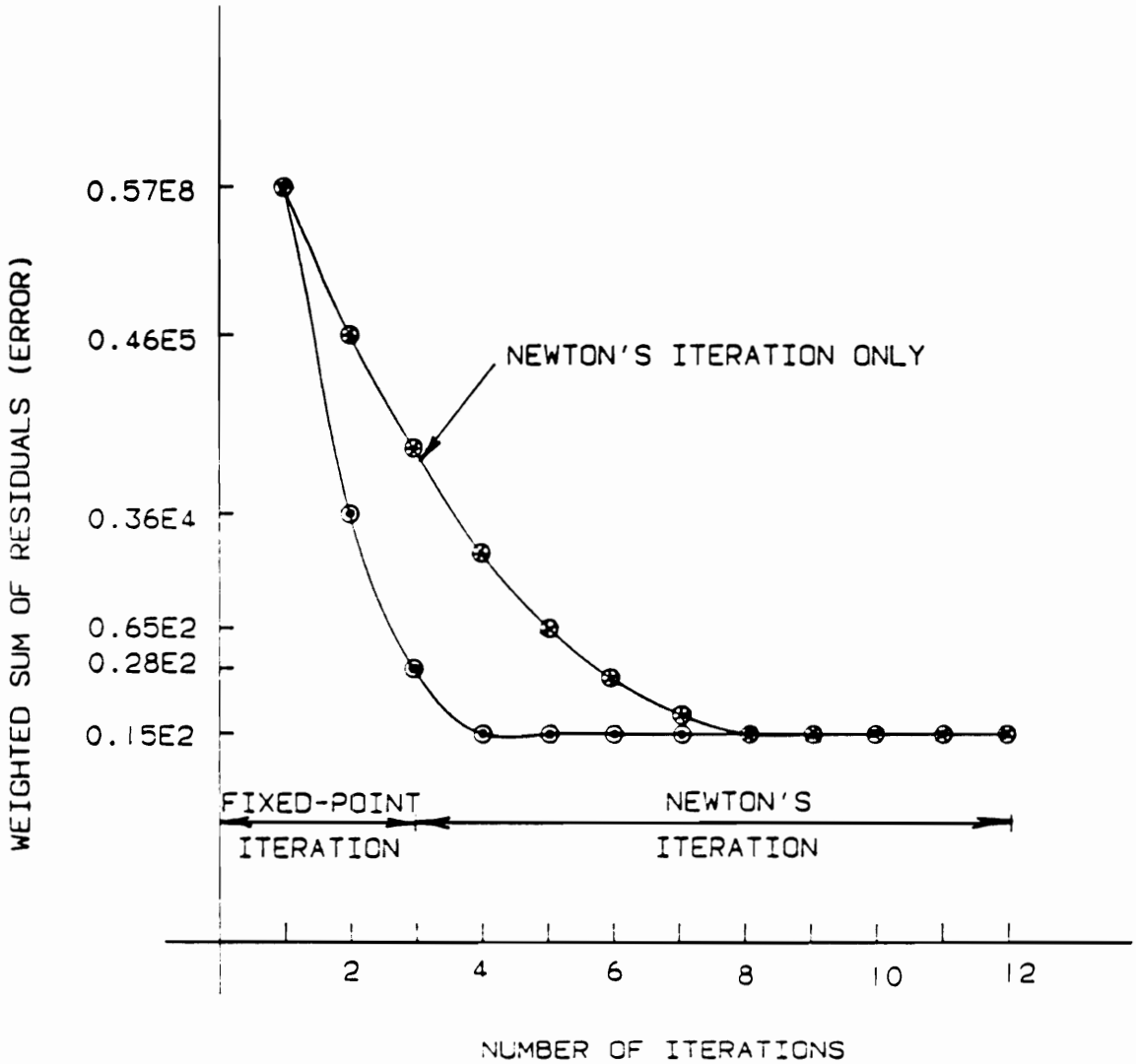

Figure 5.12 Faster convergence of proposed method (cube example; complex model)

convergence. However, if only Newton's method is used, 8 iterations are required for convergence.

Figure 5.13 shows the weighted sum of residuals (r.m.s. error) as a function of the number of iterations. It is seen that when more measurements are taken, the estimates get better and the r.m.s. residual error reduces. It is better therefore to include measurements away from the joint in the estimation. Tables 5.13 and 5.14 show the estimated values, length of confidence intervals (also expressed as a percentage of the estimated value) for 10 loading cases. Figure 5.14 shows the estimated value with confidence intervals of parameter k_{55} as a function of the number of iterations for 30 loading cases with measurements also away from joint. It is observed that the estimates converge after 4 iterations and that the confidence interval narrows with the number of iterations to yield better estimates.

Various standard deviation of the measurement error were considered in measuring deflections. Table 5.15 compares the sum of squares of residuals in estimation for various levels of measurement errors for the cube frame example. The sum of square errors (SOS) increases almost proportionally with the square of the measurement error.

Tables 5.16 and 5.17 give the estimated parameters and confidence intervals for various loading cases. It is observed that 20 loading cases are sufficient to give reasonable estimates with a confidence interval of 5% of the estimated value.

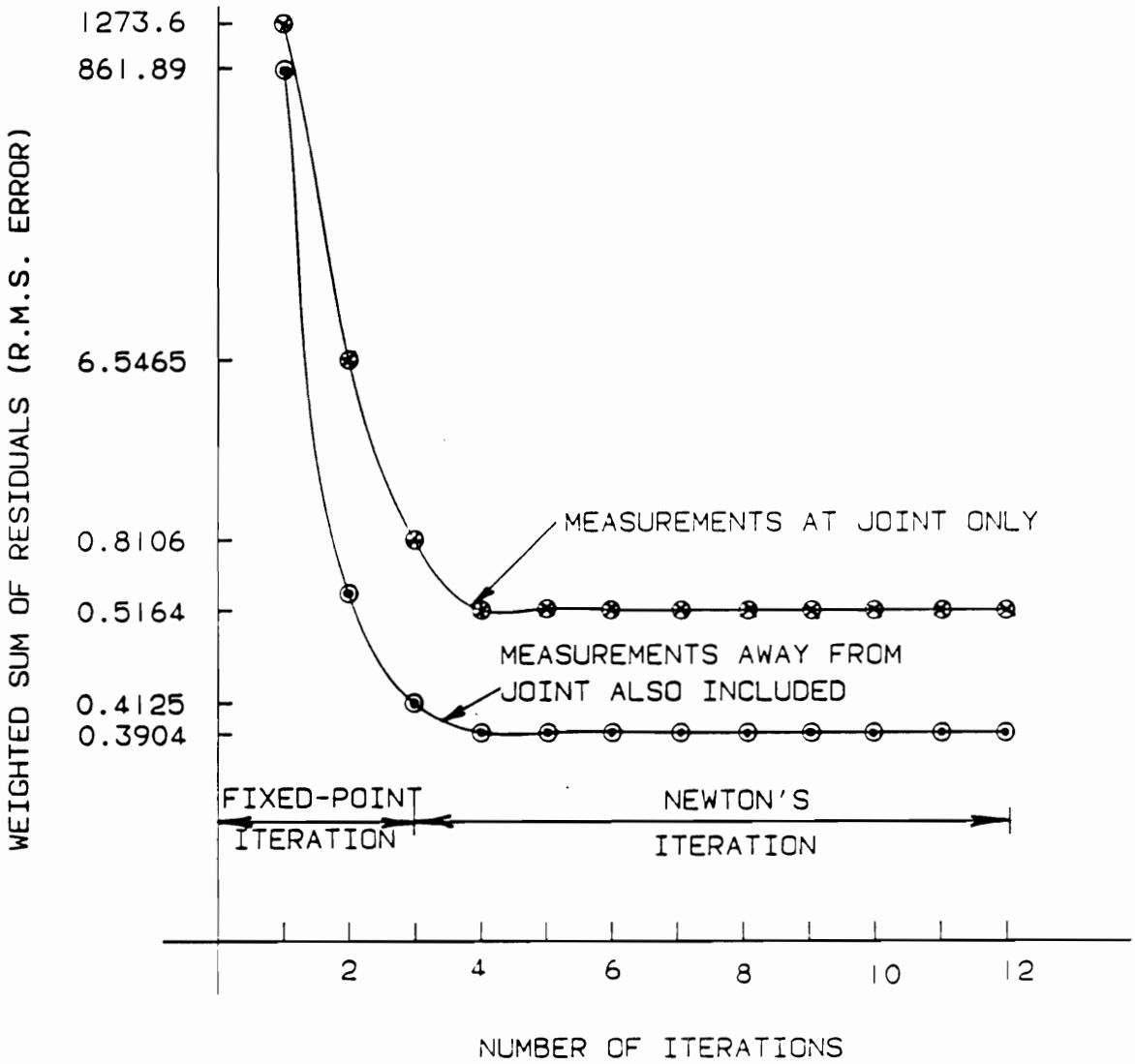

Figure 5.13 Estimation results (cube example; complex model)

Joint Stiffness Parameter	Estimated Value	Confidence Interval	Percentage of Estimate
k_{11}	0.6093E + 7	0.0519E + 7	8.52
k_{12}	-0.7237E + 6	0.0677E + 6	9.35
k_{13}	0.7896E + 5	0.0587E + 5	7.43
k_{14}	0.3134E + 5	0.0494E + 5	15.76
k_{15}	-0.1431E + 6	0.0815E + 5	5.69
k_{16}	0.2812E + 7	0.0992E + 6	3.53
k_{22}	0.6240E + 7	0.0725E + 7	11.62
k_{23}	0.7428E + 5	0.0464E + 5	6.25
k_{24}	-0.4054E + 5	0.0361E + 5	8.90
k_{25}	0.7228E + 5	0.09062E + 5	12.54
k_{26}	-0.1295E + 6	0.0692E + 5	5.34
k_{33}	0.3108E + 6	0.0127E + 6	4.09
k_{34}	-0.9172E + 3	0.0775E + 3	8.45
k_{35}	-0.2547E + 5	0.0827E + 4	3.25
k_{36}	0.1992E + 5	0.0298E + 5	14.96
k_{44}	0.3009E + 6	0.0263E + 6	8.74
k_{45}	0.8608E + 5	0.0885E + 5	10.28
k_{46}	0.7609E + 5	0.07321E + 5	9.62
k_{55}	0.6006E + 7	0.0198E + 7	2.99
k_{56}	-0.6980E + 6	0.08156E + 6	11.67
k_{66}	0.6032E + 7	0.0224E + 7	3.71

Table 5.13 Estimation results with measurements at joint only (cube example; complex model)

Joint Stiffness Parameter	Estimated Value	Confidence Interval	Percentage of Estimate
k_{11}	0.6095E + 7	0.0486E + 7	7.97
k_{12}	-0.7248E + 6	0.0622E + 6	8.58
k_{13}	0.7872E + 5	0.0516E + 5	6.55
k_{14}	0.2965E + 5	0.0461E + 5	15.54
k_{15}	-0.1463E + 6	0.0792E + 5	5.41
k_{16}	0.2818E + 7	0.0818E + 6	2.90
k_{22}	0.6171E + 7	0.0625E + 7	10.13
k_{23}	0.7643E + 5	0.0388E + 5	5.08
k_{24}	-0.3317E + 5	0.0306E + 5	9.23
k_{25}	0.1126E + 6	0.0837E + 5	7.42
k_{26}	-0.1375E + 6	0.0419E + 5	3.04
k_{33}	0.3111E + 6	0.0986E + 5	3.17
k_{34}	-0.1129E + 4	0.0627E + 3	5.55
k_{35}	-0.2548E + 5	0.0814E + 4	3.19
k_{36}	0.2217E + 5	0.0216E + 5	9.74
k_{44}	0.3091E + 6	0.0235E + 6	7.60
k_{45}	0.7952E + 5	0.0819E + 5	10.29
k_{46}	0.7702E + 5	0.0662E + 5	8.59
k_{55}	0.6078E + 7	0.0112E + 7	1.84
k_{56}	-0.7022E + 6	0.0783E + 6	11.15
k_{66}	0.6044E + 7	0.0213E + 7	3.52

Table 5.14 Estimation results with measurements also away from joint (cube example; complex model)

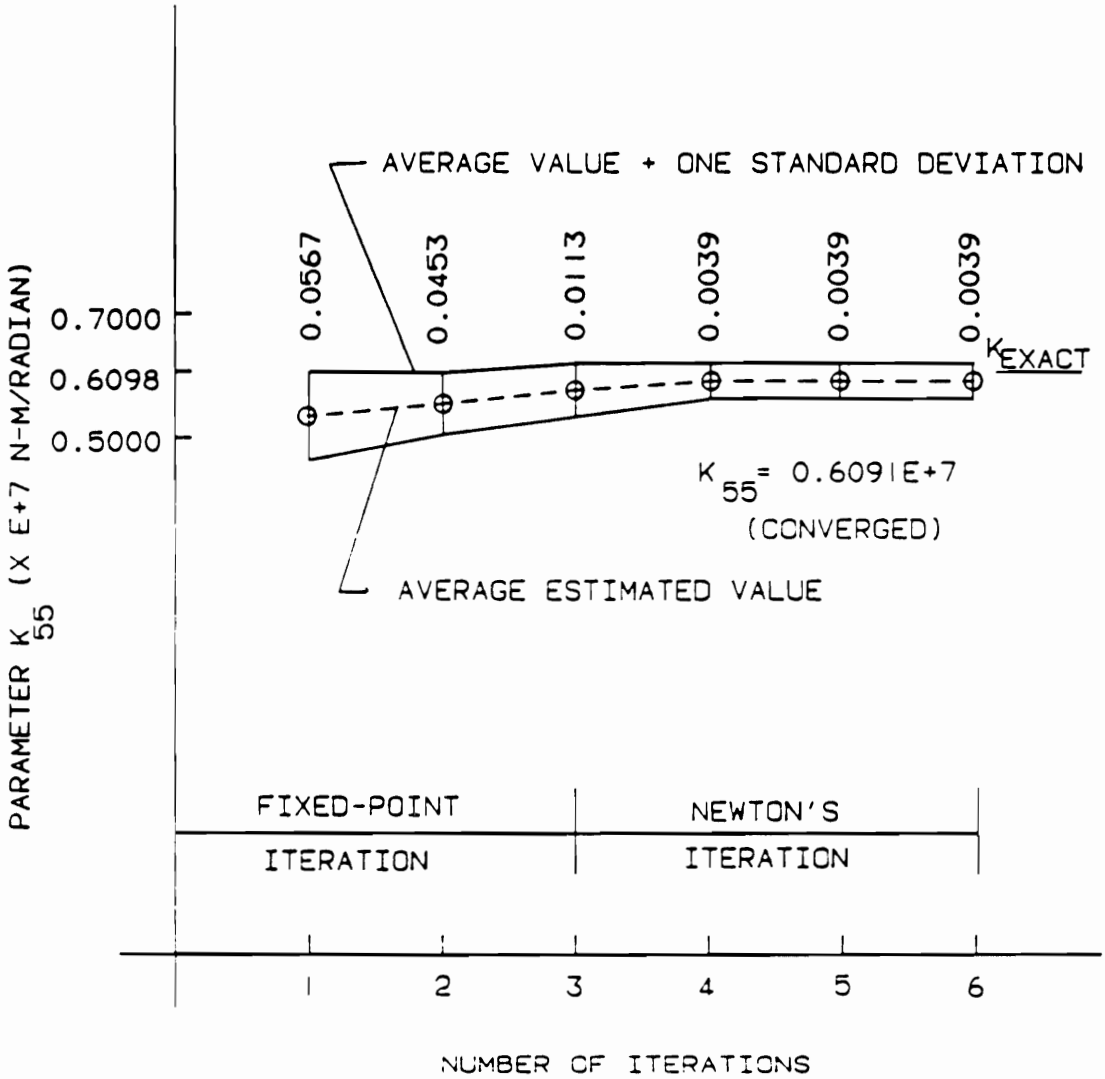

Figure 5.14 Confidence interval for k_{55} (cube example; complex model)

Error Value (percent)	Sum of Squares of Residuals (mm^2)
2	0.1473E-2
5	0.1125E-1
10	0.3836E-1

$$\text{Sum of squares of residuals} = |U_m - U_{predicted}|^2$$

Table 5.15 Effect of error variation (cube example; complex model)

Joint Stiffness Parameter	10 loading cases	20 loading cases	30 loading cases
k_{11}	0.6095E + 7	0.6096E + 7	0.6097E + 7
k_{12}	-0.7248E + 6	-0.7250E + 6	-0.7252E + 6
k_{13}	0.7872E + 5	0.7875E + 5	0.7821E + 5
k_{14}	0.2965E + 5	0.2876E + 5	0.2806E + 5
k_{15}	-0.1463E + 6	-0.1479E + 6	0.1493E + 6
k_{16}	0.2818E + 7	0.2820E + 7	0.2826E + 7
k_{22}	0.6171E + 7	0.6156E + 7	0.6125E + 7
k_{23}	0.7643E + 5	0.7692E + 5	0.7763E + 5
k_{24}	-0.3317E + 5	-3043E + 5	-0.2819E + 5
k_{25}	0.1126E + 6	0.1595E + 5	0.1236E + 6
k_{26}	-0.1375E + 6	-0.1419E + 6	-0.1471E + 6
k_{33}	0.3111E + 6	0.3116E + 6	0.3119E + 6
k_{34}	-0.1129E + 4	-0.1295E + 4	-0.1475E + 4
k_{35}	-0.2548E + 5	-0.2549E + 5	-0.2550E + 5
k_{36}	0.2217E + 5	0.2316E + 5	0.2438E + 5
k_{44}	0.3091E + 6	0.3096E + 6	0.3136E + 5
k_{45}	0.7952E + 5	0.7919E + 5	0.7874E + 5
k_{46}	0.7702E + 5	0.7726E + 5	0.7825E + 5
k_{55}	0.6078E + 7	0.6083E + 7	0.6091E + 7
k_{56}	-0.7022E + 6	-0.7105E + 6	-0.7192E + 6
k_{66}	0.6044E + 7	0.6051E + 7	0.6077E + 7

Table 5.16 Effect of loading cases on parameters (cube example; complex model)

Joint Stiffness Parameter	10 loading cases	20 loading cases	30 loading cases
k_{11}	0.0486E + 7	0.0265E + 7	0.0173E + 7
k_{12}	0.0622E + 6	0.0339E + 6	0.0184E + 6
k_{13}	0.0516E + 5	0.0284E + 5	0.0125E + 5
k_{14}	0.0461E + 5	0.0226E + 5	0.0099E + 5
k_{15}	0.0792E + 5	0.0377E + 5	0.0152E + 5
k_{16}	0.0818E + 6	0.0398E + 6	0.0201E + 6
k_{22}	0.0625E + 7	0.0336E + 7	0.0174E + 7
k_{23}	0.0388E + 5	0.0201E + 5	0.0092E + 5
k_{24}	0.0306E + 5	0.0143E + 5	0.0071E + 5
k_{25}	0.0837E + 5	0.0452E + 5	0.0225E + 5
k_{26}	0.0419E + 5	0.0226E + 5	0.0134E + 5
k_{33}	0.0986E + 5	0.0537E + 5	0.0306E + 5
k_{34}	0.0627E + 3	0.0349E + 3	0.0182E + 3
k_{35}	0.0814E + 4	0.0426E + 4	0.0239E + 4
k_{36}	0.0216E + 5	0.0109E + 5	0.0092E + 5
k_{44}	0.0235E + 6	0.0175E + 6	0.0088E + 6
k_{45}	0.0819E + 5	0.0465E + 5	0.0295E + 5
k_{46}	0.0662E + 5	0.0353E + 5	0.0186E + 5
k_{55}	0.0112E + 7	0.0075E + 7	0.0039E + 7
k_{56}	0.0783E + 6	0.0421E + 6	0.0237E + 6
k_{66}	0.0213E + 7	0.0127E + 7	0.0078E + 7

Table 5.17 Effect of loading cases on confidence intervals (cube example; complex model)

Figure 5.15 shows the parameter k_{44} as a function of the number of loading cases with confidence intervals for both both the biased and unbiased cases. Bias in resulting estimates does not converge to zero as the number of loading cases tends to infinity.

5.4.2 Illustrative Car Model Example

For the car model, the procedure described in section 5.4.1. is repeated. The length corresponding to a joint stiffness matrix that gives the potential energy that lies half way between the rigid and totally flexible joint is $2.0 \times 10^{-2} m$. The actual values of the joint stiffness parameters are given in Table 5.18. Figure 5.16 demonstrates that the use of fixed point iteration is beneficial as compared to using only Newton's method in the identification process. The standard deviation of the error is 5% of the actual rotation. When fixed point iteration was used along with Newton's method, only 5 iterations were needed for convergence. However, if only Newton's method is used, 8 iterations are required for convergence.

Figure 5.17 shows the weighted sum of residuals (r.m.s. error) as a function of the number of iterations for the car model when only the joint degrees of freedom are considered as the boundary degrees of freedom and when degrees of freedom other than the joint degrees of freedom are considered as the boundary degrees of freedom. It is seen that when more measurements are taken, the estimates get better and the r.m.s. residual error reduces. It is better therefore to include

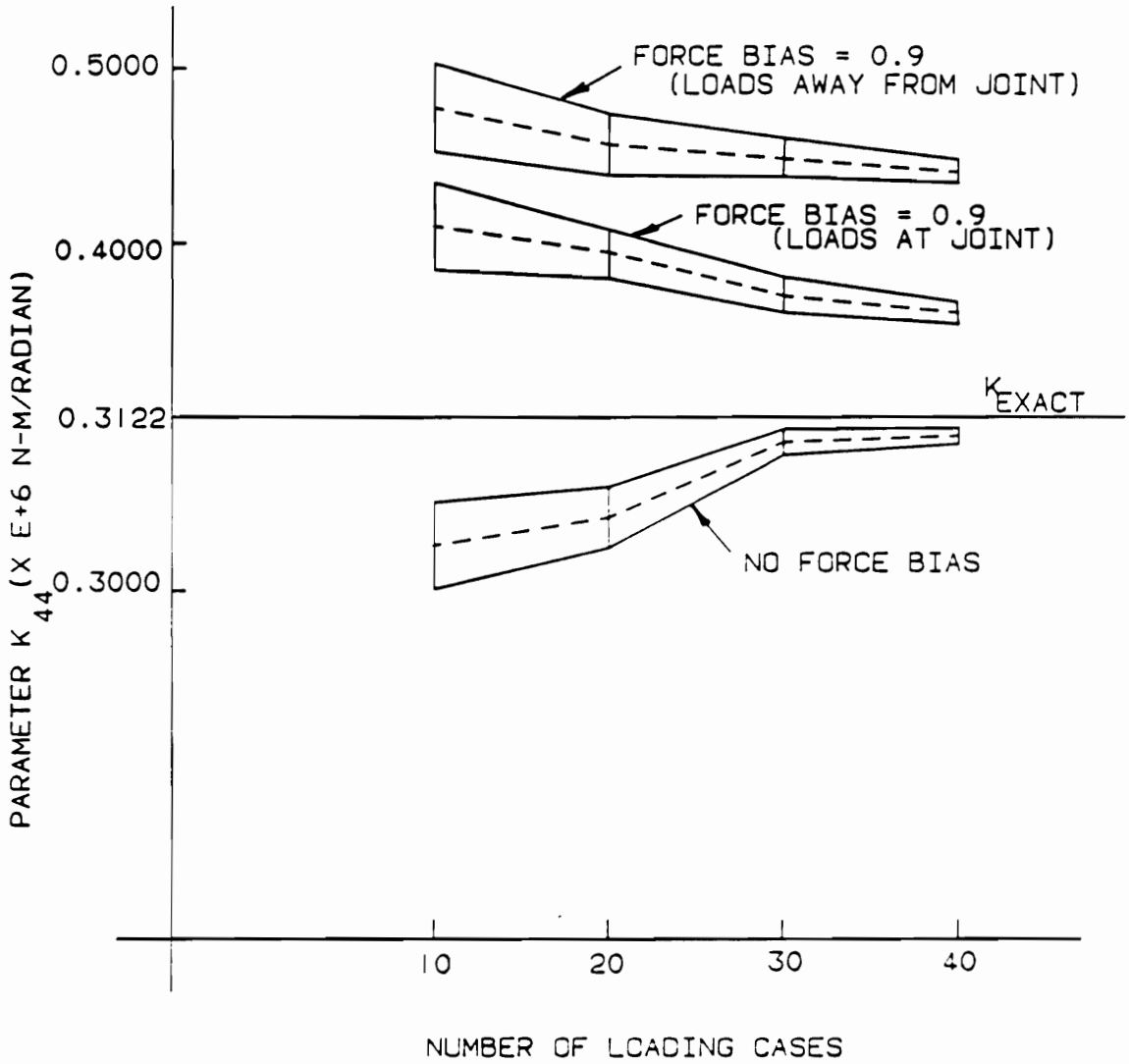

Figure 5.15 Biased and unbiased estimation results (cube example; complex model)

Joint Stiffness Parameter	Value $N-m/radian$
k_{11}	0.3607E + 07
k_{12}	-0.1321E + 06
k_{13}	0.2355E + 05
k_{14}	0.2355E + 05
k_{15}	-0.1321E + 06
k_{16}	0.9408E + 06
k_{22}	0.3607E + 07
k_{23}	0.2355E + 05
k_{24}	-0.7697E + 04
k_{25}	-0.1321E + 06
k_{26}	-0.1321E + 06
k_{33}	0.1567E + 06
k_{34}	0.4648E + 03
k_{35}	-0.7697E + 04
k_{36}	0.2355E + 05
k_{44}	0.1567E + 06
k_{45}	0.2355E + 05
k_{46}	0.2355E + 05
k_{55}	0.3607E + 07
k_{56}	-0.1321E + 06
k_{66}	0.3607E + 07

Table 5.18 Actual values of joint stiffness parameters (car example ; complex model)

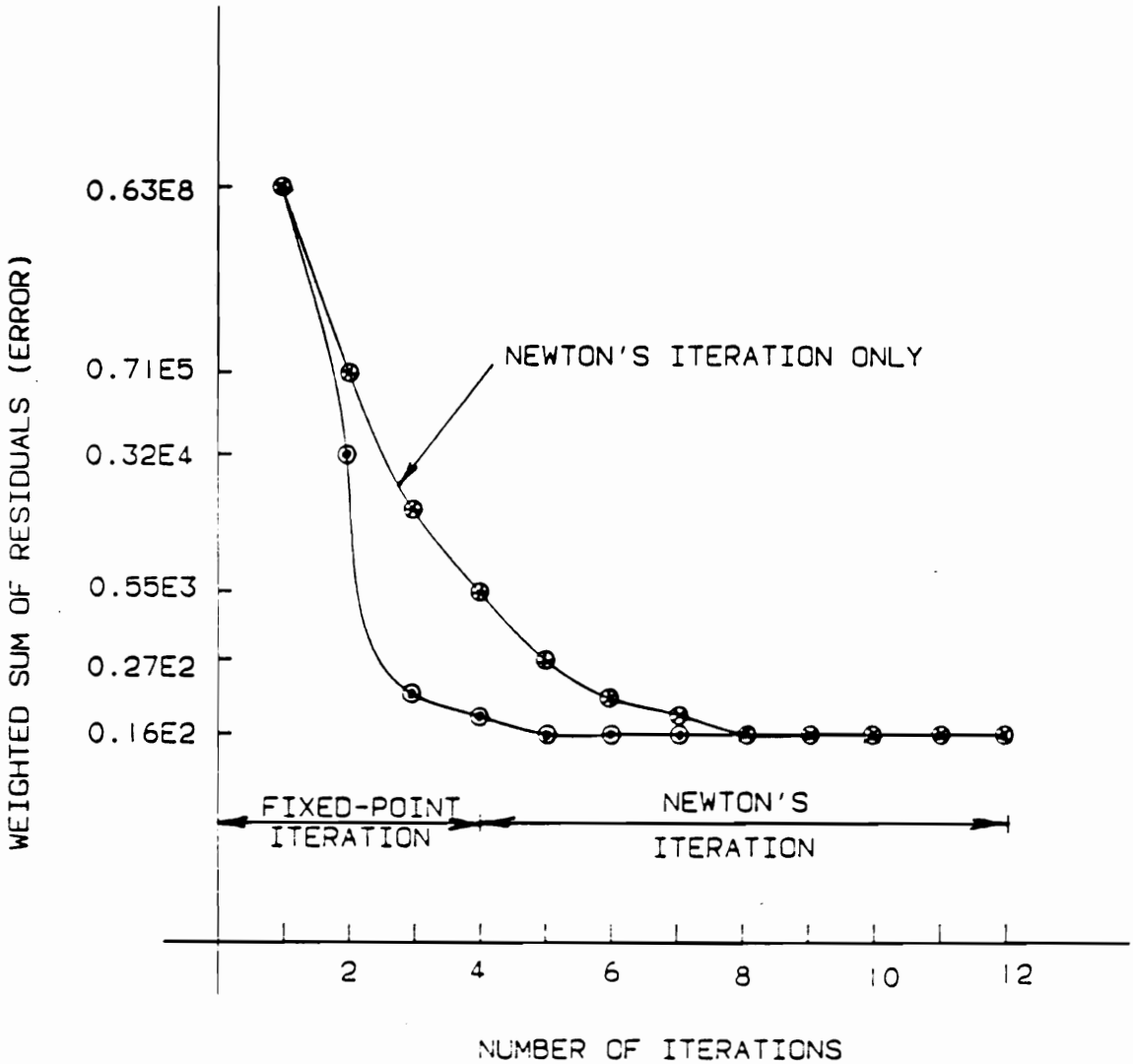

Figure 5.16 Faster convergence of proposed method (car example; complex model)

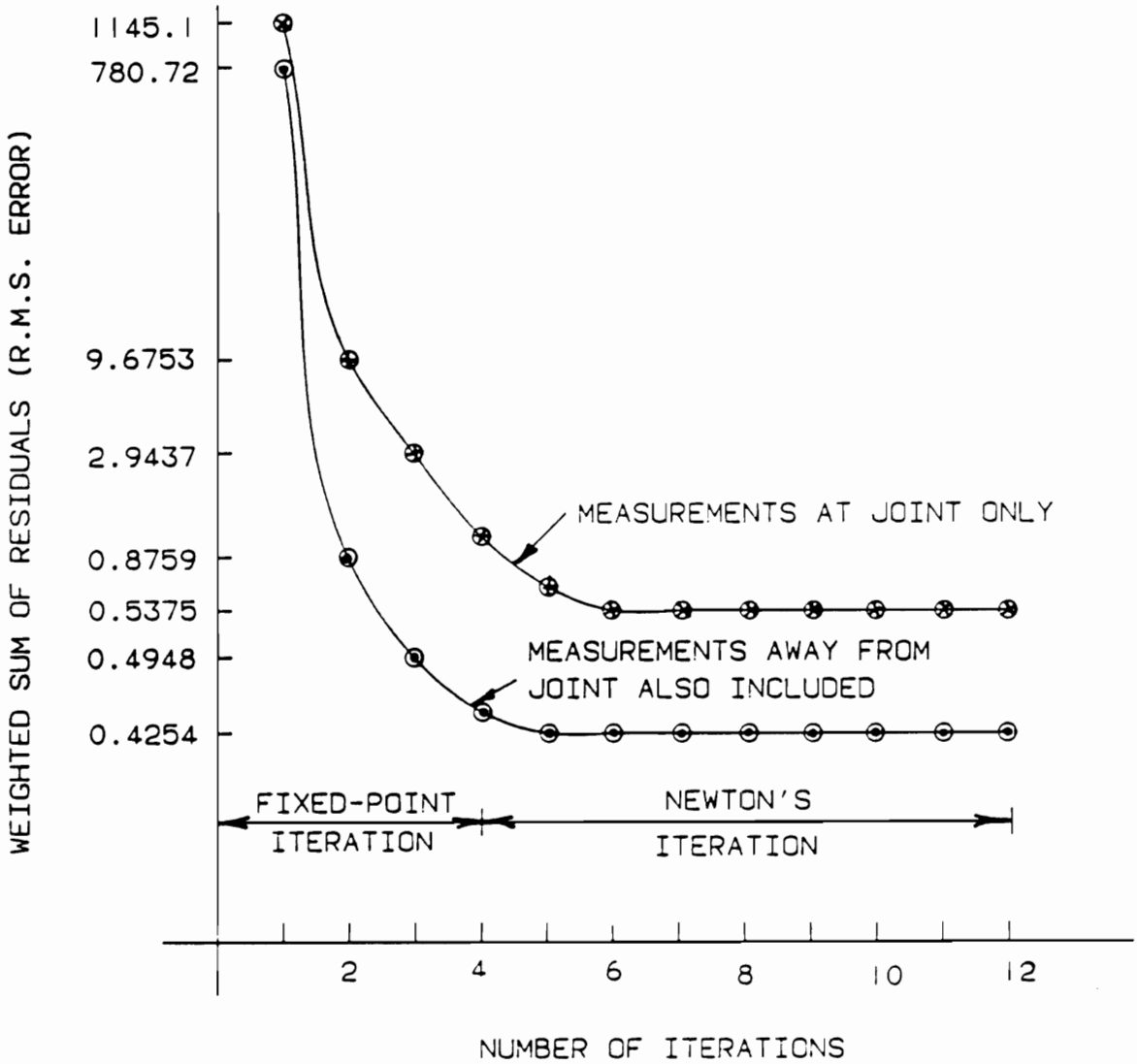

Figure 5.17 Estimation results (car example; complex model)

measurements away from the joint in the estimation. Tables 5.19 and 5.20 show the estimated values, length of confidence intervals (also expressed as a percentage of the estimated value) for both cases for 10 loading cases. Figure 5.18 shows the estimated value with confidence intervals of parameter k_{33} as a function of the number of iterations for 30 loading cases with measurements also away from joint. It is observed that the estimates converge after 5 iterations and that the confidence interval narrows with the number of iterations to yield better estimates.

Table 5.21 shows the comparison of sum of squares of residuals in estimation for various levels of measurement errors for the car frame example. The sum of square errors (SOS) increases almost proportionally with the square of the measurement error. Tables 5.22 and Table 5.23 give the estimated parameters and confidence intervals for various loading cases. It is observed that 20 loading cases are sufficient to give reasonable estimates with a confidence interval of 5% of the estimated value.

Figure 5.19 show the parameter k_{22} as a function of the number of loading cases with confidence intervals for both both the biased and unbiased cases. It is observed that 20 loading cases are enough to obtain reasonable estimates with confidence interval of about 5 percent of the estimates. The bias in resulting estimates does not converge to zero as the number of loading cases tends to infinity.

Joint Stiffness Parameter	Estimated Value	Confidence Interval	Percentage of Estimate
k_{11}	0.3572E + 7	0.0259E + 7	7.26
k_{12}	-0.1498E + 6	0.0768E + 5	5.13
k_{13}	0.2123E + 5	0.0102E + 5	4.82
k_{14}	0.2206E + 5	0.0119E + 5	5.39
k_{15}	-0.1178E + 6	0.0101E + 6	8.56
k_{16}	0.8893E + 6	0.0625E + 6	7.03
k_{22}	0.3426E + 7	0.0181E + 7	5.28
k_{23}	0.2513E + 5	0.0142E + 5	5.67
k_{24}	-0.7546E + 4	0.0464E + 4	6.15
k_{25}	-0.9650E + 5	0.09392E + 5	9.74
k_{26}	-0.1536E + 6	0.0665E + 5	4.33
k_{33}	0.1407E + 6	0.0558E + 6	3.97
k_{34}	0.4457E + 3	0.0242E + 3	5.42
k_{35}	-0.6581E + 4	0.0326E + 4	4.95
k_{36}	0.2506E + 5	0.0222E + 5	8.86
k_{44}	0.1728E + 6	0.0854E + 5	4.94
k_{45}	0.2286E + 5	0.0213E + 5	9.32
k_{46}	0.2306E + 5	0.01421E + 5	6.15
k_{55}	0.3751E + 7	0.0150E + 7	4.01
k_{56}	-0.1436E + 6	0.01046E + 6	7.27
k_{66}	0.3512E + 7	0.0184E + 7	5.26

Table 5.19 Estimation results (car example; complex model): Measurements at joint only

Joint Stiffness Parameter	Estimated Value	Confidence Interval	Percentage of Estimate
k_{11}	0.3581E + 7	0.0248E + 7	6.93
k_{12}	-0.1472E + 6	0.0746E + 5	5.07
k_{13}	0.2205E + 5	0.0102E + 5	4.61
k_{14}	0.2247E + 5	0.0120E + 5	5.33
k_{15}	-0.1206E + 6	0.0101E + 6	8.39
k_{16}	0.8965E + 6	0.0606E + 6	6.76
k_{22}	0.3482E + 7	0.0142E + 7	4.09
k_{23}	0.2494E + 5	0.0128E + 5	5.12
k_{24}	-0.7553E + 4	0.0451E + 4	5.97
k_{25}	-0.9728E + 5	0.08692E + 5	8.93
k_{26}	-0.1505E + 6	0.0589E + 5	3.92
k_{33}	0.1429E + 6	0.0526E + 6	3.68
k_{34}	0.4483E + 3	0.0233E + 3	5.19
k_{35}	-0.6793E + 4	0.0330E + 4	4.86
k_{36}	0.2529E + 5	0.0221E + 5	8.73
k_{44}	0.1712E + 6	0.0832E + 5	4.86
k_{45}	0.2295E + 5	0.0204E + 5	8.89
k_{46}	0.2314E + 5	0.0137E + 5	5.93
k_{55}	0.3722E + 7	0.0139E + 7	3.76
k_{56}	-0.1417E + 6	0.0972E + 5	6.86
k_{66}	0.3533E + 7	0.0174E + 7	4.93

Table 5.20 Estimation results (car example; complex model): Measurements also away from joint

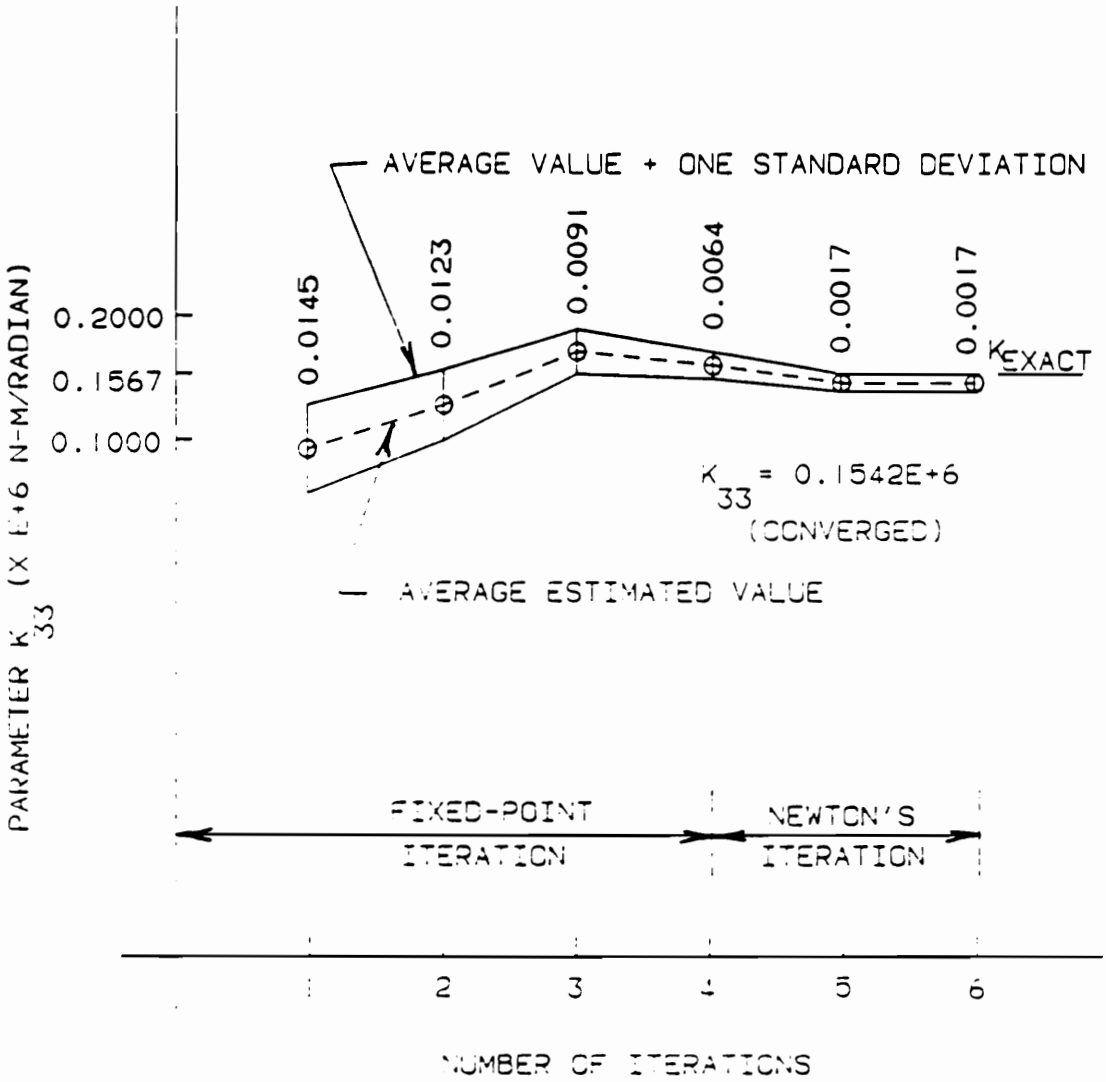

Figure 5.18 Confidence interval for k_{33} (car example; complex model)

Error Value (percent)	Sum of Squares of Residuals (mm^2)
2	0.9866E-3
5	0.8294E-2
10	0.3649E-1

$$\text{Sum of squares of residuals} = |\mathbf{U}_m - \mathbf{U}_{predicted}|^2$$

Table 5.21 Effect of error variation (car example; complex model)

Joint Stiffness Parameter	10 loading cases	20 loading cases	30 loading cases
k_{11}	0.3581E + 7	0.3593E + 7	0.3598E + 7
k_{12}	-0.1472E + 6	-0.1433E + 6	-0.1372E + 6
k_{13}	0.2205E + 5	0.2286E + 5	0.2307E + 5
k_{14}	0.2247E + 5	0.2270E + 5	0.2313E + 5
k_{15}	-0.1206E + 6	-0.1278E + 6	-0.1318E + 6
k_{16}	0.8965E + 6	0.9026E + 6	0.9319E + 6
k_{22}	0.3482E + 7	0.3561E + 7	0.3587E + 7
k_{23}	0.2494E + 5	0.2462E + 5	0.2291E + 5
k_{24}	-0.7553E + 4	-0.7588E + 4	-0.7663E + 4
k_{25}	-0.9728E + 5	-0.1108E + 6	-0.1265E + 6
k_{26}	-0.1505E + 6	-0.1466E + 6	-0.1378E + 6
k_{33}	0.1429E + 6	0.1473E + 6	0.1542E + 6
k_{34}	0.4483E + 3	0.4509E + 3	0.4592E + 3
k_{35}	-0.6793E + 4	-0.6982E + 4	-0.7314E + 4
k_{36}	0.2529E + 5	0.2510E + 5	0.2417E + 5
k_{44}	0.1712E + 6	0.1688E + 6	0.1605E + 6
k_{45}	0.2295E + 5	0.2304E + 5	0.2326E + 5
k_{46}	0.2314E + 5	0.2321E + 5	0.2333E + 5
k_{55}	0.3722E + 7	0.3713E + 7	0.3634E + 7
k_{56}	-0.1417E + 6	-0.1391E + 6	-0.1367E + 6
k_{66}	0.3533E + 7	0.3568E + 7	0.3591E + 7

Table 5.22 Effect of loading cases on parameters (car example; complex model)

Joint Stiffness Parameter	10 loading cases	20 loading cases	30 loading cases
k_{11}	0.0248E + 7	0.0179E + 7	0.0062E + 7
k_{12}	0.0746E + 5	0.0393E + 5	0.0213E + 5
k_{13}	0.0102E + 5	0.0068E + 5	0.0041E + 5
k_{14}	0.0120E + 5	0.0052E + 5	0.0038E + 5
k_{15}	0.0101E + 6	0.0049E + 6	0.0035E + 6
k_{16}	0.0606E + 6	0.0351E + 6	0.0197E + 6
k_{22}	0.0142E + 7	0.0085E + 7	0.0053E + 7
k_{23}	0.0128E + 5	0.0049E + 5	0.0031E + 5
k_{24}	0.0451E + 4	0.0264E + 4	0.0193E + 4
k_{25}	0.0869E + 5	0.0497E + 5	0.0305E + 5
k_{26}	0.0589E + 5	0.0218E + 5	0.0104E + 5
k_{33}	0.0526E + 5	0.0296E + 5	0.0168E + 5
k_{34}	0.0233E + 3	0.0132E + 3	0.0088E + 3
k_{35}	0.0330E + 4	0.0174E + 4	0.0092E + 4
k_{36}	0.0221E + 5	0.0102E + 5	0.0049E + 5
k_{44}	0.0832E + 5	0.0405E + 5	0.0193E + 5
k_{45}	0.0204E + 5	0.0112E + 5	0.0066E + 5
k_{46}	0.0137E + 5	0.0678E + 5	0.0391E + 5
k_{55}	0.0139E + 7	0.0062E + 7	0.0033E + 7
k_{56}	0.0972E + 5	0.0488E + 5	0.0215E + 5
k_{66}	0.0174E + 7	0.0096E + 7	0.0052E + 7

Table 5.23 Effect of loading cases on confidence intervals (car example; complex model)

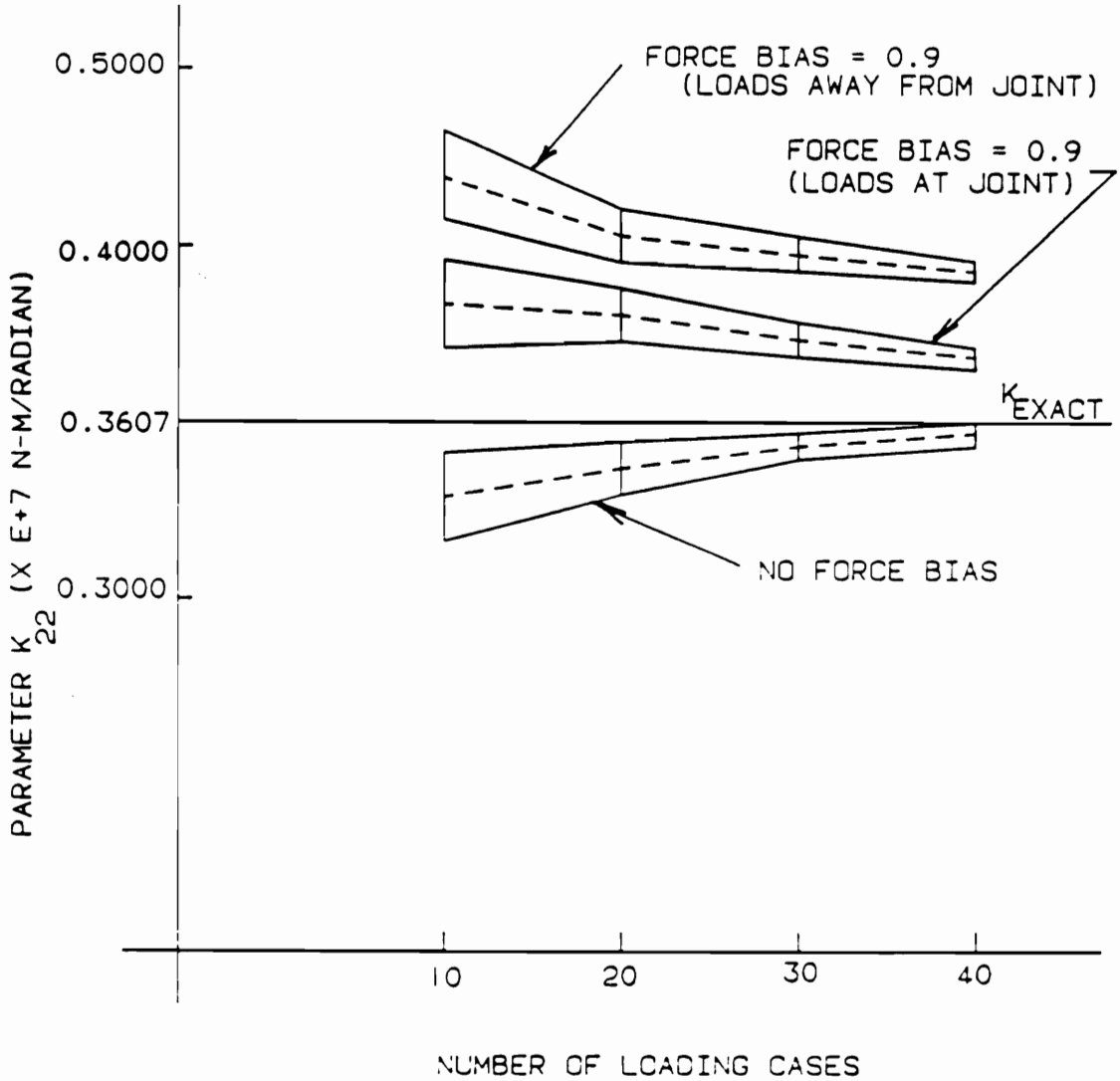

Figure 5.19 Biased and unbiased estimation results (car example; complex model)

Chapter 6: Comparison of Joint Models

6.1 Overview

In this chapter, the simple and complex joint models for both the cube and car examples are compared. For the purpose of examples, it is assumed that the actual joint behaves according to the assumptions stated in section 1.4. Therefore, the complex model can predict the behavior of the actual joint. Simulated measurements obtained from complex model are used to estimate the parameters of the simple model. Finally, the two models are compared in terms of their ability to predict static response.

6.2 Comparison Process

The complex model is more realistic because it accounts for the coupling between the motions of the joint branches. On the other hand, it is more complicated than the simple model. It is interesting to explore the importance of coupling by

comparing both joint models. The following procedure is used for such comparison:

Consider an actual joint. An actual joint is one that is observed in practice. In this comparison, with the assumptions stated in section 1.4, the complex model is idealized to the actual structure. Hence, the measurements obtained from the complex model is taken as measurements obtained from the actual joint. The stiffness matrix of this joint is assembled with that of the remaining structure to form the global stiffness matrix. The structure with the flexible joint is loaded and measured displacements are simulated by the procedure described in section 5.2. Both models are identified from the simulated measurements. Then, apply the same loads to each structure and compare the resulting displacements and strain energies. The comparison process is shown in Figure 6.1.

The two models predict different responses for the same loading. Among all possible loadings, there is one that corresponds to the largest difference between the strain energies of the two models. This loading case will be called maximum difference in strain energies (MDSE) loading. MDSE loading is determined by minimizing the ratio of the difference between the strain energies of the two models normalized by the length of the forcing vector. Therefore, maximize the following quantity,

$$\frac{E_{complex} - E_{simple}}{L_f} \tag{34}$$

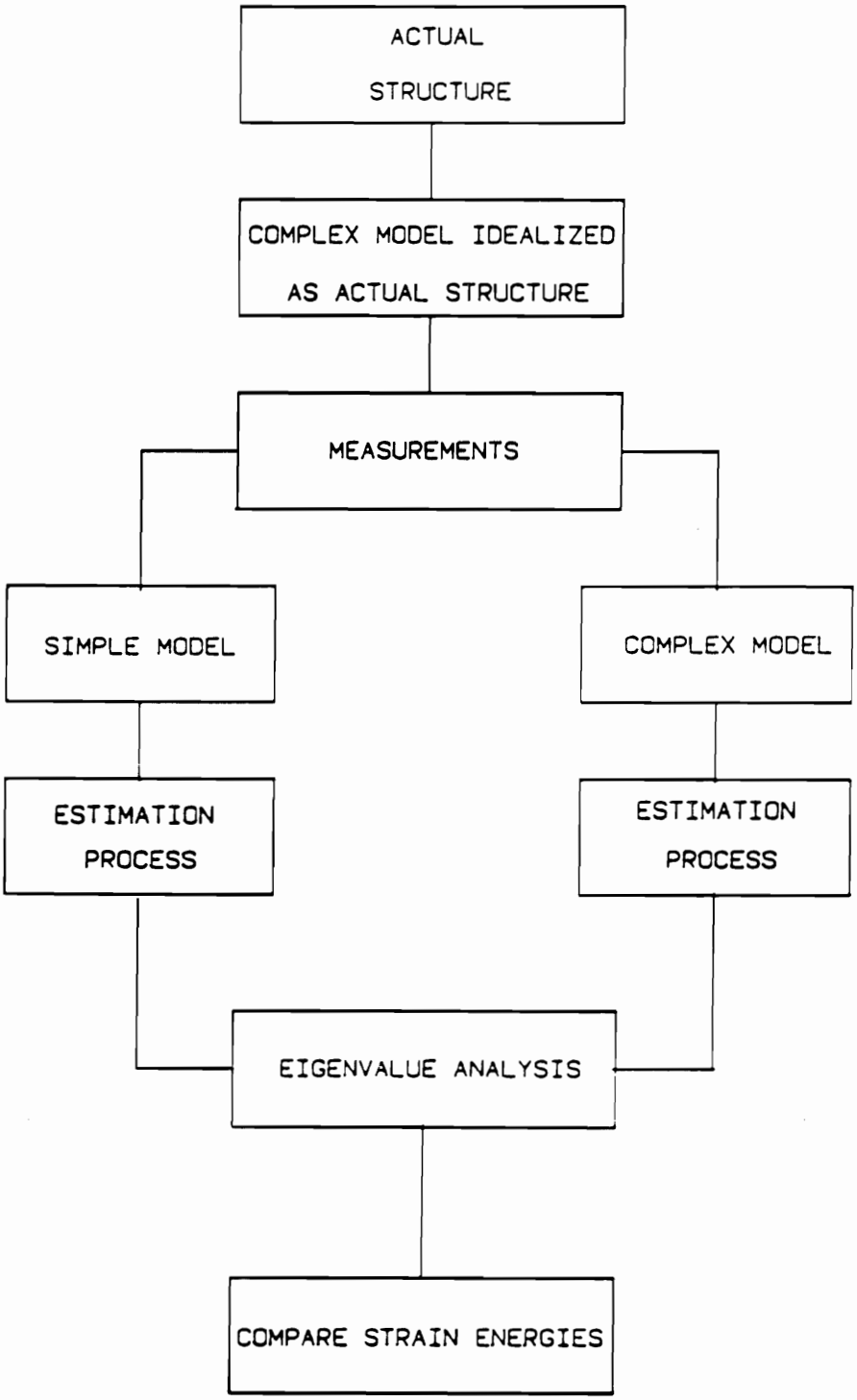

Figure 6.1 Comparison process for simple and complex models

where, $E_{complex}$ and E_{simple} are the strain energies of the complex model and the simple model respectively. L_f is the square of the length of force vector. These are given by,

$$E_{complex} = \frac{1}{2} \mathbf{F}^T \mathbf{K}_{complex}^{-1} \mathbf{F} \tag{35a}$$

$$E_{simple} = \frac{1}{2} \mathbf{F}^T \mathbf{K}_{simple}^{-1} \mathbf{F} \tag{35b}$$

$$L_f = \frac{1}{2} \mathbf{F}^T \mathbf{F} \tag{35c}$$

It can be shown that the load vector that maximizes the normalized difference in strain energies is the eigenvector that corresponds to the largest eigenvalue of the matrix which is the difference of the flexibility matrices of the complex and the simple model [38]. This procedure is applied to the cube and car examples to study the effect of coupling in flexible joint structures.

6.3 Cube Frame Example

It is assumed that the actual joint behaves according to the assumptions stated in section 1.4. Therefore, the complex model can exactly predict its behavior. The stiffness matrix of the actual joint is specified in Table 6.1. More specifically, entries of its reduced stiffness matrix, $\mathbf{K}_C$, are presented in the second column.

Joint Stiffness Parameter	Complex Model Actual	Complex Model Estimated	Simple Model Estimated
k_{11}	0.6098E + 7	0.6093E + 7	0.166E + 7
k_{12}	-0.7255E + 6	-0.7237E + 6	0.0
k_{13}	0.7805E + 5	0.7896E + 5	0.0
k_{14}	0.2627E + 5	0.3134E + 5	-0.4847E + 6
k_{15}	-0.1502E + 6	-0.1431E + 6	0.0
k_{16}	0.2830E + 7	0.2812E + 7	0.0
k_{22}	0.6098E + 7	0.6240E + 7	0.3281E + 7
k_{23}	0.7805E + 5	0.7428E + 5	0.0
k_{24}	-0.2551E + 5	-0.4054E + 5	0.0
k_{25}	0.1374E + 6	0.7228E + 5	-0.7254E + 6
k_{26}	-0.1502E + 6	-0.1295E + 6	0.0
k_{33}	0.3122E + 6	0.3108E + 6	0.4401E + 6
k_{34}	-0.1530E + 4	-0.9172E + 3	0.0
k_{35}	-0.2551E + 5	-0.2547E + 5	0.0
k_{36}	0.2627E + 5	0.1992E + 5	-0.1941E + 6
k_{44}	0.3122E + 6	0.3009E + 6	0.1328E + 7
k_{45}	0.7805E + 5	0.8608E + 5	0.0
k_{46}	0.7805E + 5	0.7609E + 5	0.0
k_{55}	0.6098E + 7	0.6006E + 7	0.2553E + 7
k_{56}	-0.7255E + 6	-0.6980E + 6	0.0
k_{66}	0.6098E + 7	0.6032E + 7	0.2063E + 7

Table 6.1 Actual and estimated parameters of complex and simple joint models (cube example)

The stiffness matrices of the identified simple and complex models are also presented in Table 6.1.

Next, evaluate the MDSE loading corresponding to the two estimated models. One of the joint branches is clamped as shown in Figure 3.3, so that the joint becomes statically determinate. The calculated MDSE loading is presented in Table 6.2. This loading practically constitutes a unit moment in the θ_{x_2} direction which corresponds to the parameter k_{44} . This result can be explained by considering the flexibility matrices of the two models. It is observed that entry corresponding to degree of freedom θ_{x_2} has the largest value in the matrix which is the difference between the flexibility matrices of both models.

Table 6.3 compares the strain energies stored in the two joint models subjected to MDSE loading. Table 6.4 shows the comparison of displacements at the joint degrees of freedom for the case of an isolated joint. It is evident that these models are widely different. The difference in the behavior of the two models can only be attributed to the coupling between the motions of the joint branches because the only difference between the two models is in accounting for such coupling. Thus, coupling is important in this example.

In Figure 6.2, the two finite element models for the cube which incorporate the estimated simple and complex joint models are compared. This figure presents the strain energies of the two cube-joint assemblies subjected to the MDSE loading corresponding to these assemblies. In the same figure, the strain energy

Direction	Load
θ_{x_1}	-0.0786
θ_{y_1}	0.0083
θ_{z_1}	0.0051
θ_{x_2}	1.0000
θ_{y_2}	-0.0197
θ_{z_2}	-0.0162

Table 6.2 MDSE loading for an isolated joint (cube example)

Strain Energy		Relative
$E_{complex}$	E_{simple}	Difference R (%)
0.3358E-5	0.0808E-5	75.93

The unit for strain energy is $N - radian/m$

$$R = \frac{E_{Complex} - E_{simple}}{E_{complex}}$$

Table 6.3 Strain energy ratio for an isolated joint (cube example)

Joint Degree of Freedom	Complex Model	Simple Model
θ_{x1}	-0.7072E-8	0.1920E-6
θ_{y1}	0.2172E-7	0.8609E-9
θ_{z1}	0.2109E-7	0.8337E-8
θ_{x2}	0.3356E-5	0.8230E-6
θ_{y2}	-0.5728E-7	-0.7460E-8
θ_{z2}	-0.4794E-7	-0.7043E-8

Table 6.4 Comparison of joint displacements for isolated joint models (cube example)

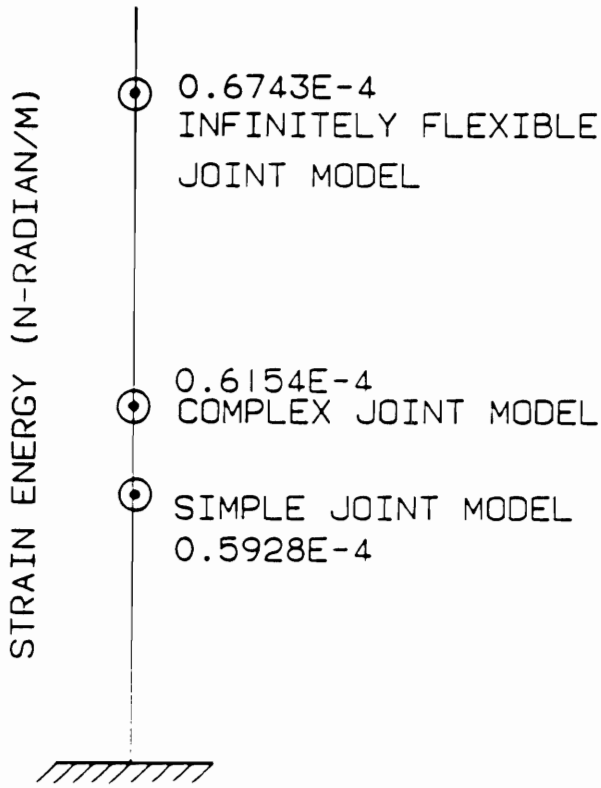

Figure 6.2 Strain energy ratios for joint-cube assembly (cube example)

of a cube-joint assembly in which the joint is infinitely flexible when the assembly is subjected to MDSE loading is presented. Table 6.5 shows the comparison of displacements at the joint degrees of freedom for the case of a cube-joint assembly. It is observed that there is no significant difference between the three models when the overall structure is analyzed. This is because only one joint was considered as being flexible. However, since the two joint models are significantly different, the small difference in strain energies in the overall structural response can be explained by the fact that only one joint was considered flexible. The error in strain energies when the simple model replaces the complex is roughly 30% of the resulting error if the joint is idealized as infinitely flexible. Therefore, the error when using the simple joint model is significant when considering the overall structural response.

The MDSE loading was used as an additional loading case apart from the loading cases used before and the two joint models were estimated again. The estimation was based on the measurements obtained from the this new set of loading cases. The newly estimated parameters are given in Table 6.6. The difference between the estimated parameters with and without the measurements from the MDSE loading taken into account (Tables 6.1 and 6.6 respectively) was very small (less than 2%). The strain energies of the isolated joint models obtained from 11 loading cases are shown in Table 6.7. The same quantities for the joint-cube assemblies are compared in Figure 6.3. As it should be expected, the responses of the complex and the simple models were significantly different again. The response to the MDSE loading is heavily exercised by the coupling

Joint Degree of Freedom	Complex Model	Simple Model
θ_{x1}	0.9186E-5	0.1410E-5
θ_{y1}	-0.6189E-6	-0.4580E-6
θ_{z1}	0.9876E-7	0.2978E-7
θ_{x2}	0.4234E-5	0.3730E-5
θ_{y2}	-0.8164E-6	-0.6819E-6
θ_{z2}	0.1624E-6	0.9190E-7
θ_{x3}	0.1148E-5	0.2264E-5
θ_{y3}	-0.7751E-5	-0.7216E-5
θ_{z3}	-0.2333E-6	-0.2006E-6

Table 6.5 Comparison of joint displacements for joint-cube assembly (cube example)

Joint Stiffness Parameter	Actual Joint	Estimated Complex Model	Estimated Simple Model
k_{11}	0.6098E + 7	0.6097E + 7	0.1671E + 7
k_{12}	-0.7255E + 6	-0.7422E + 6	0.0
k_{13}	0.7805E + 5	0.7705E + 5	0.0
k_{14}	0.2627E + 5	0.2892E + 5	-0.4860E + 6
k_{15}	-0.1502E + 6	-0.1470E + 6	0.0
k_{16}	0.2830E + 7	0.2803E + 7	0.0
k_{22}	0.6098E + 7	0.6204E + 7	0.3272E + 7
k_{23}	0.7805E + 5	0.7457E + 5	0.0
k_{24}	-0.2551E + 5	-0.2636E + 5	0.0
k_{25}	0.1374E + 6	0.6820E + 5	-0.7274E + 6
k_{26}	-0.1502E + 6	-0.1602E + 6	0.0
k_{33}	0.3122E + 6	0.3149E + 6	0.4406E + 6
k_{34}	-0.1530E + 4	-0.1246E + 4	0.0
k_{35}	-0.2551E + 5	-0.2516E + 5	0.0
k_{36}	0.2627E + 5	0.1906E + 5	-0.1943E + 6
k_{44}	0.3122E + 6	0.3066E + 6	0.1329E + 7
k_{45}	0.7805E + 5	0.8890E + 5	0.0
k_{46}	0.7805E + 5	0.8190E + 5	0.0
k_{55}	0.6098E + 7	0.5995E + 7	0.2536E + 7
k_{56}	-0.7255E + 6	-0.7009E + 6	0.0
k_{66}	0.6098E + 7	0.6049E + 7	0.2061E + 7

Table 6.6 Estimated parameters of complex and simple joint models for 11 loading cases (cube example)

Strain Energy		Relative
$E_{complex}$	E_{simple}	Difference R (%)
0.3386E-5	0.0841E-5	75.16

The unit for strain energy is $N - radian/m$

$$R = \frac{E_{Complex} - E_{simple}}{E_{complex}}$$

Table 6.7 Strain energy ratio for an isolated joint for 11 loading cases (cube example)

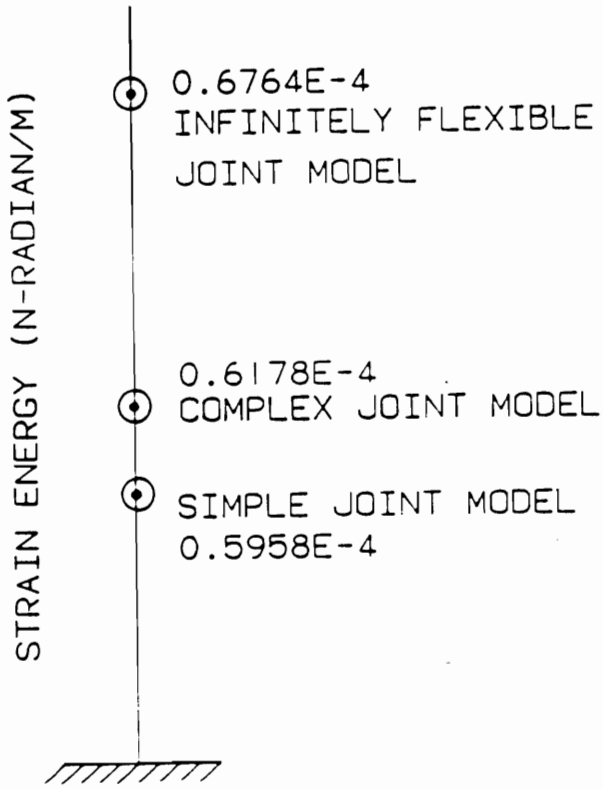

Figure 6.3 Strain energy ratios for a joint-cube assembly for 11 loading cases (cube example)

between the motions of the joint members. Consequently, the difference between the simple and complex models should be attributed to the importance of coupling and not on possible poor design of the experiments.

6.4 Car Model Example

The comparison process used for the cube example is repeated for the car example. The stiffness matrix of the actual joint and that of the identified simple and complex models are presented in Table 6.8.

The MDSE loading corresponding to the two estimated models is presented in Table 6.9. This loading practically constitutes a unit moment in the θ_{z_1} direction which corresponds to the parameter k_{33} . The strain energies stored in the two joint models when subjected to MDSE loading are compared in Table 6.10. Table 6.11 shows the comparison of displacements at the joint degrees of freedom for the case of an isolated joint. Again, as for the cube example, these models are widely different. The difference in the behavior of the two models can only be attributed to the coupling between the motions of the joint branches. Thus, coupling is important in the car example also.

In Figure 6.4, the two finite element models which incorporate the identified simple and complex joint models are compared as for the cube example. The strain energies of the two car-joint assemblies subjected to the MDSE loading corresponding to these assemblies are presented in Figure 6.4. The strain energy

Joint Stiffness Parameter	Actual Joint	Estimated Simple Model	Estimated Simple Model
k_{11}	0.3607E + 7	0.3572E + 7	0.1158 + 7
k_{12}	-0.1321E + 6	-0.1498E + 6	0.0
k_{13}	0.2355E + 5	0.2123E + 5	0.0
k_{14}	0.2355E + 5	0.2206E + 5	-0.3097E + 6
k_{15}	-0.1321E + 6	-0.1178E + 6	0.0
k_{16}	0.9408E + 6	0.8893E + 6	0.0
k_{22}	0.3607E + 7	0.3426E + 7	0.2814E + 7
k_{23}	0.2355E + 5	0.2513E + 5	0.0
k_{24}	-0.7697E + 4	-0.7546E + 4	0.0
k_{25}	-0.1321E + 6	-0.9650E + 5	-0.2551E + 7
k_{26}	-0.1321E + 6	-0.1536E + 6	0.0
k_{33}	0.1567E + 6	0.1406E + 6	1.3922E + 7
k_{34}	0.4618E + 3	0.4457E + 3	0.0
k_{35}	-0.7697E + 4	-0.6581E + 4	0.0
k_{36}	0.2355E + 5	0.2506E + 5	-0.6536E + 7
k_{44}	0.1567E + 6	0.1728E + 6	0.7008E + 6
k_{45}	0.2355E + 5	0.2286E + 5	0.0
k_{46}	0.2355E + 5	0.2306E + 5	0.0
k_{55}	0.3607E + 7	0.3751E + 7	0.2903E + 7
k_{56}	-0.1321E + 6	-0.1436E + 6	0.0
k_{66}	0.3607E + 7	0.3512E + 7	0.6852E + 7

Table 6.8 Actual and estimated parameters of complex and simple joint models (car example)

Direction	Load
θ_{x_1}	-0.0021
θ_{y_1}	-0.0067
θ_{z_1}	1.0000
θ_{x_2}	-0.0062
θ_{y_2}	0.0025
θ_{z_2}	-0.0185

Table 6.9 MDSE loading for an isolated joint (car example)

Strain Energy		Relative
$E_{complex}$	E_{simple}	Difference R (%)
0.8429E-5	0.1426E-5	83.08

The unit for strain energy is $N - radian/m$

$$R = \frac{E_{Complex} - E_{simple}}{E_{complex}}$$

Table 6.10 Strain energy ratio for an isolated joint (car example)

Joint Degree of Freedom	Complex Model	Simple Model
θ_{x1}	-0.1870E-7	-0.4659E-8
θ_{y1}	-0.5535E-7	-0.8025E-8
θ_{z1}	0.7128E-5	0.1278E-6
θ_{x2}	-0.5453E-7	-0.1094E-7
θ_{y2}	0.1109E-7	0.9902E-8
θ_{z2}	-0.1038E-7	-0.1192E-7

Table 6.11 Comparison of joint displacements for isolated joint models (car example)

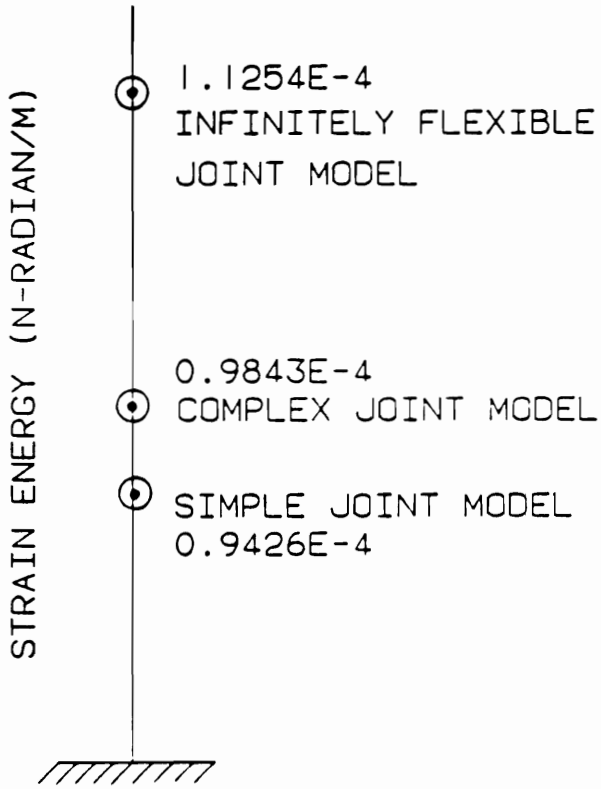

Figure 6.4 Strain energy ratios for joint-car assembly (car example)

of a car-joint assembly in which the joint is infinitely flexible when the assembly is subjected to MDSE loading is also presented in Figure 6.4. Table 6.12 shows the comparison of displacements at the joint degrees of freedom for the case of a car-joint assembly. It is observed that there is no significant difference between the three models when the overall structure is analyzed. This is because only one joint was considered as being flexible. However, since the two joint models are significantly different, the small difference in strain energies in the overall structural response can be explained by the fact that only one joint was considered flexible. As it was mentioned earlier, for this example, the actual joint can be exactly represented by the complex model. It is observed that the error in strain energies when the simple model replaces the complex is roughly 30% of the resulting error if the joint is idealized as infinitely flexible. Therefore, the error when using the simple joint model is significant when considering the overall structural response.

Using the MDSE loading as an additional loading case apart from the loading cases used before, the two joint models were estimated again (Table 6.13). As for the cube example, a very small difference of less than 3% was observed between the estimated parameters and those in Table 6.13. Table 6.14 and Figure 6.5 compare the strain energies of the isolated joint models and the car-joint assembly using the estimated parameters obtained from additional loading case. It is observed that, as for the cube example, the complex and the simple models are significantly different. This difference between the simple and complex models

Joint Degree of Freedom	Complex Model	Simple Model
θ_{x1}	0.5399E-6	0.5014E-6
θ_{y1}	-0.4359E-6	-0.6427E-7
θ_{z1}	0.6082E-4	0.4865E-4
θ_{x2}	-0.9786E-6	-0.8532E-6
θ_{y2}	-0.1193E-6	-0.1024E-6
θ_{z2}	0.1069E-5	0.9088E-6
θ_{x3}	0.5269E-6	0.4819E-6
θ_{y3}	-0.2260E-7	-0.2357E-7
θ_{z3}	0.2254E-5	0.1874E-5

Table 6.12 Comparison of joint displacements for joint-car assembly (car example)

Joint Stiffness Parameter	Actual Joint	Estimated Simple Model	Estimated Simple Model
k_{11}	0.3607E + 7	0.3514E + 7	0.1175 + 7
k_{12}	-0.1321E + 6	-0.1245E + 6	0.0
k_{13}	0.2355E + 5	0.2148E + 5	0.0
k_{14}	0.2355E + 5	0.2274E + 5	-0.3136E + 6
k_{15}	-0.1321E + 6	-0.1195E + 6	0.0
k_{16}	0.9408E + 6	0.8436E + 6	0.0
k_{22}	0.3607E + 7	0.4014E + 7	0.2956E + 7
k_{23}	0.2355E + 5	0.2722E + 5	0.0
k_{24}	-0.7697E + 4	-0.7267E + 4	0.0
k_{25}	-0.1321E + 6	-0.1542E + 6	-0.2691E + 7
k_{26}	-0.1321E + 6	-0.1459E + 6	0.0
k_{33}	0.1567E + 6	0.1368E + 6	1.3853E + 7
k_{34}	0.4618E + 3	0.4798E + 3	0.0
k_{35}	-0.7697E + 4	-0.6692E + 4	0.0
k_{36}	0.2355E + 5	0.2761E + 5	-0.6567E + 7
k_{44}	0.1567E + 6	0.1633E + 6	0.7119E + 6
k_{45}	0.2355E + 5	0.2491E + 5	0.0
k_{46}	0.2355E + 5	0.2467E + 5	0.0
k_{55}	0.3607E + 7	0.3432E + 7	0.3146E + 7
k_{56}	-0.1321E + 6	-0.1502E + 6	0.0
k_{66}	0.3607E + 7	0.3592E + 7	0.6749E + 7

Table 6.13 Estimated parameters of complex and simple joint models for 11 loading cases (car example)

Strain Energy		Relative
$E_{complex}$	E_{simple}	Difference R (%)
0.8488E-5	0.1475E-5	82.62

The unit for strain energy is $N - radian/m$

$$R = \frac{E_{Complex} - E_{simple}}{E_{complex}}$$

Table 6.14 Strain energy ratio for an isolated joint for 11 loading cases (car example)

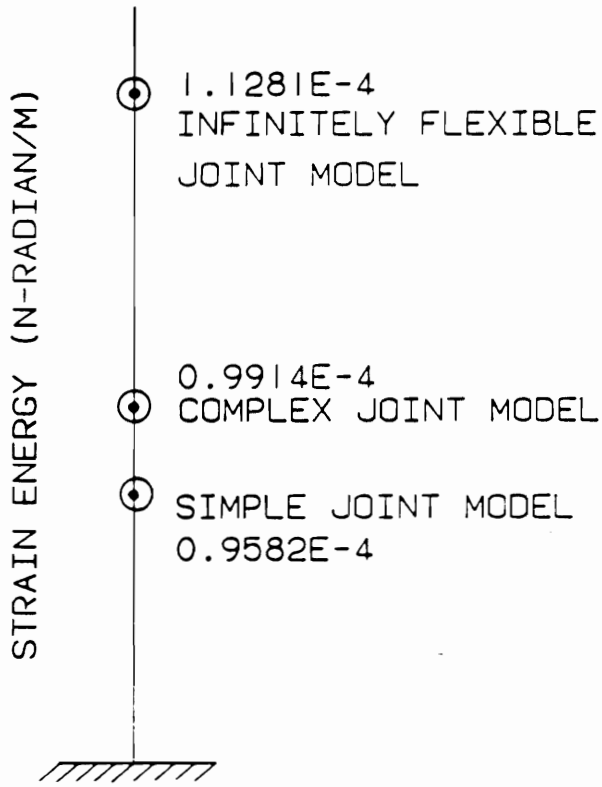

Figure 6.5 Strain energy ratios for a joint-car assembly for 11 loading cases (car example)

is again attributed to the importance of coupling and not on possible poor design of the experiments.

Chapter 7: Conclusions and Future Work

7.1 Contributions of this Dissertation

(i) A black-box approach to static condensation method was developed and employed in the proposed probabilistic system identification method. Comparison of computer times indicates that the use of static condensation can reduce computation times significantly and the black-box approach is only slightly less efficient than the standard implementation of static condensation. The ease of implementation of the black-box approach recommends its use with general purpose finite-element codes that do not have a built-in facility for static condensation.

(ii) Two generic flexible joint models called the simple joint model and the complex joint model were developed to represent the compliant behavior of flexible joints. The simple model includes torsional springs restraining the relative rotation of the joint branches in the three planes, while all branches are assumed

to have the same linear displacements. Coupling between the motions in different planes is neglected. The complex model of the flexible joint, however, takes into account the coupling between the parameters in the various planes. These joint models are incorporated in the finite element analysis of the overall vehicle and the stiffness parameters of this model are identified using simulated experimental displacements.

(iii) A methodology for identification of flexible joint stiffness parameters was developed and was found to be able to estimate model parameters in a small number of iterations. Fixed point iteration was used for convergence to the neighborhood of correct values of the parameter and Newton's method was then used for immediate convergence. The black-box approach developed was used for finding the sensitivity derivatives of displacements with respect to the joint stiffness parameters required in Newton's method. In the solution procedure, the combination of fixed-point iteration scheme and Newton's method yields a faster convergence than Newton's method alone.

(iv) Errors resulting from approximations and idealizations on which the finite element model is based, constitute for the systematic bias in the stiffness of the structure and the joint. In this study, this systematic bias is introduced in the estimation process through the forces by increasing or decreasing the applied forces. It was found that the effect of modeling error that induces bias in the parameter estimates cannot be reduced by increasing the number of loading cases.

(v) Probabilistic system identification is preferable to a method that estimates the parameters from a number of displacements equal to the number of parameters. Moreover, in the probabilistic method, the parameters were identified with confidence intervals which give the quality of the estimates.

(vi) It is found that the coupling between the motions of the joint branches plays an important role in representing the compliant behavior of flexible joints. If coupling is ignored when modeling the joint, the resulting model cannot predict static displacements accurately. Hence the complications induced by considering coupling are justified.

7.2 Suggestions for Future Work

Since flexible characteristics of welded joints are important in the design of automotive structures, further efforts should be made to achieve a better understanding of these characteristics. This can be achieved by the following measures:

(i) Develop flexible joint models that are flexible in translations, and do not rotate about the same point. These models should be used to represent some real life structures with flexible joints. The results must be compared to those from this thesis. Such a comparison will help to decide how complex a joint model needs to be.

(ii) The effect of modeling error in identifying the joints should be further explored.

(iii) The proposed methodology could be applied to other body components. For example, it could be applied to extract local compliance parameters from the suspension and engine mount attachment structures.

(iv) A methodology should be developed to effectively design static experiments in a way that the effect of errors in measuring displacements and in modeling the car body is minimized.

References

(1) Barone, M. R., and Chang, D. C., 'Finite Element Modeling Automotive Structures', Modern Automotive Structural Analysis, Chapter 4, pp. 116-158, edited by Kamal, M. M., and Wolf, J. A., and published by Van Nostrand Reinhold Co., New York, 1982.

(2) Chon, T. C., Mohammedtorab, H., and El-Essowi, M., 'Generic Stick Model of a Vehicular Structure', Proceedings of the 6th. International Conference in Vehicle Structural Mechanics, published by the Society of Automotive Engineers, pp. 235-241, 1986.

(3) Chang, D. C., 'Effects of Flexible Connections on Body Structural Response', SAE Transactions, 1974, Paper No. 740041.

(4) Chen, W. F., and Lui, E. M., 'Effects of Joint Flexibility on the Behavior of Steel Frames', Computers and Structures, Vol. 26, No. 5, 1987, pp. 719-732.

(5) Garstecki, A., 'Optimal Design of Joints in Elastic Structures', Acta Mechanica, pp. 63-76, 1988.

(6) Ioannidis, G. J., and Kounadis, A. N., 'The Effect of Joint Flexibility on the Non-Linear Buckling Load of Metal Portal Frames', Mechanics Research Communications, Vol. 15, no. 3, pp. 189-197, 1988.

(7) Morman, Jr., K. N., 'A Method for the Identification and Modeling of Complex Component Behavior in Large-Scale Vehicle Systems Models', SAE Transactions, 1984, Paper No. 840738.

(8) Berman, A., and Nagy, E. J., 'Improvement of a large Analytical Model Using Test Data,', AIAA Journal, Vol. 21, No. 28, 1983.

(9) Boroski, V. J., Steury, R. L., and Lufkin, J. L., 'Finite Element Dynamic Analysis of an Automobile Frame', Paper 730506 presented at SAE Automobile Engineering Meeting, Detroit, May, 1983.

(10) Baruch, M., 'Methods of Reference Basis for Identification of linear dynamic systems', Technical note, AIAA Journal, Vol. 22, No.4, pp. 561-564, 1984.

(11) Baruch, M., and Zemel, Y., 'Mass Conservation in the Identification of Space Structures', AIAA/ASME/ASCE/AHS 30th. Structures, Structural Dynamics, and Materials Conference., Mobile, Alabama, April 3-5, 1989.

(12) Yun, C. B., and Shinozuka, M., 'Identification of Non-Linear Structural Dynamic Systems', Journal of Structural Mechanics Vol. 8, No. 2, pp. 187-203, 1980.

(13) Collins, J. D., et al., 'Statistical Identification of Structures', AIAA Journal, Vol. 12, No. 2, pp. 185-190, 1974.

(14) Draper, N. R., and Smith, H., Applied Regression Analysis Second Edition, John Wiley and Sons, 1981.

(15) Collins, J. D., et al., 'Statistical Analysis of the Modal Properties of Large Structural Systems', SAE Paper No. 710785, SAE National Aeronautic and Space Engineering Meeting, Los Angeles, California, Sept. 1971.

(16) Baruch, H., and Khatri, M. P., 'Identification of Modal Parameters in Vibrating Structures', AIAA/ASME/ASCE/AHS 28th. Structures, Structural Dynamics, and Materials Conference., 1987.

(17) Butkunas, A. A., et al., 'Procedures of Structural System Identification Applied to Automotive Structures', Proceedings of the Sixth International Conference on Vehicle Structural Mechanics, pp. 93-108, 1986.

(18) Allen, J. J., and Martinez, D. R., 'Automating the Identification of Structural Model Parameters', pp. 728-736, AIAA Journal, 1989.

(19) Chen, J. C., and Garba, J. A., 'Analytical Model Improvement Using Modal Test Results', AIAA Journal, Vol. 18, pp. 684-690, 1980.

(20) Hart, G. C., and Martinez, D. R., 'Improving Analytical Dynamic Models Using Frequency Response Data Application', AIAA SDM Conference, Paper 82-0637, 1982.

(21) Martinez, D. R., 'Estimation Theory Applied to Improving Dynamic Structural Models', Report SAND82-0572, Sandia National Laboratories, Nov. 1984.

(22) Chrostowski, J. D., and Hasselman, T. K., 'MOVER II - A Computer Program for Verifying Reduced-Order Models of Large Dynamic Systems', SAE Technical Paper 861790, 1986.

(23) Isenberg, J., 'Progressing from Least Squares to Bayesian Estimation', ASME Winter Annual Meeting, New York, N.Y., Paper 79-A/DSC-16, December 1979.

(24) Adelman, H. M., and Haftka, R. T., 'Sensitivity Analysis of Discrete Structural Systems', AIAA Journal, Vol. 24, No. 5, pp. 823-832, May 1986.

(25) Nguyen, D. T., and Arora, J. S., 'Fail-Safe Optimal Design of Complex Structures with Substructures', Journal of Mechanical Design, Vol. 104, pp. 861-868, Oct. 1982.

(26) Arora, J. S., and Govil, A. K., 'An Efficient Method for optimal Structural Design by Substructuring', Computers and Structures, Vol.7, no. 4, pp. 507-515, Aug. 1977.

(27) Arora, J. S., and Govil, A. K., 'Design Sensitivity Analysis with Substructuring', Journal of Engineering Mechanics Division of ASCE, Vol. 103, EM4, pp. 537-548, Aug. 1977.

(28) Kirsch, U., Reiss, M., and Shamir, U., 'Optimum Design by Partitioning into Substructures', Journal of Structural Division of ASCE, 98(STI), pp. 249-267, Jan. 1972.

(29) Botkin, M. E., and Yang, R. J., 'Three Dimensional Shape Optimization with Substructuring', Proceedings of the AIAA/ASME/ASCE/AHS/ASC 30th Structures, Structural Dynamics and Materials Conference, held in Mobile, Alabama, part 1, pp.564-568, April 3-5, 1989.

(30) Guyan, R. J., 'Reduction of Stiffness and Mass Matrices', AIAA Journal, Vol. 3, no. 2, p. 380, Feb. 1965.

(31) MacNeal-Schwendler Corporation, 'NASTRAN User Manuals, Vol. 1 and 2', Los Angeles, California, July 1984.

(32) Chon C. T., 'Sensitivity of Overall Vehicle Stiffness to Local Joint Stiffness', Sensitivity Analysis in Engineering, NASA Conference Publication 2457, (H. M. Adelman and R. T. Haftka, editors), Proceedings of Symposium, pp. 97-112, held in Hampton, Virginia, Sept. 25-26, 1986.

(33) Haftka, R. T., and Kamat, M. P., 'Elements of Structural Optimization', Martinus Nijhoff Publishers, 1986.

(34) Bard, Y., 'Non-Linear Parameter Estimation', Academic Press, New York, 1974.

(35) Lewis, T.O., and Odell, P.L., Estimation in Linear Models, Prentice-Hall, Englewood Cliffs, 1971.

(36) Gangadharan, S. N., Haftka, R. T., and Nikolaidis, E., 'An Easily Implemented Static Condensation Method for Structural Sensitivity Analysis', Communications in Applied Numerical Methods', (in press).

(37) Hartley, H.O., 'The Modified Gauss-Newton Method for Fitting of Non-Linear Regression Functions by Least Squares,' Technometrics, Vol. 3, 1961, pp. 269-280.

(38) Strang, G., 'Linear Algebra and its Applications', 2nd. Edition, Academic Press Inc., 1976.

(39) Gangadharan, S. N., Nikolaidis, E., and Haftka, R. T., 'Probabilistic System Identification of a Simple Flexible Joint Model', 'AIAA/ASME/ASCE/AHS 31st.

SDM Conference', Long Beach, California, April 2-4, 1990 (accepted for presentation).

(40) Gangadharan, S. N., Haftka, R. T., and Nikolaidis, E., 'An Alternate Static Condensation Method for Sensitivity Analysis of Structures', 'CSME: Mechanical Engineering Forum 1990', Toronto, Canada, June 3-9, 1990 (accepted for presentation).

(41) Gangadharan, S.N., Nikolaidis, E., and Haftka, R. T., 'Probabilistic System Identification of a Complex Flexible Joint Model', 'AMSE International Conference', Greensboro, North Carolina, October 29-31, 1990 (accepted for presentation).

(42) Gangadharan, S. N., Nikolaidis, E., and Haftka, R. T., 'Probabilistic System Identification of Two Flexible Joint Models', 'AIAA Journal', (intended publication).